2006

Security enhancement in passive optical networks through wavelength hopping and sequences cycling technique

Walid Suleiman Shawbaki
Iowa State University

Recommended Citation

Shawbaki, Walid Suleiman, "Security enhancement in passive optical networks through wavelength hopping and sequences cycling technique " (2006). *Retrospective Theses and Dissertations*. 1305.
https://lib.dr.iastate.edu/rtd/1305

Security enhancement in passive optical networks through wavelength hopping and sequences cycling technique

by

Walid Suleiman Shawbaki

A dissertation submitted to the graduate faculty

in partial fulfillment of the requirements for the degree of

DOCTOR OF PHILOSOPHY

Major: Computer Engineering

Program of Study Committee:
Doug W. Jacobson, Co-major Professor
Ahmed E. Kamal, Co-major Professor
Thomas E. Daniels
Douglas D. Gemmill
Yong Guan

Iowa State University

Ames, Iowa

2006

Graduate College
Iowa State University

This is to certify that the doctoral dissertation of

Walid Suleiman Shawbaki

has met the dissertation requirements of Iowa State University

Signature was redacted for privacy.

Co-major Professor

Signature was redacted for privacy.

Co-major Professor

Signature was redacted for privacy.

For the Major Program

DEDICATION

I dedicate this dissertation with love and admiration to my parents for their everlasting support in my life, and to my wife, brothers, and sisters for their constant encouragement in pursing my higher education.

TABLE OF CONTENTS

LIST OF FIGURES

LIST OF TABLES

LIST OF ABBREVIATIONS

1-D: One dimensional

2-D: Two dimensional

3-D: Three dimensional

AES: Advanced encryption standard

AOTF: Acousto-optical tunable filters

APON Asynchronous transfer mode passive optical networks

ASK: Amplitude shift keying

ATM: Asynchronous transfer mode

B&S: broadcast and select

BER: Bit error rate

BPON: Broadband passive optical networks

CATV: Cable television

CDMA: code-division multiple access

CDR: Clock data recovery

CO: Central office

CRU: Clock recovery unit

CSMA/CD: Carrier sense multiple access with collision detection

DA: Destination address

DBR: Distributed Bragg reflectors

DES: Data encryption standard

DFB: Distributed feed back

DVB: Digital video broadcast

DWDM :Dense wave division multiplexing

DSL: Digital subscriber line

EOTF: Electro-optical tunable filters

EPON: Ethernet passive optical networks

EQC: Extended quadratic congruence

FH: Frequency hopping

FFH: Fast-frequency hopping

FFH-CDMA: Fast optical frequency-hop code division multiple access

FSK: Frequency shift keying

FTTB: Fiber-to-the-Building

FTTC: Fiber-to-the-Curb

FTTD: Fiber-to-the-Desktop

FTTH: Fiber-to-the-Home

FWM: Four-wave mixing

GCSR: Grating coupler sampled reflector

GVD: Group velocity dispersion

HFC: Hybrid fiber coax

HDTV: High definition television

IEEE: Institute of Electrical and Electronic Engineers

IM: Intensity modulation

ISI: Inter symbol interference

ISO: International Standards Organization

ITU: International Telecommunication Union

LAN: Local area network

MAC: Medium access control

MAI: Multiple access interference

MI: Modulation instability

MPCP: Multi-point control protocol

MPEG: Motion picture expertise group

MW: Multiple wavelength

NAS: Network area storage

NRZ: Non-return to zero

NZ-DSF: Nonzero dispersion-shifted fiber

OAM: Operation, administrative, and maintenance

OCDMA: Optical code division multiple access

OLT: Optical line terminal

ONU: Optical network unit

OOC: Optical orthogonal code

OOK: On-off-keying

OSI: Open Systems Interconnect

OSNR: Optical signal to noise ration

P2MP: point to multi-point

PMD: Polarization mode dispersion

PN: Pseudorandom noise

PON: passive optical networks

PPM: Pulse position modulation

PRBS: Pseudo random binary signal

PS: Prime sequences

PSC: Passive star coupler

PSL: Phase shift keying

PSO: Pseudo orthogonal

QCC: Quadratic congruence codes

QoS: Quality of service

RF: Radio frequency

RIN: Relative intensity noise

RTT: Round trip time

RZ: Return to zero

SA: Source address

SAC: Spectral amplitude coding

SAN: Storage area network

SDBR: Sectional distributed-Bragg reflection

SMDR: Side mode suppression ratio

SMF: Single-mode fiber

SMPTE: Society of Motion Picture and Television Engineers

SPM: Self-phase modulation

SRS: Stimulated Raman scattering

SSL: Secure sockets layer

TDMA: time-division multiple access

TPS: Triple play services

TS/WH: Time-spreading/wavelength-hopping

VCSEL: Vertical cavity surface emitting laser

WDM: Wave division multiplexing

WDMA: Wavelength-division multiple access

XPM: Cross-phase modulation

ACKNOWLEDGEMENTS

I owe gratitude to many people for completing this dissertation, starting with my program of study committee members for their comments and questions during the preliminary and final oral examinations. I am deeply indebted to my co-major professor, Dr. Ahmed Kamal, for his constant support and guidance in my research. I appreciate his efforts for making time to have one-on-one meetings throughout the research activities and pointing me in the right direction. Dr. Kamal's positive attitude, dedication, and enthusiasm for research and his background in optical systems made it a pleasure to work with him. I would like also to thank my co-major professor Dr. Doug Jacobson for his efforts in providing me with the knowledge and background through his security courses that were useful in extending my research interest to secure optical networks. Many thanks to my committee members Dr. Thomas Daniels, Dr. Douglas Gemmill, and Dr. Yong Guan for their advice, time and patience that are highly appreciated. Their knowledge and experience in the area of network security had clarified many doubts that I had at the early stages of my Ph.D. research, and I offer my appreciation for taking interest in my work and providing ideas and suggestions during the preliminary and final oral exams.

My graduate education and research has been possible through the support of my employer Rockwell Collins, which I fully admire as an employer of choice. I would like to thank the continuing education team at Rockwell Collins for their support, and I would like to express my regards and appreciation to my immediate manager Mr. Ken Mc Elereath for his continuous support to pursue my higher education, and facilitating the way to help me achieve my goal of higher education.

Finally, I would like to thank my parents for their constant support over the years. The encouragement and love that they have selflessly and tirelessly invested in me is undoubtedly the greatest source of my ambition, inspiration, dedication, and motivation. They have taught me far more than words can express.

ABSTRACT

Growth in the telecommunication industry continues to expand with requirements evolving around increased bandwidth and security. Advances in networking technologies have introduced low cost optical components that has made passive optical networks (PON) the choice for providing huge bandwidth to end users. PON are covered by established standards such as IEEE 802.3ah and ITU-T G.983.1/984.1, with star topology of broadcast and select (B&S) on shared fiber links that poses security vulnerability in terms of confidentiality and privacy.

The focus of research and reports in the literature center around increasing cardinality via coding schemes that lack in addressing security, which was left for implementation in application layers via cryptography. In this dissertation, an approach is presented on the subject of security in PON at the network level using slow wavelength hopping techniques and diffusion of data packets among dense wave division multiplex (DWDM). Orthogonal wavelength sequences are generated by mapping an ITU-T G694.1 based wavelength grid matrix and code matrices. The arrangement of wavelengths in the wavelength grid matrix, which can be changed frequently (i.e, on an hourly basis) serves as the first key of secure operation. Allocation of generated wavelength sequences distributed in multiple quantities to nodes based on their security level serve as second individual keys for the nodes. In addition, an improved level of security provided via the cycling order of those allocated wavelength sequences to nodes is the third key (shared secret) between the central office (CO) and a node. The proposed approach to PON security provides three new keys available outside the world of cryptography.

Various coding techniques are used, and the result shows that even time spreading/ wavelength hopping based on symmetric prime numbers provided the least wavelength sequences; however, it provided excellent correlation properties and level of security. A PON simulation model was implemented to investigate channel impairments in DWDM with 64 channels spaced at 25GHz carried over a 25 KM ITU-T G.655 compliant shared fiber cable, and security performance evaluation included analytical studies in the classical probabilities to capture the correct order of wavelength hopping sequence using exhaustive search, in addition to reverse construction of matrices from monitored channels. Encouraging results obtained support the feasibility of the proposed technical approach for security.

CHAPTER 1: PASSIVE OPTICAL NETWORKS

Massive growth in demand for broadband services by end users requires networks with performance and capabilities that satisfy increasing organizational as well as residential demand for bandwidth. The trend in increasing demand for bandwidth, illustrated in Figure 1, exhibits a sharp rise as more connectivity requirements at home and office for services such as high definition television, video, mail, and digital audio as well as full internet connections via user-friendly graphic user interfaces drives the demand on bandwidth [1]. The need exists for supporting connectivity for triple play services (TPS), which include audio, video, and data [2].

The technology that has the potential to satisfy the increasing demand for bandwidth is optical networking technology, which includes wave division multiplexing (WDM) or dense WDM (DWDM[1]), optical code division multiple access (OCDMA), etc. However, the maturity of some technologies to deal with high data rates (i.e., OCDMA) and cost are among many factors that played major roles in the slow adaptation of such technologies in fiber connectivity to end users in the local loop [3]. Fortunately, the cost barrier is coming down due to development of passive optical networks (PON) with their attractiveness associated with their low cost and high performance [4]. PON use shared fiber links with a broadcast and select (B&S) type of transmission as shown in Figure 2, which makes them vulnerable to different types of attacks that are applicable to optical networks [5]. B&S makes transmitted data available at all nodes location (optical network units—ONUs) where robust security must be provided in order to gain subscribers' confidence in a network. In addition to the security concern, comprehensive study of the various other issues and challenges faced in the design of any multicast technique based on B&S protocols is reported in [6].

The objective of this dissertation is to introduce a novel scheme for providing security enhancement in PON as a countermeasure against eavesdropping and impersonation types of attacks. The dissertation outline is as follows: In this chapter, background about optical networks focusing on PON is provided, in addition to standards, enabling technologies, and

[1] DWDM is often used to describe systems supporting a large number of channels with the channels very tightly spaced.

the organization of this dissertation. Chapter 2 discusses the types of attacks against PON and current schemes used for protection and reviews the literature in relation to PON vulnerability. The motivation section discusses the need for security in PON and justification for the cost in addition to the contribution of this dissertation. In Chapter 3, the proposed security enhancement is presented with details of the simulation used to provide proof of the concept of the feasibility of the technical approach, along with considerations related to system deployment. In Chapter 4, analysis and evaluation of the proposed security enhancement in PON is included. Finally, the conclusion and future work is presented in Chapter 5.

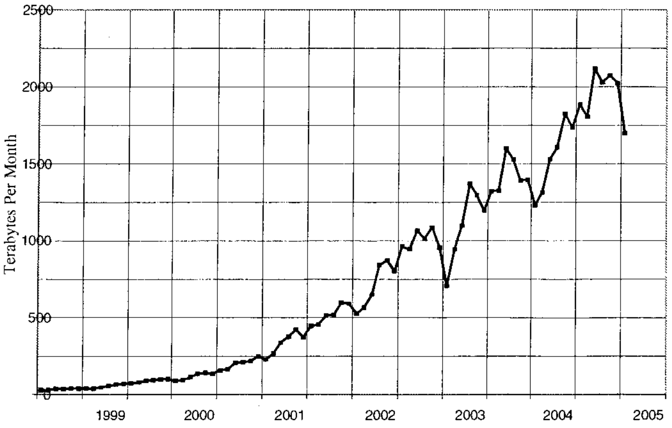

Figure 1: Customers traffic volume trend (Source: SurfNet www.gigaport.nl)

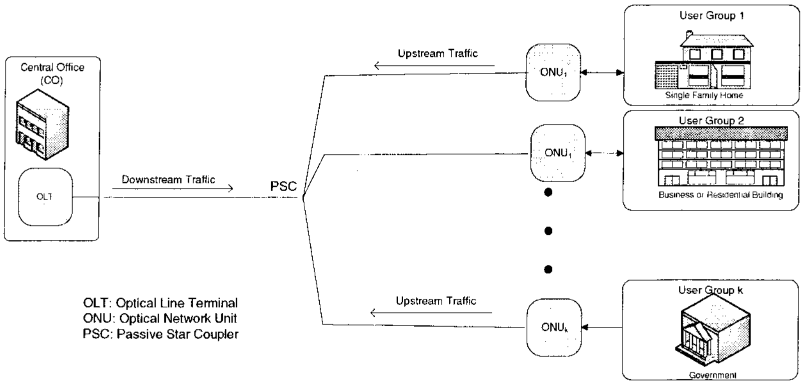

Figure 2: Passive optical network (PON) topology

1.1 Introduction to Optical Networks

Optical networks, as the name implies, implement optical light to transfer data from one end to another such that with the use of optical networking technologies and characteristics of fiber connectivity of handling high bandwidth meet the demand by customer. However, there is a strong correlation between the increasing demand for bandwidth and the cost of bandwidth, but technological advances in optical networking have succeeded in continuously reducing the cost of bandwidth [7].

The optical networking market is roughly divided into three main segments for ease of analysis as well as customer focus [8]: size of network, line rates, and distances/geographical locations. Traditionally, there is a three-tiered hierarchy:

- Long-Haul Core Network: usual distance ranges of 300 to 2000 km and considered as regional or continental networks connecting different cities and supporting massive data transfer.
- Metro Core Transport Network: extending 75 to 300 km and found in a ring configuration to support longest transmission.
- Metro Access Network: at edge of the networks and usually connected to a metro core transport network, which extends to 75 km in distance. This is where the PON usually are connected, and is also the focus of the this dissertation.

Successful implementation of optical technologies in backbone networks to transport massive data provided a need to extend fiber connectivity to remove bottleneck in access networks. Existing access networks built on top of existing copper wire infrastructure have their limitations in supporting the increasing demand for bandwidth, where future services are expected to satisfy, for example, TPS, which include data, audio, and video with high definition television (HDTV), as well as full Internet connections via user-friendly graphic user interfaces [1]. It is estimated that more than 75 Mb/s per subscriber is required for convergence services such as TPS, and among several types of high speed access network technologies, wavelength division multiplex PON is the most favorable [2]. The estimate is conservative for today's requirements; however, access networks will be used to deliver multiple HDTV broadcasts to the home, requiring a data rate in the order of 1 Gb/s [3]. TPS will be part of the next wave in access network deployment, and Fiber-to-the-Building (FTTB), Home (FTTH), or Curb (FTTC) are the ultimate level of access, allowing end users to access the backbone networks through the gigabit capacity of a fiber optic cable [9]. Figure 3 provides information about revenue for PON world wide spending projections [11] and shows, along with the trend shown in Figure 1, a clear picture of access networks moving toward optical connectivity in which PON are the baseline for future connectivity for businesses and residential alike.

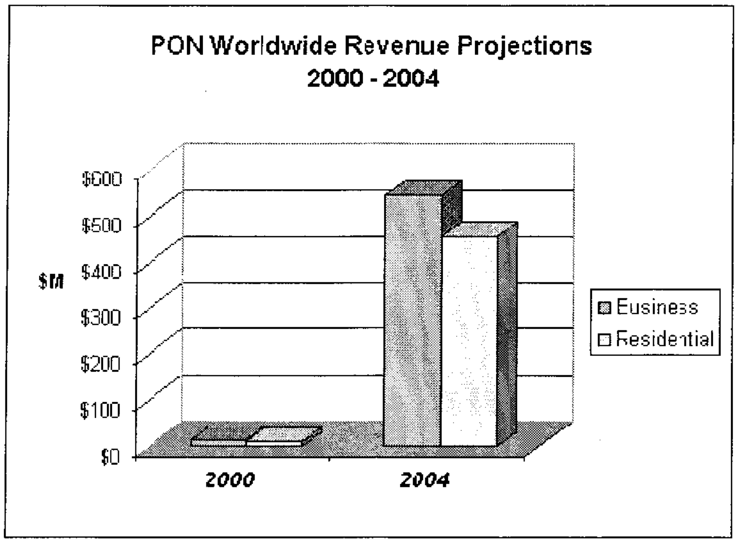

Figure 3: PON world revenue (Source: CIBC world market)

PON has been proposed in [12] and [13] as the potential baseline providing speeds at low cost, compared to existing technologies, with the use of passive components. When PON is combined with optical networking technologies such as WDM, data are pumped across the networks at higher capacity making fiber connectivity in access networks more realizable to achieve FTTH, FTTB, and/or FTTC.

1.2 Current Status of Access Networks

Telephone networks and connectivity to homes or offices is considered the origin of access networks based on copper wire pairs designed for transmission of analog voice signals. Thereafter, demands for extra services and enormous demand for Internet services by businesses and households focused on the need for higher bandwidth connectivity, preferably using existing telephone lines. Starting with modems that supported data service rates up to 56Kbps, then the need for higher bandwidth to access what is known as the "information superhighway" for residential customers, required new technologies capable of improving the performance and capacity of these access networks.

Broadband and data service deployment were launched initially on overlay infrastructures adding cost and complexity of deployment and reducing operational scalability of these services [10]. For example, investment went into using the existing infrastructure of access networks that led to the development of the digital subscriber line (DSL) using existing telephone twisted pair systems, and cable television (CATV), which uses coax cables. Actually, fiber connectivity was introduced in access networks in a hybrid architecture that includes hybrid fiber coax (HFC) with coax being the bottleneck for further expansion of bandwidth. However, existing metal-based infrastructure has its saturation point and new generation optical access networks are emerging, which include for example FTTC, FTTB, and FTTH. The gradual penetration of optical fiber into the access network (which is known also as the local loop) is one way to respond to the increase in demand for bandwidth, but it is clear that cost is the cause of such slow adaptation of full optical networking in the local loop.

Various schemes with more focus are used in access networks to provide more nodes/ users access to the network through bandwidth sharing techniques. Some of the schemes in place include time-division multiple access (TDMA), wavelength-division multiple access (WDMA), and code-division multiple access (CDMA) as illustrated in Figure 4. TDMA has limited growth since it is a bottleneck when considering the increase in the number of users and their demand for bandwidth as illustrated in Figure 1. Optical access networking, such as PON shown in Figure 2, provides an excellent solution to meet future demand as an access network. PON is a point to multi-point (P2MP) network that implements passive elements between nodes such as the passive star coupler (PSC), and accordingly, lowers the cost barrier for implementation as compared to active elements.

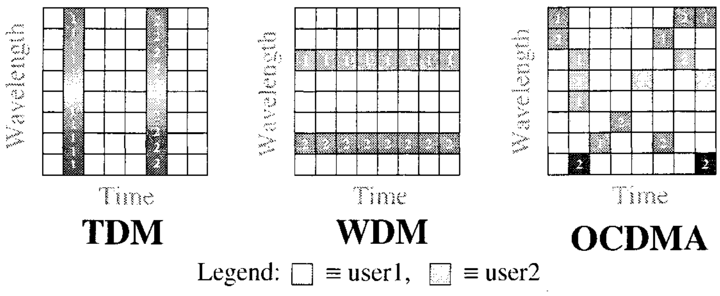

Figure 4: Various access scheme in optical networks

PON topology shown in Figure 2 consists of an optical line terminal (OLT) located at the local central office (CO) and *k* ONUs that serve up to *K* user groups, where a user group can be a single or multiple residential homes, public/government institutions, or businesses.

PON have two types of traffic: downstream and upstream. Downstream traffic is B&S on a single wavelength, while upstream traffic direction is on different wavelengths with centralized control and scheduling within the OLT.

Extension of fiber connectivity to end users to solve the bandwidth bottleneck in metro/ access networks drove the establishment of different standards by the Institute of Electrical and Electronic Engineers (IEEE) and the International Telecommunication Union (ITU). The main purpose of establishing standards is to provide guidance and recommendations for a broadband optical access network, which regulates and accelerates the installation of fiber in access network. Standards are based on PON topology shown in Figure 2, and have the basic principle of sharing a central OLT and the feeder fiber over as many ONUs.

Two well-known standards are in place to support implementation of PON technology. The first is governed by the ITU-T G983.1/984.1 standard (the second T stands for Telecommunication), and the second is IEEE 802.3ah Ethernet PON (EPON).

1.2.1 ITU-T Passive Optical Networks Standard

ITU-T G983.1/984.1 provides rules for broadband optical access systems [12], which are based on PON in asynchronous transfer mode (ATM) (abbreviated APON), which is also known as the broadband PON (BPON). ITU-T-G983.1 includes recommendations that describe systems with nominal symmetrical line rates of 155.520 Mbit/s and asymmetrical line rates of 155.520 Mbit/s upstream and 622.080 Mbit/s downstream, with fixed packet size to 56 bytes [12]. The physical infrastructure of the BPON (APON) uses single fiber PON in most implementations [12]. Both directions of communication are supported using WDM. The downstream direction uses the 1550 nm window, while the upstream uses the 1310 nm window. This arrangement saves cost over dual fiber arrangements by reducing the amount of fiber deployed and eases operational concerns, as there is less chance of fiber misconfiguration.

1.2.2 IEEE 802.3ah Ethernet Passive Optical Networks (EPON) Standard

Ethernet based PON (EPON), unlike APON (ITU-T G983.1 standard), utilize the economies of scale of Ethernet [13]. The Ethernet as mature technology provides simple, easy to manage connectivity due to fully deployed Ethernet-based systems. The same idea of using a PON-based system in which the number of subscribers can be a single customer or a group of customers connected to a single ONU, all ONUs are connected to the (OLT located in the CO, as illustrated in Figure 2.

In the original IEEE 802.3 standard Ethernet, two configurations are defined: Carrier sense multiple access with collision detection (CSMA/CD) is used in shared medium, and switched network configuration uses full duplex links. Properties of an EPON system based on IEEE 802.3ah are such that it cannot be considered either a shared medium or a point-to-point network; rather, it is a combination of both protocols [15]. In an EPON system, all data are encapsulated in Ethernet packets for transmission, which are compatible with IEEE 802.3 Ethernet standards [13][16]. Extraction of data from the main downstream traffic on the shared fiber link by a specific ONU is based on its medium access control (MAC) address. A single wavelength is used for each direction of traffic (upstream and downstream) with TDM slots used for ONUs in the downstream and TDMA for upstream. TDMA is scheduled by OLT, and line data rates can be different per ONU; therefore, the TDMA scheme can be a bottleneck for bandwidth-hungry ONUs.

The principle of sharing the same link among ONUs in the downstream may be tolerated for some applications, however, a problem arises in the upstream direction where the EPON system must employ a MAC mechanism to arbitrate access to shared medium for collision avoidance. It is still also responsible for the efficient sharing of upstream transmission bandwidth among all ONU.

Arbitration in EPON uses polling protocol for transmissions from ONU to OLTs, which facilitates the dynamic bandwidth allocation and arbitrating the transmissions of multiple ONUs. Polling resides in OLTs' MAC control layer and has two operation modes: NORMAL and AUTO-DISCOVERY. In the NORMAL mode, the OLT sends the GATE message to ONUs, which is permission to transmit at a specific time, for a specific duration, and the ONUs send a REPORT message to the OLT, which is a message used by an ONU to report its local conditions to the OLT [13]. Both messages are used in the allocation of bandwidth to each ONU. In addition, the GATE message is used by the OLT to allocate transmission windows to individual ONUs.

The AUTO-DISCOVERY mode is a process by which the OLT finds a newly attached and active ONU in the P2MP PON to enable exchanging registration information between the OLT and ONUs [13]. The OLT is responsible for the required synchronization time and, with sufficient information collected during the NORMAL and AUTO DISCOVERY modes, OLT provides the maximum number of pending grants and is responsible for scheduling ONUs for access to PON in the upstream direction.

Due to different fiber lengths and locations of ONUs on the access network, ranging will be necessary, which is a procedure by which the propagation delay between the OLT and ONUs is measured. The round trip delay computation performed by the OLT uses the timestamp in messages from the ONUs.

IEEE 802.3ah standard defines the Ethernet frame structure (shown in Figure 5), which consists of a number of blocks plus a special frame start and stop marker [13]. The header is common to all Ethernet frames, and each frame is preceded and trailed by an inter packet GAP (IGP) of 14 bytes. The standard Ethernet has the following blocks:

- Destination Address (DA);
- Source Address (SA): carries the individual MAC address associated with the port;
- Length/Type: type encoded and carries the Slow Protocols Type field value;
- Subtype: identifies the specific Slow Protocol being encapsulated;

- Flags: contains status bits;
- Code: identifies the specific OAMPDU;
- Data/Pad: contains the OAMPDU data and any necessary pad;
- Frame Check Sequence (FCS).

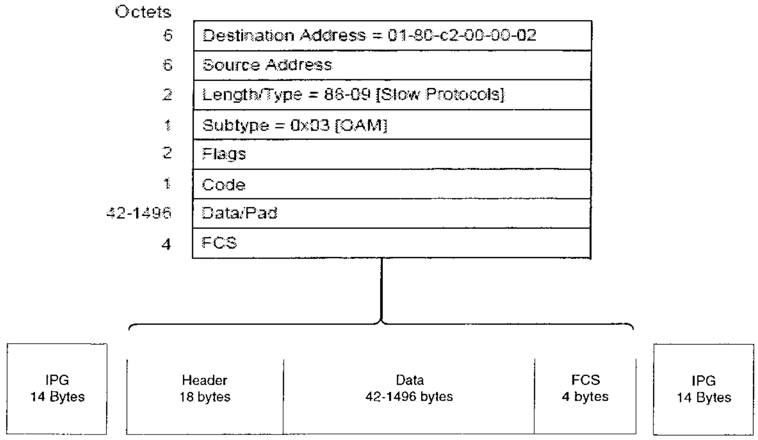

Figure 5: Ethernet frame structure defined in IEEE 802.3ah

1.3 Enabling Technologies for Passive Optical Networks

Laser is the enabling technology used in both OLTs and ONUs for transmission and reception in PON. WDM provides an increase of capacity of optical fiber, and tunable lasers could emit light at different wavelengths by using some physical characteristics of the lasing media that facilitated the change in emitted wavelength. Tunable laser source provides convenience and economies of scalability when considering WDM with large number of channels because it would be impractical to use a large amount of fixed wavelength transmitters.

One of the key requirements for a great expansion of optical networks is low-cost, high-performance tunable lasers that are easily packaged and coupled to fiber [17]. Tunable laser components must accommodate good dynamic ranges of operations in terms of tuning, sensitivities, and stability for absolute wavelength that is necessary, especially when operating with small channel[2] spacing in WDM operation, where the channel defined throughout this dissertation by its wavelength, frequency, or both will be used to mean channel.

[2] Channel designated by its frequency in THz, or wavelength in nm.

In long haul communication optical networks, the attenuation of fiber necessitates the use of repeaters at regular intervals, but this will not be necessary in a PON-based access network due to the shorter distance (less than 40 km). The attractiveness of PON is due to their low cost and high performance, which makes the need for compact optical transceivers urgently in demand in order to spread PON [4]. In addition, the maturity of Ethernet opens the door for PON as the next generation access network; already some have been designed, tested, and implemented to be used in FTTH or Fiber-To-The-Desktop (FTTD) as reported in [18].

In the following sections is a brief review of optical components included in this dissertation to establish the foundation of the DWDM PON simulation model as discussed in section 3.5.3. The review is very brief; for theory of operation and structure of actual optical components, the reader is referred to academic textbooks that discuss optical components technologies in more detail. References [7] and [20] are good sources for more in-depth information about the basic laser components structure and theory of operation.

1.3.1 Laser Transmitter Components

The basic principle for laser transmitters/filters, whether they are tunable or fixed, is the same: The transmitter is a semiconductor device that converts electrical information to optical, while the laser receiver (i.e., filter and detector) works in the opposite manner. The narrow band of light with small optical spectral (line width), in addition to fast responses (tunability), and the ability to couple a significant amount of energy are some of the expected performance parameters that are required in optical networking [8]. Some of the popular tunable lasers are mechanically tuned lasers that are known for their wide range tuning, however, they have slow tuning speed that will make them disadvantaged in wavelength hopping applications.

Acousto-optically, electro-optically, and injection-current tuned lasers are some of the available technologies. For example, when an application requires faster wavelength tunable lasers, laser's refractive index, which determines the lasing wavelength, can be changed by controlling the amount of current injected into the laser cavity or the laser's wavelength control section. The refractive index in the laser cavity can be controlled very rapidly by controlling the current injected into the laser. The wavelength switching speed is a few nanoseconds [21], and semiconductor lasers based on PN junction are the most common with operation in wavelength ranges of interest between 1528 nm and 1560 nm that are favorable for the proposed PON security enhancement in this dissertation.

Vertical cavity surface emitting laser (VCSEL)[3] is the preferred choice for gigabit speed operation, but it is available only for wavelengths no longer than 850 nm [8], which is outside the wavelengths of interest in this dissertation.

PON covered by both ITU and IEEE standards in [12]and [13], respectively, are based on only two wavelengths, while WDM, with tunable resources, supports higher bandwidth greater than what is established in those standards.

1.3.1.1 Laser Components Performance Parameters

WDM operation places great restrictions on laser transmitter and receiver implementation, and tuning range is an important factor to the implementation of WDM expressed by $\Delta\lambda$ and represents the maximum number of wavelengths (λ_i) supported. Cooling requirements and other parameters are important, but these requirements are outside the scope of this dissertation where the discussion will focus on components' parameters related to the simulation model application in section 3.5.2.

Several technologies available provide tunable lasers, which vary between wide range and slow tuning characteristics, but the most suitable technology for use in WDM is the sectional distributed-Bragg reflection (SDBR) tunable lasers, which is based on having different cavities with different currents used to create different wavelengths. SDBR is an extension of the distributed Bragg reflectors (DBR[4]) where feedback is essential for maintaining lasing threshold [8]. The three section DBR tunable laser, for example, has one section associated with gain and considered the active region, followed by a section that provides phase shift of the reflected wave and a Bragg grating third section as the DBR. More details about the structure are found in [20].

[3] VCSEL emits the laser light perpendicular to the plane of P-N junction and the structure proving the laser feedback arranged in the vertical direction as compared to the normal laser diode.

[4] Optical feedback is realized by placing the P-N junction in a cavity that has fully reflecting walls on all but one side and a partial reflector on the remaining side, in addition to insertion of grating (corrugated surface) within the cavity.

1.3.1.1.1 Tuning Speed and Range

Tuning speed and range are the important parameters for tunable laser components to be included in DWDM implementation. Tuning time (speed) is the time required for the laser to tune from one wavelength to another, while tuning range ($\Delta\lambda$) refers to the range of wavelengths over which the laser may be operated. The technology for providing components with wide tuning range and high speed tuning are available commercially by using the grating coupler sampled reflector (GCSR) and sampled grating DBR that have achieved a speed of 5 ns and tuning over 50 nm range as reported in [22] and [23].

Different ways can be used to provide tunable wavelengths, however, architecture systems that employ digital non-mechanical tunable lasers potentially offer the stability, reliability, and repeatability which is necessary for DWDM and telecommunication grade systems [24].

Output of tunable laser devices can be continuously changeable to any other wavelength, or discretely tunable to preset predefined wavelengths such as those in the ITU recommendations ITU-T G694.1 wavelength grid [26]. The approach to compensate for slow tuning in the proposed solution in this dissertation is to have a minimum of dual transmitters/ filters such that when one is being used, the other is tuned to the next wavelength, thus providing a ready resource for the next wavelength. Both discrete ITU-T G694.1 wavelengths channel tuning and implementation of multiple tuning resources (transmitters and filters) in each node will be part of the approach in providing PON's security enhancement as proposed in this dissertation.

1.3.1.1.2 Line Width of a Laser

As a prime requirement in DWDM with several simultaneous channels (wavelengths) being on shared fiber link, a narrow line width and stable channel frequencies of the laser sources provide protection of the spectrum from being spilled over to adjacent channels. Laser line widths for single mode lasers, for example, typically are less that 1 Å[5] as transmitted by the source [28]. Therefore, it is required that in DWDM operation each channel has to have a very narrow spectral width in order to avoid cross talk with an adjacent

[5] Å designates an angstrom, which is a unit of measure equal to 1 hundred-millionth of a centimeter.

channel. Fortunately, the distributed feed back (DFB) laser diode meets the narrow line width requirements where a typical line width is 10 MHz and a maximum of 40 MHz, which also has an inverse relationship to output power; , for example, for a DFB laser radiating at 30mW, the line width can be as narrow as 1 MHz [20].

1.3.1.1.3 Stability of the Laser Source

The variation in output power of a laser source affects line width, and consequently, cross talk between channels occurs that we need to avoid or keep under control in WDM system design. This is a condition in which channel separation in a stable manner reduces crosstalk between channels to a minimum. In the PON DWDM simulation model in section 3.5.2, stability of channels is monitored and checked in spectrums around the center frequency of the channel and compared to the channel spacing 25GHz (.2nm) used.

1.3.1.1.4 Side-Mode Suppression Ratio (SMSR)

The side mode suppression ratio (SMSR) is a measure of the intensity difference between the main longitudinal mode and the side mode. The typical SMSR specified in the data sheets is around 40dB, which is a comparison of the main mode intensity to the side mode intensity expressed in dBs. This important property is considered in the implementation of DWDM because suppression of the side modes is required to avoid crosstalk.

DFB laser has a narrow line width, but also provides a better SMSR since side modes are severely suppressed. For example, the GCSR laser diode was built with a fast wavelength tunable transmitter offering 100 (0.4 nm spaced) accessible wavelength channels with a tuning range of 44 nm (1523.77–1567.77 nm) and an output SMSR of at least 30dB [19].

1.3.1.1.5 Chirp

Chirping is a rapid change in the center frequency of the transmitted optical signal with reference to time [8]. For example, the laser diode is very sensitive to back reflected light[6], which is a major cause for chirping and relative intensity noise (RIN[7]). Some solutions to avoid chirping include the use of optical isolators to prevent back reflected light from

[6] Back reflected light is the light reflected from the fiber optic cable back into the Laser Diode (LD) active region, which causes a deterioration of the laser diode performance.

[7] RIN is defined as the ratio of the mean square optical intensity noise to the square of the average optical power.

penetrating the active region of the laser diode. In addition, chirp is a fast variation in the laser peak radiating frequency in response to a change in a driving (modulation) current that results in broadening of the light pulse. In WDM operation, chirp has to be eliminated, which means that direct modulation (intensity modulation) will not be suitable in WDM operation. External modulation (discussed next) is used to reduce the effect of chirp due to lasing effect [8].

1.3.1.1.6 Modulation: Direct and External

The type of laser diode as a source provides expected quality of generated laser light; however, in order to make laser source useful in data transmission, modulation[8] technique is used. Modulation is achieved by coupling data to the laser source in two common ways: direct or external modulation.

The simplest and most widely used is the on-off-keying (OOK) modulation scheme, which is direct modulation; laser current is considered as the input signal turning the signal ON or OFF by coupling the data stream to the drive current of the laser source [7]. This OOK modulation is referred to also as intensity modulation (IM), which has a drawback in terms of bandwidth restriction due to diodes relaxation frequency and chirp, as was discussed in previously. Chirp is a limiting factor in the DFB laser where it is not recommended in WDM implementation, especially with high channels count [8].

External modulation is based on leaving the diode radiating continuously and the laser current source being kept constant with an external device used to modulate the laser light source. External modulation covers for the shortcomings of the direct or IM, namely the bandwidth restriction and chirp.

External modulation implementation is the proposed PON security enhancement in this dissertation. In addition, external modulation provides stability of the source and avoids the nonlinearity of excessive chirp in DWDM.

[8] Modulation is defined as superimposing a data stream onto a carrier signal by altering one of the virtues of the carrier signal with respect to a change in the data stream.

1.3.1.1.7 Digital Data Format

Digital data transmitted on fiber lines carry modulation of the optical carrier (at a certain wavelength) by the modulation technique used. For example, amplitude shift keying (ASK), frequency shift keying (FSK), or phase shift keying (PSK) are some of the modulation techniques; however, in optical systems, ASK with the external modulation technique is widely used since light is non coherent and phase information is not used [65].

A single bit 1 can be represented in two different formats. The simplest way is to provide light for the duration of a "one" bit time and turn the light off for the duration of a "zero" bit time. This technique is known as non-return to zero (NRZ) modulation. The other way is to turn the light on for a one bit, but to turn it off before the bit time is over, allowing the signal to go dark, and this is called return to zero (RZ).

The main advantage of NRZ representation of a bit is that the bandwidth associated with this format is smaller than the RZ format by a factor of 2. However, the choice for NRZ is not always the right choice because of the dispersive and nonlinear effects that can distort the optical pulses during transmissions [25]. A long string of 1 bits can make it difficult to extract the clock information, and because the NRZ format occupies the entire time slot for a bit, problems can arise from pulses broadening during the transmission online, which make the system vulnerable to inter symbol interference (ISI).

The duration of the NRZ bit can be represented by T_b, which can be expressed in terms of data rate B as $T_b = 1/B$. In the RZ format, the pulse duration is actually shorter than the allocated bit time slot, and when there are two or more 1's, the pulses are spaced apart by T_b. It is common to use a 50% duty cycle[9], but other duty cycles can be chosen to meet system design goals [8].

1.3.2 Optical Laser Receivers

Another critical element of an optical network is the optical receiver, which must tune and detect one out of all the wavelengths incoming on the shared fiber line. The detection is achieved by coherent or direct (non-coherent) detection methods. Coherent detection technique uses phase information of the signal and requires a local oscillator and the direct

[9] Duty cycle: In RZ system, the ratio of the time allocated for the pulse (T_p) over the total time for the bit (T_b) is referred to as the duty cycle = T_p/T_b.

detection of incoming signal converted to electrical signal by a PN diode. Coherent detection provides better selectivity when considering the background noise but adds hardware complexity and cost. For PON, direct detection is the preferred choice due to its lower cost and ease of implementation.

Because a photo diode will be the basis for detection, which itself detects broad band of wavelengths, the photodiode must be preceded by a wavelength filter to limit the range of detection to wavelengths of interest; therefore, tunable optical filters include interferometer filters, filters based on mode coupling, filters based on resonant amplification, and grating based filters.

1.3.2.1 Optical Filters

Similar to the case of laser transmitters, fast and broad tuning ranges are desired in the laser receiver module. The laser receiver module will be operating in the 1550 nm band with fast tuning to support the wavelength hopping. In addition, stability of those two components in terms of the important performance parameters needs to be determined in order to realize the wavelength hopping.

The key limitation to the DWDM system is that the receiving end since laser line widths for single mode lasers are typically less than 1 Å (or 10MHz) as transmitted by the source [28]. There are many filtering technologies and different types of tunable filters available to support implementation in WDM networks. A tunable optical filter has the ability to track the signal wavelength variation over its operating wavelength range. The tuning of optical filters, similar to laser transmitters, will have the characteristic that the wider you make the tuning range, the slower the tuning time will be. Generally, tunable optical filters from an application point of view can be divided into two main categories [30]:

- Slow-speed tunable, with tuning times up to a few milliseconds, relevant for circuit-switched networks, and
- High-speed tunable, in the microsecond and nanosecond range, relevant for packet- and cell-switching networks.

Some filtering schemes include mechanical tunable filters such as the Fabry–Perot tunable filter, which consists of a single cavity built by two mirrors that, with their movements, form a resonant cavity. The Fabry-Perot filter tunes by changing the distance between the mirrors, i.e., moving one of the mirrors. Because it mechanically moves one lens, the tuning latency is large and therefore it is not ideal for implementation in a fast wavelength hopping WDM network.

On the fast tuning speed side, one filter is the acousto-optical tunable filter (AOTF), which is another method for filter tuning using radio frequency (RF) waves passed through a transducer. A transducer is a piezoelectric crystal that converts sound waves to mechanical movement. The sound waves change the crystal's index of refraction and enables the crystal to act as a grate. By changing RF waves, a single optical wavelength can be chosen to pass through the material. An AOTF controller built, for example, where the switching response is as fast as 6 μs, satisfies the recommendation of Society of Motion Picture and Television Engineers (SMPTE) for video switching [29]. The tuning range for acousto-optic receivers covers the 1300 nm to 1560 nm spectrum with tuning time usually on the order of microseconds, thus making AOTFs eligible for high-speed switching applications [20][30].

Electro-optical tunable filters (EOTF), the other fast tuning type filter, uses crystals whose index of refraction can be changed by electrical current. Electrodes resting in the crystal are used to supply current to the crystal. The current changes the crystal's index of refraction, which in turn allows some wavelengths to pass. The tuning time and tuning range of these types of filters are 10 ns and 16 nm, respectively. Electro-optic filters have low tuning latencies, while acousto-optic filters have a broad tuning range and support multi-wavelength filtering by applying multiple acoustic frequencies [20][30].

1.4 PON and Increasing Demand for Bandwidth

The demand for higher data rate, which requires more bandwidth drives the access networks and local area networks toward the implementation of simultaneous transmissions of many high bit rates channels [31], which can be met via DWDM that provide more capacity for data pumping. However, the medium carrying the multiple wavelengths has physical characteristics that can restrict the performance of WDM system and introduces impairments in the individual channels that can be challenging to system designers.

1.4.1 DWDM in PON

The system capacity depends on many factors including, for example, optical bandwidth, data rate, and channel density. In general, WDM system design must account for many parameters that could degrade the performance of the planned system of the signal in the optical path such as noise and signal distortions. Channel impairment effects can accumulate while signals travel between OLTs and ONUs in PON topology, as shown in Figure 2, which cause significant signal degradation due to fiber line physical characteristics.

The transmission impairments induced by non-ideal physical layer components can be classified into two categories: linear and nonlinear [36]. Some important linear impairments are amplifier noise, polarization mode dispersion (PMD), group velocity dispersion (GVD), component crosstalk, etc.; and some important nonlinear impairments are four-wave mixing (FWM), self-phase modulation (SPM), cross-phase modulation (XPM), scattering, etc.

Linear impairments are independent of signal power. Their effects on end-to-end light path might be estimated from link parameters, and hence could be handled as a constraint [37]. In this dissertation, because the approach for PON security enhancement depends totally on DWDM with small channel spacing (25 GHz), a proof of the concept through a simulation model is included in section 3.2.5 to serve as an investigation tool for impairments and support of feasibility of DWDM implementation in PON.

1.4.1.1 Optical Fiber Cable and Impairment Factors

In a typical PON topology similar to that shown in Figure 2, optical fiber cable and splitter, which is a PSC, are the only two components in the field between both ends of PON. Current technology supports a splitting ratio of the PSC up to N = 64 [35]. The length of fiber cable depends on the data rate (i.e., 1 Gbps) and provides a distance of 20 km [12][13][38][58], which is based on a system design that supports b(P2MP) on optical fiber for a 1Gbps bit error rate (BER) greater than or equal to 10^{-12}. However, new types of fibers operating in C and L bands have technological advances such that it is possible to extend the range much farther. For example, with GPON operation of 2.488 Gbit/s downstream and 1.244 Gbit/s upstream a distance reached of over 135 km was reported [39] giving performance consistent with ITU-T standards.

Attractiveness of PON is associated with having low cost, maintenance free, passive components in the field between both ends of PON. However, physics of light in fiber lines actually plays an important role and determines the performance of optical networks. The different lights from different sources travel in the shared fiber medium at different velocities affected by what is known as the refractive index[10]. Some optical phenomena include reflections, refractions, birefringence, polarization, and dispersion [8]. The important phenomena are the last three: birefringence, polarization, and dispersion.

Birefringence is due to variation of the refractive index as a function of the incident light ray and polarization [8][20] and causes non-polarized rays to be refracted into two orthogonal polarized light rays. Polarization is the basics of light where the electric field (E) and magnetic fields (M) of the light are orthogonal to each other and travel in an orthogonal direction to the direction of both E and M. When light travels and interacts with the medium through which it is traveling it leads to the situation where the E and M are no longer equal in magnitude and direction, known as PMD. The degree of polarization will depend on the angle of incidence where the light ray enters the medium (fiber end), the refraction index, and the scattering profile of the medium itself.

Dispersion on the other hand, is an inherent property that causes spreading of an optical pulse in time domain. PMD management requires that the time-average differential time delay between two orthogonal states of polarization be less than a fraction of the bit duration, T = 1/B, where B is the bit rate [37]. Dispersion effects usually limit 1550 nm transmission distances in metro/provincial networks, which can be approximately +17 ps/nm/km in the 1550 nm region, limiting transmission distances to 80 to 100 km for many transmitters, and the reach can be much shorter for some transmitters such as directly modulated 10 Gb/s lasers [42]. For example, RFC[11] 4054 for optical layer routing provides estimation for newer fibers with a PMD parameter of 0.1 picoseconds per square root of km; the maximum length of the transparent segment (without PMD compensation) is limited to 10000 km and 625 km for bit rates of 10Gb/s and 40Gb/, respectively [40]. In addition, for 10-Gbitls linear transmission, conventional step-index single-mode fiber (SMF) allows for uncompensated

[10] Refractive Index for a particular medium is the ratio of speed of light in vacuum (c_0) to the speed of light in the medium (c_m), c_0/c_m.

[11] RFC: Request for Comments are references that are published by Internet Engineering Task Force (IETF).

distances of 60 km with a 1 dB eye-opening[12] penalty; nonzero dispersion-shifted fiber (NZ-DSF) extends the uncompensated distance by as much as an order of magnitude [41].

The figures above assure that implementation of the new fibers in the local loop in PON should not cause serious problems in terms of non linearities since PON usually are limited to less than 40 km. On the other hand, nonlinear effects are significantly more complex and some parameters will be important when considering DWDM. It was reported in [43] that 40 Gbps was supported for distances up to 80 km by using fiber cable compensation techniques.

In both SMF and NZ-DSF, effects of dispersion and nonlinearity cannot be isolated from one another. Fiber nonlinearities that complicate dispersion compensation can be classified into two categories: the single-channel nonlinear effects, such as SPM and modulation instability (MI); and multichannel nonlinear effects, such as PM, FWM, and stimulated Raman scattering (SRS) [41].

PON architecture has the advantage of not using optical fiber amplifiers on lines between CO and ONUs where amplifiers are a major source of nonlinearities. Nonlinearities also impact BER due to SPM and MI; multi channel nonlinear effects, such as XPM, FWM, and SRS are associated with DWDM [41].

The most common type of fiber used is the SMF, and ITU defines different types of fibers governed by ITU standardization [8]. Fiber requirements of metro/provincial networks are now starting to approach those of long haul networks in some ways as higher bit rates and DWDM systems are deployed [42]. ITU G.655 compliant fiber cables are the most suitable for application in DWDM, which is selected for use in the PON simulation model in section 3.5.1. ITU G.655 supports higher bit rates and longer distances since it is a NZ-DSF, and SMFs has chromatic dispersion that is greater than a non zero value throughout the C band (1500nm). The ITU G.655 based optical fiber reduces the effect of non-linear ties such as FWM, SPM, and XPM and is best suited to operate between 1500 and 1600nm [8].

Long haul optical fiber links that implement DWDM is the major cause of non-linearity due to Kerr effect [44], which includes FWM, SPM, and XPM. The effect of FWM can be

[12] Eye opening is related to the eye pattern diagram used to provide preliminary and initial indication of the quality of the signal, which is made of superimposing the received 011 and 101 digital signals where cross talk and inter-symbols interference can be investigated.

nearly eliminated by managing the fiber dispersion or channel spacing [45]. As the capacity requirement of optical fiber systems increases, channels with narrower channel spacing will be used in WDM systems. As a result, the two dominant nonlinear effects, XPM and FWM become more and more pronounced [47]. Both nonlinear effects introduce intensity fluctuations that are dependent on the neighboring channels.

In principle, impairments generated at the nodes can be bounded by system engineering rules because the node elements can be designed and specified in a uniform manner. This approach is not feasible with PMD and noise because neither can be uniformly specified. Instead, they depend on node spacing and the characteristics of the installed fiber plant, neither of which are likely to be under the system designer's control [40].

1.4.1.1.1 Self-Phase Modulation (SPM)

Self-phase modulation (SPM) arises because the refractive index of the fiber has an intensity dependant component, and this non-linear index causes an induced phase shift proportional to the intensity of the pulse. SPM is caused by variations in optical signal power. It introduces variations in the phase of signal. In phase shift keying systems, these variations may lead to a degradation of the system performance since the receiver relies on the phase information. Additionally, SPM causes spectral broadening of pulses because the variations in a signal's phase results in instantaneous variations of frequency around the signal's central frequency. This may lead to spreading of pulses, thereby, affecting the maximum bit rate.

1.4.1.1.2 Cross-Phase Modulation (XPM)

On the other hand, cross-phase modulation (XPM) is a shift in the phase of a signal. It is caused by a change in the intensity of a signal propagating at different wavelengths. XPM may lead to asymmetric spectral broadening. The combined effect of XPM and SPM may affect pulse shape.

1.4.1.1.3 Four-Wave Mixing (FWM)

FWM is a product of three waves with frequencies $(f_{1,}, f_2, f_3)$ propagating over the same fiber link interacting to give rise to a fourth wave with a frequency defined as $f_4 = (f_{1,} + f_2 - f_3)$, which is a combination of the three waves frequencies. As a result, power from one channel leaks into another channel, causing an increase of BER[13] in addition to inter-channel cross talk.

FWM depends upon channel spacing, power intensity of contributing signals, chromatic dispersion of fiber, fiber length, and refractive index. FWM degrades the SNR and causes cross talk, limits the transmission capacity of the fiber because of the inter-channel cross talk, and is worst when the channels used are an equally spaced WDM system and operating at high power [8][45].

The effect of FWM cross talk is a potential problem in all DWDM systems. This problem has been recently solved by an unequal-spaced-wavelength technique [46]. However, unequal spacing, which is known also as channel detuning, resulted in an increase of bandwidth requirement compared to equally spaced channel allocation [48]. This is due to the constraint of the minimum channel spacing between each channel and that the difference in the channel spacing between any two channels must be assigned to be distinct. As the number of channels increases, the bandwidth for the unequally spaced channel allocation methods increases in proportion.

FWM can be reduced by a nonzero local dispersion, which either reduces the walk-off distance of channel-by-channel nonlinear interactions or increases the phase mismatch for FWM [41]. The FWM effect reaches its maximum effect at the zero-dispersion zone of the fiber cable, but many solutions such as the NZ-DSF [20] have been found to counter this problem.

In [48], a method for channel allocation is proposed to reduce the FWM effect so as to improve WDM system performance without inducing additional cost, in terms of bandwidth, which allows the computation of a channel allocation set to result in an optimal point whereby degradation caused by inter-channel interference and FWM is minimal.

In some applications, optical fiber FWM nonlinear phenomenon is used for wavelength conversion as mentioned in [49] for ring type transport protocols that can be adapted for any dense wavelength-reuse WDM networks.

[13] BER: Bit error rate is a measure of digital channel faithfulness in its ability to transfer digital.

The approach in this dissertation uses published standard wavelengths (channels) from the ITU-T G694.1 wavelength grid [26] with 25 GHz channel spacing. The use of wavelength hopping will minimize the problem associated with equal channels spacing as will be demonstrated in the PON simulation model in section 3.5.2.2 since wavelengths online will be selected according to a code matrix and hopping patterns reduces the impact of FWM.

The impact of the non-linear impairments are seen as a problem for the long haul fiber links (>100 km), however, it can also be a problem in the short hauls where channel spacing and increased power provide an increase to FWM.

1.4.1.2 Optical Network Performance Evaluation Parameters

In order to provide some metrics that will be used in the DWDM simulation model as discussed in section 3.5.1, some performance parameters will be used that are typically used in optical networking technologies as discussed in the following subsections.

1.4.1.2.1 Bit Error Rate (BER)

In section 1.4.1.1.3, it was mentioned that FWM causes power from one channel to leak into another channel, causing an increase of bit error rate (BER). BER is a measure of digital communication system faithfulness and its ability to transport binary data from transmitter to receiver, or the ability of the receiver to provide a good decision in decoding the received bit.

BER quantifies the rate of errors as the probability of an error occurring per transported bit. Typical benchmarks for BER are rates of 10^{-9} and 10^{-12} [8]. As guidance, [12] provides an average transmission quality that should have a very low bit error rate of less than 10^{-9} across the entire PON. ITU-T recommendation G.957 standard defines the objective error rate required for optical components to be better than 10^{-10}. In summary, BER can be used to describe system performance [98] in addition to a related Q factor that is discussed in the next section.

1.4.1.2.2 Q Factor

In addition to BER, Q factor is a parameter that provides a qualitative description of the receiver performance because of its function to optical signal to noise ration (OSNR), which is a measurable quantity. The logarithmic value of Q is related to OSNR provided in (1) below.

$$Q_{dB} = 20\log\sqrt{OSNR}\sqrt{B_o / B_c} \tag{1}$$

The B_o/B_c provides the ratio of optical bandwidth (B_o) to the end device (i.e., photo detector) to the electrical bandwidth (B_c) of the receiver filter. A higher Q factor is an indication of better quality of the optical signal, because with control of minimum OSNR in the network design process, the Q factor can be decided from (1) where a specific BER can be obtained in accordance to the complementary error function (*erfc*[14]) relation in (2) below [8].

$$BER = \frac{1}{2} erfc(\frac{Q}{\sqrt{2}}) \tag{2}$$

As can be seen from OSNR in (1), the Q factor is related to analog signals, and it gives a measure of the propagation impairments caused by optical noise, non-linear effects, polarization effects, and chromatic dispersion, which is a measure of how noisy a pulse is for diagnostic purposes.

1.4.1.2.3 Eye Pattern

In addition to BER and Q factor discussed in sections 1.4.1.2.1 and 1.4.1.2.2, respectively, the eye pattern is a representation of the top level system performance by superimposing digital signals 010 and 101 in order to check for cross talk and ISI. Eye pattern is used as a quick tool to look for impairments, allows quick verification of signals that meet performance specifications, and is used for evaluating system performance providing visual depiction of the waveform being transmitted. Figure 16 provides an illustration of eye pattern, where wider opening of the eye corresponds to minimal signal distortion, and accordingly, provides an indication of the signal quality.

[14] The error function is denoted as erf(x); the complementary error function is denoted as erfc(x). Also, erfc(x) = 1 - erf(x). The error function is very closely related to the standard normal distribution function, p (x). It can be obtained as follows: erf(x) = 2 * p(x * sqrt(2)) - 1 and erfc(x) = 2 * (1 - p (x * sqrt(2))).

In typical modern instrumentation, an eye pattern oscilloscope generates a report that shows what the Q factor number is as opposed to what the "ideal" Q factor is. This will be provided in the simulation model DWDM in PON in section 3.5.1 of this dissertation.

1.4.1.2.4 Forward Error Correction (FEC)

Forward error correction (FEC) is a technique that adds overhead bits to the signal in order to make it easy for receiver detection function, and when implemented, much lower rates of BER can be accepted. Such a technique removes the dependence on controlling the optical phase in the system.

The fact is that FEC is still expensive, and if the system meets the 10^{-9} BER at 1 Gb/s per user there is no need for FEC, it is preferable not to implement FEC in PON in order to meet the low cost of PON [3].

1.5 Dissertation Organization

The rest of this dissertation organized as follows:

In Chapter 2, an overview of security vulnerabilities in optical networks is provided with a focus on the PON, in addition to a review of current practices of protection as covered by existing PON standards. The chapter discusses the need for PON network security level with consideration of the cost of implementation, and includes comments on previous work and a literature review about security in optical networks. The chapter provides motivation for the work proposed in this dissertation and lists its main contributions.

Chapter 3 provides an introduction to the novel conceptual approach for security enhancement in PON based on diffusion of transmitted Ethernet frames/packets[15] over several wavelengths (channels) in a hopping mode as part of protection at the network security[16] level. The proposed solution in this dissertation uses slow wavelength hopping, which is suitable for implementation at network security as opposed to applications security,

[15] In this dissertation, the Ethernet frames is the fixed length units representing transmitted/received data per wavelength hop; also fixed length packet across the network can be used in the data diffusion process in the same manner as the Ethernet frames.

[16] The term network security means that protection provided at the physical and data link layers of the OSI model, while applications security refers to protection (i.e., cryptography) at the upper layers of the OSI model.

or simply implementation in data link and physical layers of a typical Open Systems Interconnect (OSI) model defined by International Standards Organization (ISO) for communication networks.

The challenges for implementation of DWDM in relation to small channel spacing and fiber non linearities and impairment are included. A proof of the concept using OptSim™ 4.5-simulation software is provided to support rationale and soundness to the technical approach in the proposed solution. The chapter ends with some implementation and deployment recommendations.

In Chapter 4, security analysis is used to provide a proof and illustrates the robustness of the proposed solution to security enhancement in PON. Some assumptions are made about the background of attackers and the proposed solution for security enhancement subjected to brute force type of attack against an eavesdropper, and analyzing the probability of capturing the correct order of wavelength sequences assigned to a specific ONU. In addition, reverse analysis is used in which the attacker knows captured traffic with synchronization and the task is to analyze the captured wavelength on tapped fiber and try to reconstruct matrices used to generate the wavelength sequences. The probabilities of successful reconstruction of matrices derived indicates a level of difficulty to reverse construct such matrices.

In Chapter 5, some concluding remarks are made and potential future research directions identified.

CHAPTER 2: SECURITY VULNERABILITIES OF PON

Passive optical networks (PON) have the potential to meet the bandwidth requirement and be the baseline for the connectivity to homes and businesses However, more and more end users relying on such networks create users' dependency for day-to-day transactions. Such dependency requires security to support the privacy and confidentiality of users. The ITU-T standard X.805 associates privacy with the identity of users and their online activities such as purchasing habits, Internet sites visited, etc., while confidentiality relating to the protection of the data against unauthorized access to data contents.

Encryption in PON provides security for data, however, the nature of B&S traffic makes the data available at each ONU, which potentially have the capability to operate in a promiscuous mode and pick up others' ONU traffic (plain or encrypted), having time for eavesdropping without even being detected.

In Ethernet traffic, encryption usually covers the payload of the traffic, and Ethernet-based networks are popular due to the ease of implementation and cost. However, security has never been a strong part of Ethernet networks [15]. For example, having the Ethernet frames online with DA and SA in plain sight violates the privacy of the users' online behaviors. In addition, the sophistication of attackers and tools is where the privacy of communication against eavesdroppers will be a major problem, especially in access networks that are based on B&S types of traffic. This chapter addresses the vulnerabilities of optical networks in general, with some focus on PON that use B&S traffic.

2.1 Types of Attacks on Passive Optical Networks

Access networks, as part of local area networks (LANs), have become a major tool for many organizations in meeting data processing and data communication needs [51], and the role of access networks will increase as higher bandwidth is provided through PON-based networks such as FFTH, FFTB, and FFTC where the focus will need to shift to security.

Security threat is a potential violation of security, which can be considered as active or passive threats. Active threats are those cases in which the state of the systems are changed, while passive threats are related to unauthorized disclosure of information without changing the state of the system. Passive threats, for example, include eavesdropping activities to capture messages on line (whether clear or encrypted), while active threats can be in several forms such as masquerading as an authorized entity and denial of service.

Several theoretical methods for detecting intentional attacks upon the infrastructure of an all-optical network were discussed in [52], which also listed the categorization of attacks into six areas based on the goal of the attacker: (1) traffic analysis, (2) eavesdropping, (3) data delay, (4) service denial, (5) quality of service (QoS) degradation, and (6) spoofing.

Prior to the use of LANs, most processing and communications were centralized and the information and control were centralized as well. Now LANs logically and physically extend data processing and communication facilities across the organization, and security services that protect the data, processing, and communication facilities must also be distributed throughout the LAN [51]. For example, sending sensitive files that are protected with stringent access controls on one system over a LAN to another system that has no access control protection defeats the efforts made on the first system. Therefore, basic security may necessitate including two requirements, secrecy and authenticity [53].

Secrecy can be divided into two types: ephemeral secrecy, which means preventing an unauthorized user from receiving the transmitted data, and long-time secrecy, which is usually protected by complex cryptography. Cryptography is part of semantic security, which is the protection of the meaning of the data even when an attacker has access to the received stream [54].

In general, the security policy for the organization needs to be in place by upper management, and secure architecture in the network should provide methods and techniques that can be used to prevent or lessen the impact of the above threats [55]. This dissertation focuses on the concept as stated here where security enhancement in the PON plan is to provide protection and make it difficult for an eavesdropper to collect good samples that can be used for cryptanalysis. Other security measures need to be in place depending on the individual's or organization's security needs.

Authorization and access control with the proposed security enhancement in PON provides protection against disclosure of information, theft of service, and protection against unauthorized access. Additional security measures need to be available for use in PON such as the process of limiting access to system resources and allowing only authorized users, programs, processes, or other systems to access the OLT since it is the most vital part and needs to be protected accordingly.

The network//information security should provide confidence in the information and services available on the network and protect access to unauthorized users. This is of great concern to customers especially when the medium is shared among many users and the need arises for providing security at the network level, which is the focus of this dissertation: the prevention of eavesdropping as a countermeasure in PON. An assumption is made that threats are coming from sophisticated hackers who can be outsiders or an insiders to the organization.

2.1.1 Eavesdropping

The downstream traffic from OLTs to ONUs in PON, as specified in [12] and [13] is characterized as a B&S transmission type on a single wavelength, which means that downstream traffic will be available at all ONUs. Selection by an ONU is based on the time slot, and usually the DA of the Ethernet frame can be used after selection by the ONU. Potential tapping by an outsider to the fiber links network is an allocated responsibility of the operation, administrative, and maintenance (OAM) protocol of the network. In a typical network, shared medium security concerns are minimized because users belong to a single administrative domain and are subject to the same set of policies. However, the situation is different, as illustrated in Figure 6, where several locations on the networks are vulnerable to tapping/ eavesdropping. The tapping can be internal or external to the network, and it is assumed that with the external tapping the OAM does not detect the drop in signal level. Internal tapping into the network can be simply one or more nodes (ONUs) operating in a promiscuous mode, which presents a higher threat in terms of passive attacks than outsider tapping [53]. The danger from an ONU eavesdropping on data transfer that belongs to another ONU arises from the difficulty of detecting their passive attacks especially when they have the time available to monitor and collect data without being detected, which makes it difficult to ensure PON security and guarantee subscriber privacy.

Security must be provided as a mechanism to control subscribers' access to the infrastructure and prevent ONUs from receiving traffic other than what is intended for its reception. In LANs, lack of privacy that results from a subscriber's susceptibility to eavesdropping by neighbors is considered higher in value than susceptibility of the service provider to theft-of-services by attackers and can jeopardize the success of the future Fiber-To-The-Home (FTTH) concept.

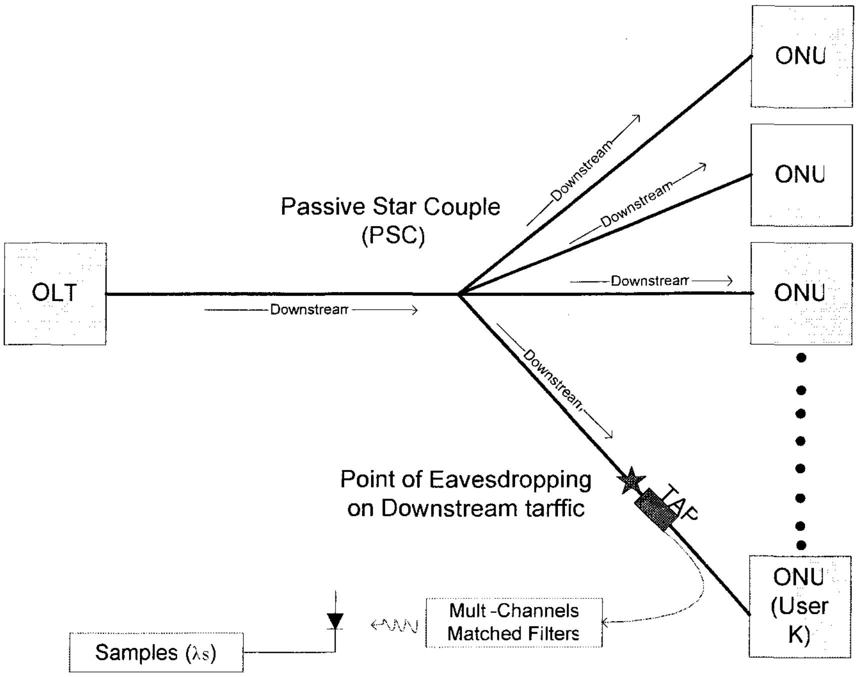

Figure 6: Typical PON topology with possible points of attacks on network

2.1.2 Impersonation

The IEEE 802.3ah standard in [13] includes downstream transmission with a P2MP discovery process, which is a process by which an OLT finds a newly attached and active ONU in the P2MP network, and the OLT and ONU exchange registration information [13]. As was discussed in section 1.2.2, OLT sends a GATE flagged for discovery. GATE is a message by which the permission to transmit at a specific time and for a specific duration are granted to a node (ONU) by the master OLT. Since the process of registration of nodes (ONUs) with an OLT is standard procedure, and the OLT assigns the ONU IDs during the discovery period, for an attacker, all that is needed is a MAC address and it can masquerade as another ONU by transferring the wrong registration frame to an OLT [57]. In addition, an attacker can get access to privileged data and network resources, and it is possible that some ONUs can take the discovery period of an OLT and hijack the identity of another ONU.

2.1.3 Denial of Service

Since ONUs share the capacity of the network in the upstream data flow, the OLT assigns the bandwidth to ONUs, and one non cooperating ONU can maliciously generate a large amount of traffic intentionally [57] depriving other ONUs from the bandwidth allocation.

2.2 Current Security Schemes in Passive Optical Networks

PON, in general, are multicast in the downstream direction, and the need for protection is necessary. A protection recommended in the ITU-T standard in [12] is in the form of churning, while the standard in [13] uses Ethernet (EPON) where security has never been a strong part of Ethernet networks [15], and the IEEE standard in [13] treated encryption and authentication as a scope outside the standard.

Churning uses 8-bit key length to provide "the necessary function of data scrambling" and to offer "protection for data confidentiality." The encryption provides a tunnel communication link in the upstream direction between the OLT and ONUs. According to [56], churning as applied in the ITU-T standard in [12] to cells is at the transmission convergence (TC) layer. The standard actually provides the recommendation that if churning is not enough for a security requirement of a provided service, a suitable encryption mechanism should be employed at a higher layer than the TC layer to provide data scrambling. No recommendation for key distribution is provided.

Unfortunately, churning has many critical, even fatal, flaws, and it is trivial to defeat It was shown in [56] that it is easy to carry on passive attacks on churning, and it is possible to break the 8-bit key with an exhaustive key search.

PON users are at high risk of having their presumed private communications exposed to adversaries even with employing other security techniques—secure sockets layer (SSL) encryption, which may still inadvertently disclose information such as the identity of Web servers with which they communicate [56].

For EPON in the IEEE 802.3ah standard, it is mentioned in [15] that encryption and decryption may be implemented at the physical layer, data link layer, or in higher layers. Implementing encryption above the MAC sub-layer will encrypt the MAC frame payload only, and leave headers in plain text [15], which prevents malicious ONUs from reading the payload, but they may still learn other ONUs MAC addresses such that privacy is vulnerable. In addition, it was recommended in [15] to include an alternative method for encryption to be implemented below the MAC layer, where encryption covers the entire bit stream, including the frame headers and FCS. This will require the receiving end to decrypt the data before passing it to MAC for verification.

IEEE 802.3ah standard in [13] does not cover message authentication for upstream traffic, which involves authentication of data origin to have assurance about the identity of the party that originated the message. OLTs have no means to verify that the message received and presumably created by ONU A for example did indeed originate from ONU A. This is a threat, which can be used in masquerading (authentication) as mentioned in section 2.1.2.

In general, EPON needs strong security services of authentication, confidentiality, and access control, and there is a need for an authentication and key exchange protocol preferably using a public key mechanism [56]. Any security protocol in PON MAC layers reduces the overhead of security service, and authentication and ONU authentication can be performed separately for efficient key management and strong authentication service.

The major problem that encryption addresses is protection with various degrees of sophistication and complexity in order to make it difficult to deduce the code against time. It is known that the processing speed of computational resources are becoming available in the market, defeating simple encryption such as churning in the ITU-T standard in [12] is well within the capabilities of would-be eavesdroppers today, and PON sniffer tools could easily incorporate methods for automated real-time cryptanalysis of churning with essentially no performance impact [56].

In cryptography discussed above, the assumption is made that an attacker is able to get a sample of encrypted data, and the focus is to provide various degrees of fortification against crypto analysis. Encryption alone will not be sufficient for protection, and it needs to be supplemented by some network mechanism that provides difficulty in collecting a good sample. In addition, higher protection must be provided by making it difficult to trace the various segments of the message that are distributed among several wavelengths during transmission between the OLT and ONUs as shown in Figure 2. This is the focus of this dissertation where security enhancement is provided via the wavelength hopping techniques.

2.3 Literature Review for Other Protection Methods in Optical Networks

In the literature, several technical papers and research reports are available that discuss different approaches to providing security (with or without encryption) to optical networks, but not specific to PON. The majority of the papers focused on using OCDMA as an access scheme to the network where the objectives have been to provide higher cardinality (number of nodes on the network), but not focused on security.

OCDMA is considered to potentially provide both confidentiality and availability protection by offering some degree of jamming resistance using the OCDMA coding [68]. OCDMA is based on optical orthogonal coding (OOC); for example, starting with a single bit and using time spreading in one dimension coding (1-D), the single bit is divided into several chips (T_c) in the time domain as shown in Figure 7 where the single bit period $T_b = nT_c$.

The codeword (i.e., signature sequence) is multiplied with signal bit sequences to each uniquely distinct different user. The weight w is expressed as the number of 1's in n chips. The single wavelength is selected when $w = 1$, and no wave is selected when w = 0 during the bit duration.

The drawback of 1-D OOC is that it suffers from low cardinality (Φ) and increasing n and w impacts bandwidth [46][65][66]. An extension to two dimensional (2-D) adds more wavelengths, and in this case, every single chip in Figure 7 represented by different wavelength from several wavelengths is available for hopping.

The extension requires orthogonal codes, OOCs, in order to avoid multiple access interference (MAI). Unlike time in TDMA or WDMA, OOC is attractive because it offers asynchronous multiple access and is capable of realizing access and routing operations in a common channel without optical switches in addition to allowing flexible bandwidth assignment. Time-spreading/wavelength-hopping (TS/WH) OCDMA, utilizing both time and wavelength domain (2-D) encoding/decoding can provide more flexible codes and greater capacity than two schemes utilizing the time or wavelength domain coding.

OCDMA per bit operation is considered immature technology as compared to WDM primarily due to the difficulties in the generation, transmission, reception, and processing of ultra short pulses [60][63]. Other drawbacks are that the current state of technology for laser transmitters and filters do not support high data rates operation at bit level and total weight w in a code word could be detected as the energy level [68]. Wavelength hopping per chip duration (T_c) at bit level with data rate B requires $B\ T_c$ switching speed. For B = 10 Gbps data rate, this will impose restrictions on T_c where currently technology does not support fast tunable components with good tuning range.

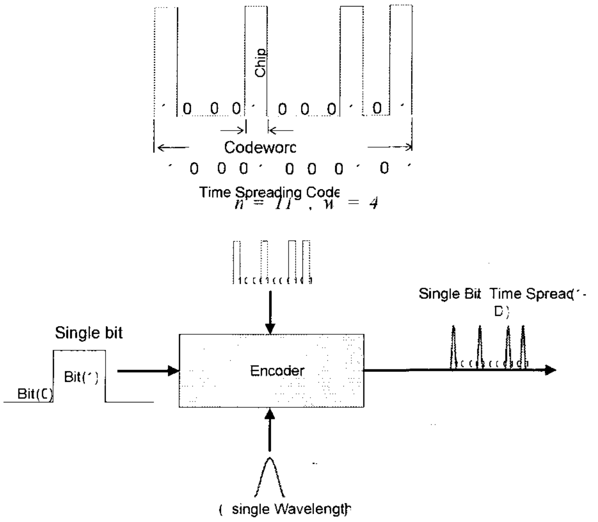

Figure 7: Code word with 11 bits and weight 4 used to represent a single bit.

Therefore, the proposed security enhancement in this dissertation will use a wider duration that covers the transmission of a complete Ethernet frame/packet designated as T_w, and $T_w >> T_c$ in time domain.

In [60], a proposal for a coding scheme directed toward providing security at the physical layer of optical networks such as backbone networks was provided. The 10 Gbps data stream encryption uses both wavelength and time domains. The technique consists of breaking the data stream into frames of N bits by M wavelengths (bit level operation). Each frame contains N x M elements representing unique time-wavelength position. Advanced Encryption Standard (AES) is implemented in counter mode to control hardware switches, and the coding scheme is based on the random permutation of the elements for each time frame. This means both the order of the bits in a stream and the wavelength in which it is transmitted may change.

The approach is based on using a switching matrix (16X16) in the active mode to achieve the permutation process, and could suffer scalability problems for higher size switching matrices. In addition, using encryption techniques via hardware implementation makes the system more rigid for future growth and changes since this will affect multiplexers, demultiplexers, and operation of switches. The proposed security scheme in [60] did not address different security levels that can coexist in the same network.

Another scheme for reduction of MAI, proposed in [61], is based on using modified pseudorandom noise (PN) coded fiber Bragg gratings with bipolar OCDMA decoders, based on having the same number of 1's and 0's to eliminate the MAI, but the proposed solution did not address the security aspect of the system.

A mix of WDMA and TDMA was proposed in [62] for providing MAC. The scheme is based on using WDM-based PON, and combining wavelength routing and power splitting in a single PON to upgrade network bandwidth and decrease accessing cost. The proposed solution in [62] was intended to solve the access scheme by ONUs in the shared bandwidth and was not focused on the security of PON.

A different approach to all-fiber fast optical frequency-hop code division multiple access (FFH-CDMA) for high-bandwidth communications was proposed in [67]. This approach does not require an optical frequency synthesizer, allowing high communication bit rates, where transmission rate of 500 Mb/s per user is supported in a system with up to 30 simultaneous users at 10^{-9} bit error rate. This is a moderate rate and does not support the individual user need in the future, which is expected to be at least 1 Gbps.

A different technique to provide security to a WDM network is discussed in [64] specific to a B&S PSC network that has N users (nodes) sharing K data channels, and $K \leq N$. The approach is based on using a fixed or tunable transmitter for each user in N and each has a receiver under a centralized control (i.e., by CO). Using a challenge-response that can be integrated in a MAC layer, it provides security by requiring every user on the network who is not scheduled to receive data to tune into a channel that does not contain sensitive data. This implies that MAC can dictate when a node is authorized to listen/transmit.

The mechanism of control in [64] requires each node to have two channels, one used for normal data and the other channel used to tune or detune the node externally based on when the node is permitted to receive data. The proposed solution in [64] did not include the assumption that a node can add supplementary receivers that can cover all the other wavelengths in the WDM grid which of course, would not be under the control of the MAC layer in this situation.

In summary, the majority of papers and research projects focused on increasing cardinality in access networks, with minimal focus on security assuming that cryptography alone will provide sufficient security.

2.4 Motivations

The two major questions that face any novel idea for providing security to PON are related to the need of security and the cost of implementation, as discussed in the following two sections.

2.4.1 The Need for Secure Passive Optical Networks

Considering the increasing demand for bandwidth discussed in Chapter 1 and illustrated by the trend shown in Figure 1, it is expected that dependency on access networks by business and residential users alike is becoming an unpleasant fact. PON are seen as the candidate to be deployed in future access networks due their capability of providing the required bandwidth per user in Gbps range and their ability to extend service distance to approximately 50 km using passive components between the extreme ends of the network that support low cost and low maintainability in the field.

However, such dependency on access networks creates a question of trust in the network for daily transactions that can be financial, personal, multimedia, sharing of large files, and multimedia services especially in a shared medium such as the PON topology in Figure 2. In addition, current standards such as IEEE 802.3ah provide privacy in the form of encryption for downstream frames/packets and not for upstream traffic where the privacy is violated. The same can be said for ITU-T G983.1/984.1 standards, which lack some strong privacy needs as discussed in section 2.2. With various types of attacks, the sophistication of attackers and their tools, and higher processing speed computers, the need arises for stronger authentication of the source and destination; all indicate that security is risk management, and needs to be addressed at the network level.

2.4.2 Cost vs. Value of Security in Passive Optical Networks

Basic security measures can be thought of as discouraging crime by making it significantly more difficult to achieve. Many factors play major roles when investing in secure networks and risk vs. cost is at the top of the list. Higher security level is always associated with higher cost, and justification for cost can be based on the basic rule that the security level and measures need to be in accordance with the assets being protected.

Security is valued by individuals or organizations in different ways. For example, for individual subscribers and residential entities, cost is related directly to how much they are willing to pay for a subscription service that protects their privacy, while the security needs of a financial institution are different from those demanded by government and military organizations. The value of data against time is another factor that needs to be considered in the cost factor.

The criteria for evidence of a secure system can be established similar to the classification discussed in [69]:

- *Computationally Secure*: if it requires a sufficiently large amount of computational resources, assets, and skills applied over a sufficiently long time, to break the code.
- *Provable Security*: This approach is concerned with reduction of security level to be considered difficult to solve relative to some other problem (i.e NP-Complete) and does not provide a proof for absolute security.
- *Unconditionally Secure:* This implies that the code cannot be broken, even with infinite computational recourses, skills, and assets (no upper bound is placed).

There must be a balance between security, cost, and usability. Though security must be a prime design consideration, it is not necessarily the overriding one, and benefits must be weighed against costs to achieve a balanced, cost-effective system [70].

The goal is to have cost effective safeguards that reduce risk to an acceptable level, since there is no absolute security in real life. Even though security is a factor in PON implementation success, cost is the major factor. Some cost can be shared such as the components at the CO, but the cost of components located at the individual ONUs on the customer's premises will depend largely on the capability of those ONUs and the importance of security to those customers.

Cost to residential users is usually driven to be extremely low to the end user in order to enable the service provider to have a large subscriber base. Low cost requirements for residential users drive the quality of components to be suboptimal. This necessitates that the downstream receiver and upstream modulator be inexpensive. This reality affects the proposed approach for security enhancement in this dissertation, and the rule for justification of investment in implementation follows organization security policy, which includes the organization's basic commitment to information security.

2.5 Dissertation Contributions

The contributions of the proposed security enhancement in this dissertation cover several different areas. One of the major contributions is a network security level scheme based on a slow wavelength hopping technique that is used in the diffusion process of data frames (or packets) into several available wavelengths in a hopping mode. The designation is slow wavelength hopping because several data bits are transmitted on the same frequency as compared to the fast wavelength hopping where a single data bit is transmitted on several frequencies (chips). The wavelength sequences generated by the proposed solution have a sequence order that is unique to each wavelength sequence and orthogonal to all other sequences in the system.

Current literature is full of research papers and reports that dealt with (OCDMA as an access scheme and its ability to handle security at bit level operation in fast wavelength hopping mode of operation. However, the state of technology of optical components (i.e., laser transmitters and filters) is not mature enough to support OCDMA in light of the high data rates in Gbps per subscriber, which requires optical components to support high switching speed [63][76][82][83]. Additional problems include cumulative shot noise and optical beat noise as the major physical channel impairments that limit the performance of OCDMA [3]. The additive noise power is composed of the relative intensity noise power in addition to shot noise power, receiver thermal noise power, and optical amplifier noise power [84]. Shot noise builds as the square root of the received optical power, proportional to the number of users. Optical beat noise can be canceled through clever control of the optical phase coherence, and a combination of OCDMA with FEC may dramatically improve the performance. However, it is expensive and impractical to implement FEC in an electrical domain at very high speed [3].

The approach in this dissertation is built on slow wavelength hopping that operates at the frame/packet transmission duration, which can be easily accommodated with existing optical components technology.

Earlier work on WDM and OCDMA in optical networking dealt with solving the access scheme and the objective always has been increasing the number of subscribers (nodes) on a network. To the best of my knowledge, no other approach discusses the implementation of slow wavelength hopping in PON or using the wavelength grids and code matrices as security keys as a viable approach to meeting security needs of future access networks such as PON. The network security level (as opposed to applications security) in PON is not addressed properly in the literature, and it was left to applications security[17] in the world of semantic security (cryptography) to provide security of data.

The important contribution in this dissertation is the introduction of a set of secure keys outside the world of cryptography that supports network security level. For example, the ITU-T G694.1 wavelength grid is arranged in a matrix, and each arrangement of wavelengths within the matrix uses a secret key in the wavelength hopping operation. The different arrangements of wavelengths within the wavelengths grid matrix have enough keys to

[17] Applications security means that protection is provided at upper layers (above thedata link layer) in the OSI model

support hundreds of years of operation based on an hourly change of keys before any key is reused.

The second set of keys is related to multiple assignments of wavelength sequences that are orthogonal with all other available sequences for the network. Each wavelength sequence is generated via mapping of orthogonal code matrices and wavelength grid matrices, and the assignment via allocation (not necessarily equally distributed) of wavelength sequences to each ONU is based on their security level.

As a derivative of the multiple assignments of wavelength sequences, the third key of implementation is the sequential order of wavelength sequences cycling for a specific ONU, which can be in any order of the factorial number of the assigned sequences. Three keys are available to enhance security at the network level, applicable in the data link and physical layer of OSI mode, thus fortifying the security of PON against eavesdroppers by making it difficult to track the wavelength sequences specific to the ONU.

The contribution of this dissertation is a novel technique that will support the security needs at the network level of future optical access networks that are based onPON. The approach requires the use of cryptography at lower layers as part of the security scheme whereby the encryption needs to be transparent to the end user and should not affect the cryptography in upper layers.

CHAPTER 3: SECURITY ENHANCEMENT IN PON

3.1 Conceptual Approach to Security Enhancement in PON

The PON security enhancement, which is referred to also as the "proposed solution," has the objective of making it very difficult for an eavesdropper to collect sample data that can be useful in cryptanalysis or to trace to a specific ONU's traffic on a shared fiber link based on the use of generic PON architecture similar to that in Figure 2. It is assumed that tailoring the OLT and ONUs operation requires tunable laser transmitters and filters across C and L bands, in addition to the associated processing algorithm to enable wavelength sequences generation for hopping schemes. Obviously, it is not feasible for everyone to invent their own systems, and the proposed solution must use established standards as a basis so that the approach will be easier to be accommodated by industry.

There are two matrices that form the core of the wavelength hopping scheme in the proposed solution: wavelength grid matrix W_{mn}^{G} with G being the grid number designation, and code matrix C_{ml}^{y} with y being the designation of the specific code matrix that has its elements take one of two values: 0 or 1. The dimensions of the matrices m & n and m & l are the number of rows and columns in W_{mn}^{xG} and C_{ml}^{y} respectively. The proposed solution is based on an overcolored[18] system in which the restriction placed on the dimensions of both matrices is that number of rows (m) in wavelength matrix W_{mn}^{xG} be equal to or larger than number of rows of code matrix C_{ml}^{y}. In addition, the number of columns (n) in wavelength matrix W_{mn}^{xG} need to be equal to or larger than the number of columns (l) of the code matrix C_{ml}^{y}.

The wavelengths grid ITU-T G694.1 in [26] is used to provide standard channels known in the industry with small channels spacing (i.e., 25 GHz) that are arranged in a wavelength matrix as shown in (5).

The conceptual drawing for the approach to security enhancement in PON is shown in Figure 8, which involves mapping (indexing) between the two matrices, W_{mn}^{xG} wavelength sub grid matrices and code matrices C_{ml}^{y} in accordance with the relation in (3) The sub grid

[18] Overcolored system implies that the number of unique wavelengths (no two wavelengths are identical) in the wavelength matix is equal to or more than the number of elements of the code matrix.

matrices W_{mn}^{xG} matrices are derived from a master network wavelength grid matrix W_{mn}^{G} simply by one complete cycle of columns rotation to generate *n* sub grid matrices (W_{mn}^{xG}).

The mapping operation (or indexing) is a process in which a wavelength from the wavelength sub grid matrix W_{mn}^{xG} is selected only if the corresponding location element of the code matrix C_{ml}^{y} is 1, and no wavelength is selected if the element of the code matrix is 0. The outcome of mapping operation in (3) is a set of unique wavelength sequences (λ_s) each designated by a sequence number *s*.

$$\lambda_s = C_{ml}^{y} \odot W_{mn}^{xG} \tag{3}$$

All sequences (λ_s) are orthogonal to each other, which can be assigned in multiple sequences to each ONU and not necessarily equally distributed among ONUs, but rather based on the security level of each ONU. For example, the classification of the security level can be associated with the number of wavelength sequences assigned to a single ONU.

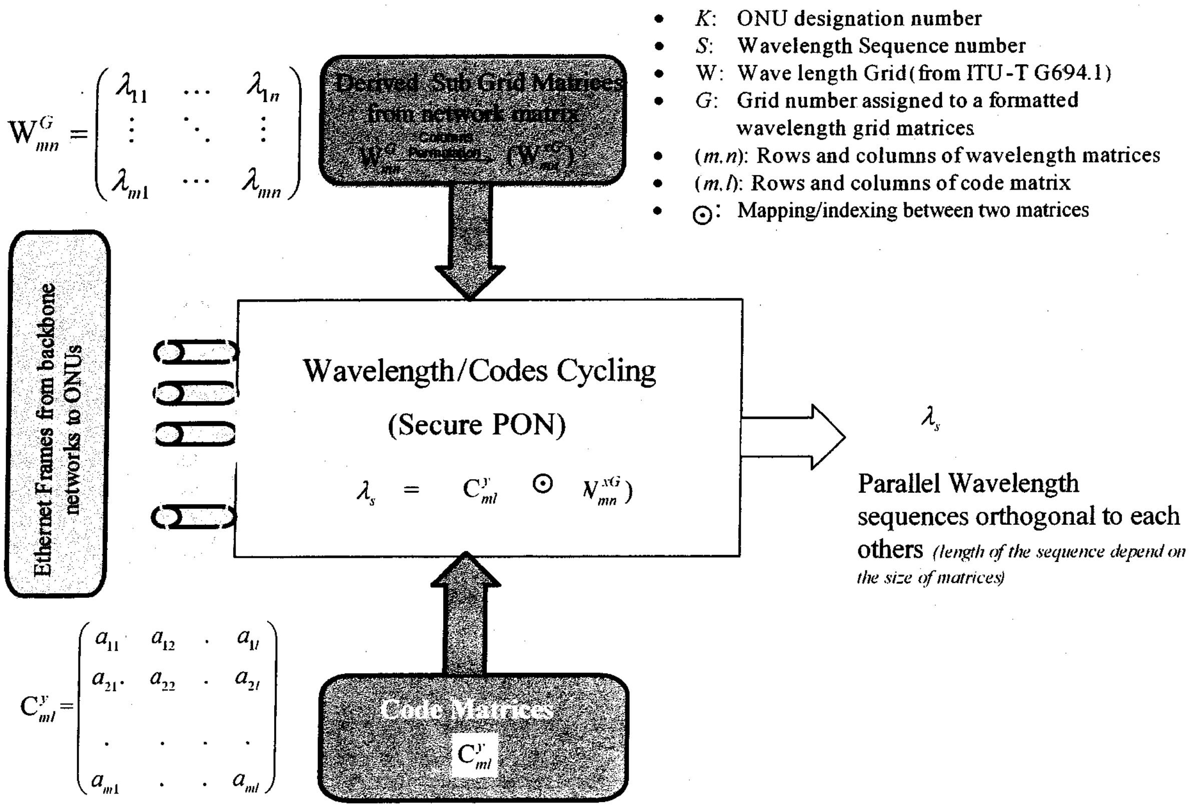
• K: ONU designation number
• S: Wavelength Sequence number
• W: Wave length Grid(from ITU-T G694.1)
• G: Grid number assigned to a formatted wavelength grid matrices
• (m.n): Rows and columns of wavelength matrices
• (m.l): Rows and columns of code matrix
• ⊙: Mapping/indexing between two matrices
$W_{mn}^{G} = \begin{pmatrix} \lambda_{11} & \cdots & \lambda_{1n} \\ \vdots & \ddots & \vdots \\ \lambda_{m1} & \cdots & \lambda_{mn} \end{pmatrix}$
Derived Sub Grid Matrices from network matrix
$W_{mn}^{G} \xrightarrow[\text{Permutation}]{\text{Columns}} (W_{mn}^{xG})$
Ethernet Frames from backbone networks to ONUs
Wavelength/Codes Cycling
(Secure PON)
$\lambda_s = C_{ml}^{y} \odot W_{mn}^{xG})$
λ_s
Parallel Wavelength sequences orthogonal to each others (length of the sequence depend on the size of matrices)
$C_{ml}^{y} = \begin{pmatrix} a_{11} & a_{12} & \cdot & a_{1l} \\ a_{21} & a_{22} & \cdot & a_{2l} \\ \cdot & \cdot & \cdot & \cdot \\ a_{m1} & \cdot & \cdot & a_{ml} \end{pmatrix}$
Code Matrices
C_{ml}^{y}

Figure 8: Conceptual drawing of the proposed security enhancement in PON

In this dissertation, an attacker (eavesdropper) is seen as one who taps into the shared fiber link or simply is one of the ONUs collecting traffic data that belongs to a different ONU on the PON shown in Figure 4. The goals of attackers were discussed in section 2.1, and the attacker's objective used in this dissertation is capturing wavelength sequences generated by (3) for a specific ONU; while learning the content of encrypted data carried by the wavelength sequences is treated as part of cryptanalytic attack, that is outside the scope of this dissertation. The strength of the proposed security enhancement in PON should reside entirely in the difficulty in determining the sequence specific to an ONU and not in the algorithm that is used to generate the wavelength sequence in (3). The wavelength sequences generated by (3) requires that ONUs and OLTs have tunable transmitters and receivers operating in slow hopping mode. This approach compensates for the problems with the technology status and its immaturity to provide high speed switching to different wavelengths as is the case for OCDMA [22].

The proposed solution in this dissertation uses slow wavelength hopping, with duration for a single wavelength being used in time T_w being the same for all wavelengths used in PON to guarantee orthogonality and synchronization purposes, which is much wider ($T_w >> T_c$) than the duration for the bit level shown in Figure 7. Wide duration $T_c << T_w$ accommodates transmission of the complete Ethernet frame/packet, and tuning time of resources (i.e., laser transmitters and filters) is expressed as $T_\tau << T_w$, which is a factor that needs to be considered in the context of timing to accommodate tuning speed and ranges of optical components.

The tuning strategy of laser components to be in place for the proposed solution requires each ONU to have a minimum of two laser transmitters and two filters. Figure 9 illustrates the tuning strategy for a typical single wavelength sequence (λ_s) generated by (3), which shows the component's wavelengths (λ^k_{mn}) in the wavelength sequence (λ_s) that belongs to ONU 13 (k = 13), and mn identifies the location in row and column of the wavelength sub grid matrix (W^{xG}_{mn}). Tuning in Figure 9 shows that when the laser transmitter (or filter) is being used at any instant, the other transmitter (or filter) will start tuning and getting ready for the next wavelength in the sequence. Each wavelength sequence (λ_s) is considered as signature associated that can be assigned to an ONU where all sequences are guaranteed by the strength of orthogonality of code matrices C_{ml}^{y}.

The wavelength sequence (λ_s) is externally (indirectly) modulated using NRZ bits due to their better utilization of bandwidth as discussed in section 1.3.1.7 Modulation covers a completely encrypted standard length Ethernet frame/packet (including SA and DA), and the same fixed length of packets is used across the PON. Fixed and equal length Ethernet frame/packets provide guarantee orthogonal wavelength sequences operation. The ITU recommendations G 983.1 standard in [12] already has a packet size limited to 57 bytes [62], however IEEE 802.3 ah EPON is required to use fixed length Ethernet frames, which is not currently in the IEEE standard 802.3ah [13].

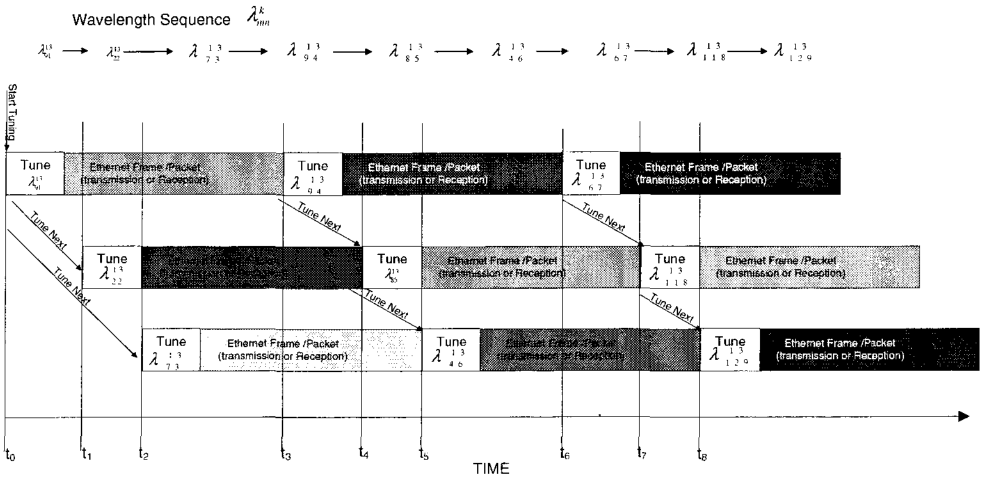
Wavelength Sequence λ_{mn}^{k}
$\lambda_{91}^{13} \rightarrow \lambda_{22}^{13} \rightarrow \lambda_{73}^{13} \rightarrow \lambda_{94}^{13} \rightarrow \lambda_{85}^{13} \rightarrow \lambda_{46}^{13} \rightarrow \lambda_{67}^{13} \rightarrow \lambda_{118}^{13} \rightarrow \lambda_{129}^{13}$
Start Tuning
Tune λ_{91}^{13}
Ethernet Frame /Packet (transmission or Reception)
Tune λ_{94}^{13}
Ethernet Frame /Packet (transmission or Reception)
Tune λ_{67}^{13}
Ethernet Frame /Packet (transmission or Reception)
Tune Next
Tune λ_{22}^{13}
Tune λ_{85}^{13}
Ethernet Frame /Packet (transmission or Reception)
Tune λ_{118}^{13}
Ethernet Frame /Packet (transmission or Reception)
Tune λ_{73}^{13}
Ethernet Frame /Packet (transmission or Reception)
Tune λ_{46}^{13}
Tune λ_{129}^{13}
Ethernet Frame /Packet (transmission or Reception)
t_0
t_1
t_2
t_3
t_4
t_5
t_6
t_7
t_8
TIME

Figure 9: Tuning strategy of laser (transmitters/filters) resources

3.2 Master Wavelength Grid Matrix W_{mn}^{G}

The master wavelength matrix W_{mn}^{G} is constructed from channels using the ITU-T G.694.1 standard for dense DWDM frequency grid [26] with the total number of wavelengths channels depending on the channel frequency spacing (Δ) used from a center frequency of 193.1 THz as expressed in (4):

$$\lambda = 193.1 + (F) \text{ x } (\Delta) \quad (4)$$

where F can be a positive or negative number including 0 and channel spacing (Δ) can be 12.5 GHz, 25 GHz, 50 GHz, 100 GHZ, or 200GHz. A wavelength matrix W_{mn}^{G} shown in Appendix A is an example of the 25 GHz channel spacing used in this dissertation's simulation model and wavelength sequence generation per (3). All channels are unique, none repeated, and are available for wavelength hopping.

The wavelength grid matrix expressed in (5) is considered the master wavelength matrix built from those wavelengths provided by (4), and in this dissertation, the number of rows (m) will be the same as that for the code matrix C_{ml}^{y}, while the columns n can have an equal or greater number of columns ($n \geq l$) than the code matrix C_{ml}^{y}.

$$W_{mn}^{G} = \begin{pmatrix} \lambda_{11} & \cdots & \lambda_{1n} \\ \vdots & \ddots & \vdots \\ \lambda_{m1} & \cdots & \lambda_{mn} \end{pmatrix} \tag{5}$$

There are many ways that the wavelengths (channels) generated by (4) can be arranged in the wavelength grid matrix in (5), with each format (arrangement of wavelengths in the matrix) assigned a grid number (G). The maximum number of wavelength grid matrices G_{max} is expressed in (6).

$$\text{Maximum wavelength grids} = G_{max} = (n!)^{m} \tag{6}$$

The limitations on m,n are related to the availability of enough channels that can be practically generated by (4) within C and L bands to form the complete ITU-T G694.1 grid [26]. For example, considering the wavelength grid matrix in Appendix A, 200 channels are available, and only 192 channels are used to fill the matrix in (5) based on m = 12, and n = 16, leaving an extra 8 wavelengths available for use as open channels (no hopping) where the case may not require security.

Applying (6) to the wavelength grid matrix in Appendix A provides $G_{max} = (16!)^{12} = 7.0378 \text{ x } 10^{159}$ wavelength grid matrices formatted simply by different arrangements of the wavelengths (channels) in Appendix A. This large number of G_{max} is a good source of keys for secure operation. Depending on the administration of security, some formats may not be suitable for security implementation due to their simple arrangement such as ascending or descending wavelength values within the matrix in (5).

Considering frequent changes of W_{mn}^{G} as a secure key of operation from those in G_{max} in (6), it is possible to have an hourly change of wavelength matrix W_{mn}^{G} in Appendix A for example from available G_{max} matrices as "key," and G_{max} supports 8.0340 x 10^{155} years of operation before any key is reused. Only one W_{mn}^{G} selected in the proposed security enhancement in PON and the selected wavelength grid matrix will be subjected to a column's complete cycle rotation to generate n sub grid matrices W_{mn}^{xG} as discussed in the next section.

3.2.1 Generation of Sub Grid Wavelength Matrix (W_{mn}^{xG})

Selected wavelength grid matrix W_{mn}^{G} out of G_{max} in (6) for use in PON secure operation is further subjected to sequential columns cycling, as shown in Figure 10, to generate sub grid (xG) matrices W_{mn}^{xG} that are considered derivatives of the selected W_{mn}^{G}. All generated wavelength sub grid matrices W_{mn}^{xG} (total n) will be mapped to code matrices (discussed in section 3.3) in order to increase the total orthogonal wavelength sequences generated in (3).

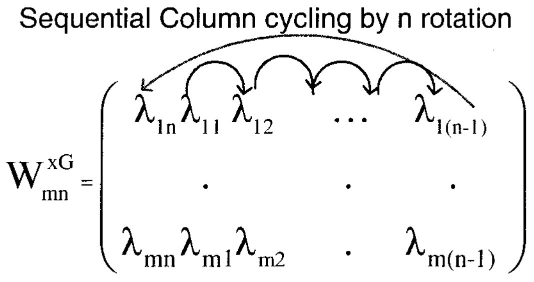
Sequential Column cycling by n rotation
$W_{mn}^{xG} =$
$\lambda_{1n}\lambda_{11}\lambda_{12} \cdots \lambda_{1(n-1)}$
$\lambda_{mn}\lambda_{m1}\lambda_{m2} \cdot \lambda_{m(n-1)}$

Figure 10 : Sequential columns cycle rotation to generate sub grid wavelength matrix

3.3 Code Matrices and their Construction Basics

In access networks with many users sharing common medium such as the fiber link in PON topology shown in Figure 2, MAI between users needs to be avoided or at least controlled. This function usually is assigned to the sublayer of the data link layer of the OSI model, or what is known as the MAC.

The success of coding schemes in a wireless network, specifically, the spread spectrum transmission and CDMA techniques provide a good foundation for OCDMA. Fiber optics networking provides the advantage of enormous bandwidth, which makes optical networks ideal medium for transmission. When applied in an optical system, incoherent detection is used because the light is energy that follows the square low of detection where unipolar coding is need and there is no representation for phase in the optical domain [72][73][76].

Codes construction methods have a different basis, but OOC and prime sequences (PS) are the most important [72]. Various methods were proposed to construct optimal codes where optimal is defined in [77] to be the codes that provide K cardinality (number of nodes) with k >> 10. Several papers [59][82][83] suggested the use of prime numbers for hopping and spreading in order to improve security and cardinality.

Coding techniques provide a means for orthogonally coded transmissions to avoid or minimize MAI depending on the coding scheme. Different classifications of coding schemes exist, and in optical system coding, one-dimensional (1-D) codes such as direct-sequence pseudo orthogonal (PSO) pulse sequences (shown in Figure 7), which are frequently referred to as 1-D OOCs [65][77], is one of them. In addition, the direct sequence bipolar codes [61] and frequency or phase encoding codes are other examples of 1-D coding [72][67][78].

The 1-D codewords using OOC cardinality are expressed as $\Phi(n, w)$, as shown in (7), where n is the codeword length (similar to the number of columns in a single row matrix) and w is the weight (number of 1s) in each row. Cardinality has an upper bound in $\Phi(n, w)$ for OOC for 1-D that was reported for odd and even n in [65][66],

$$\begin{aligned} &\text{For } n \text{ is odd, upper bound on } \Phi(n, w) \le \frac{n-1}{w(w-1)} \\ &\text{For } n \text{ is even, upper bound on } \Phi(n, w) \le \frac{n-2}{w(w-1)} \end{aligned} \tag{7}$$

The relation in (7) provides an upper bound on cardinality (number of nodes) based on using a single wavelength as shown in Figure 7, which implies more nodes. On the other hand, with increased cardinality, we need to increase the size of the code n, or reduce the weight w. However, neither solutions are desired since increasing n impacts bandwidth on the single wavelength and reducing w, for example, defeats the original purpose of security through wavelength hopping. 1-D codes do not meet the basics of data diffusion in this dissertation and therefore are not considered as part of the solution.

The second classification is the two-dimensional (2-D) and higher dimensional codes. 2-D codes can be divided into time-spreading frequency-hopping types [67], 2-D prime code types [72], spectral amplitude coding (SAC), fast-frequency hopping (FFH), pulse position modulation (PPM), and time spreading schemes [79][80]. A higher dimension such as the use of space/wavelength/time spread is considered as three-dimensional (3-D) coding [81].

The 2-D code matrix C^{y}_{ml} shown in (8) includes a_{ml} elements, where each element takes a value of 0 or 1, and when mapped (indexed) to the wavelength sub grid matrices W^{xG}_{mn} , a wavelength is selected to be in the sequences generated by (3) when a_{ml} =1 and no wavelength is selected for the case of a_{ml} =0.

$$\mathrm{C}^{y}_{ml} = \begin{pmatrix} a_{11} & a_{12} & . & a_{1l} \\ a_{21}. & a_{22} & . & a_{2l} \\ & & & \\ . & . & . & . \\ & & & \\ a_{m1} & . & . & a_{ml} \end{pmatrix} \tag{8}$$

Several coding schemes with the main purpose to provide orthogonal or pseudo-orthogonal codes are available, and each coding scheme for the construction of the matrix C^{y}_{ml} provides a maximum number of codes designated by Y_{max}.

Code matrices need to have good correlation properties in both dimensions, namely cross correlation (X_c), which provides an indication to the degree of mutual interference between two channels, and auto correlation (A_c), which facilitates the detection of the desired signal and determines how well detection is at the intended receiver (detector) with the presence of mutual inference for a certain channel [65][72]. In order to support many simultaneous users online, the maximum cross correlation value is to be as small as possible [72]. Optimum design always calls for the maximum cross correlation value to be as small as possible in order to support many simultaneous users [72].

In order to improve the codes' cross-correlation property, hamming distance (d) is another parameter that is very important. Hamming distance between two code words, each with the same number of elements, is defined as the number of positions in which the corresponding elements differ [72]. A good sources for codes construction can be found in [46][72][76][82][83][88], where codes with what is considered good correlation properties are those based on TS/WH with the same prime number representation; mainly, prime sequence for spreading, and prime for hopping. In addition, variants of TS/WH codes for extended quadratic congruence (EQC)/prime when the prime numbers for spreading is different than that for hopping [72][82][83]. The multiple wavelength OOC (MW-OOC) is another technique that can be used to generate code matrices [72][85]. This dissertation will focus on TS/WH code construction that was very well presented in [82]. However, in order to focus on the wavelength hopping for security implementation rather than as an access scheme, and to suit matrices operation, slightly different format for codes construction from that suggested in [82] will be used. The important factor in any code constructions is maximum cardinality Y_{max} and correlation properties.

The use of TS/WH codes appear to be the most promising code types for generating code spaces that are large enough to prevent successful brute force code search attacks [68]. This dissertation will focus on the TS/WH that is based on symmetric prime number as a dimension of the code matrix, which will be used in the simulation model in section 3.5.1. The review of other coding techniques is provided mainly as background, which will be used in Chapter 5 in the discussion of future work.

3.3.1 Review of Coding Techniques

The conceptual approach in section 3.1 indicated that an overcolored system (i.e., more wavelengths) be used in order to avoid wavelength reuse in the hopping mode, which dictates that the hopping/spreading ratio to be equal to or greater than 1 (hopping/spreading $\geq$ 1).

TS/WH code matrix based on symmetric prime numbers discussed in the previous section is a special case in which both dimensions of the code matrix C_{ml}^{y} are equal and based on a single prime number P, which is also referred to as a Prime/Prime based code matrix [72][82][83]. This implies that the spreading factor (P) is the same as the number of hopping factors, or hopping/spreading = 1. However, the general case for code matrix construction where the dimensions of C_{ml}^{y} are different, establishes a different pulse placement operator basis in which prime numbers are widely used in the construction of code matrices. Several classifications based on the use of prime numbers are listed in [65][72] as follows:

- Prime codes for time spreading and OOC for wavelength hopping (Prime/OOC).
- Prime codes for time spreading and prime code for wavelength hopping (Prime/Prime).
- Extended quadratic congruence (EQC) for time spreading and prime for hopping (EQC/Prime).
- Prime for hopping and extended quadratic congruence (EQC) for time spreading (Prime/EQC).
- Multiple wavelengths optical orthogonal codes (MWOOC).

The core of the approach to security enhancement in PON is to have a coding scheme that will provide large wavelength sequences (λ_s) generated per the relation in (3) to enable large multiplexing capacity in the shared fiber link in PON. The case of OOC does not support large cardinality based on (7) because of its impact on bandwidth, therefore, Prime/OOC is not considered as a candidate for the proposed solution in this dissertation.

3.3.1.1 TS/WH Code Matrices (C^{y}_{ml}) Based on Symmetric Prime Number

The code matrix in (8) is a general representation, and when used in TS/ WH schemes, implies that the number of rows m in C^{y}_{ml} expressed in (8) is related to the number of available wavelengths. In addition, the number of columns l in (8) is related to the number of time slots (i.e., code length) or the spreading of the pulses in the time domain [85]. The codes' construction in the proposed solution in this dissertation will be 2-D code matrices C^{y}_{ml}, with mxl dimension that has m rows and l columns.

Mapping operation per (3) using C^{y}_{ml} shown in (8) provides a selection of wavelengths in the same row m and column n in W^{xG}_{mn} . The mapping operation requires the numbers of rows and columns in code matrices C^{y}_{ml} to be equal to or less than the number of rows and columns in wavelength sub grid matrices W^{xG}_{mn} , respectively. In this dissertation, both matrices will have the same number of rows, while the number of columns will be $n \geq l$.

The construction of code matrix C^{y}_{ml} based on symmetric prime numbers includes a decision of the value of elements a_{ml} (0 or 1) in the code matrix shown in (8). This decision is made using a pulse placement operator based on prime codes and a linear congruent operator shown in (9) that provides a pulse placement of 1 in a row [72].

The first step is to find the prime number P in the pulse placement operator relation in (9), which will depend on the total available wavelengths generated by (4) based on selected channel spacing (Δ). For example, for Δ = 25 GHz, 200 wavelengths generated by (4), and a prime number that can be used for a symmetric TS/WH code matrix in (8), P = 13 and the code matrix dimensions are $m = l$ = 13 (i.e., 13 x 13 = 169) using symmetric dimensions.

$$a_{mn} = (y.m)Mod(p) \quad y = 1,2,3,...P, \quad m \ = 1,2,....P-1 \tag{9}$$

The relation in (9) places 1 at a certain column location in each row (m) of the y-designated code matrix. It is important to remember that the relation in (9) provides a row with no placement of 1 when $m = P$ (all rows will be 0's). Therefore, the last row is always ignored and the dimension of the produced code matrix C^{y}_{ml} will be ($m = P$ - 1) rows, and l = m columns.

Complete code matrices for P = 13 were computed using MATLAB® with the results documented in Appendix C, and each code matrix has P columns by (P - 1) rows, as shown in Figure 11, which illustrates a sample of two code matrices extracted from Appendix C for the case of P = 13, y = 7, and y = 11.

It is important to note that each row in Figure 11 includes a single location for 1 and n - 1 number of 0s, or simply can be expressed with weight w = 1. This implies that when code matrices mapped against n W^{xG}_{mn} wavelength sub grid matrices are generated by only the columns rotations shown in Figure 10, $n(m$ - 1) wavelength sequences (λ_s) are generated per the relation in (3).

The code matrix C^{y}_{ml} constructed using symmetric prime number provides excellent correlation properties that were reported to be 0 for autocorrelation A_c, and 1 for cross correlation X_c [47][48][61], which is also demonstrated in the simulation model in section 3.5 making the prime hop sequence ideal for supporting multiple simultaneous users.

The symmetric based TS/WH code matrix C^{y}_{ml} used throughout the dissertation in the simulation and analysis, and a review of other coding schemes are provided next.

$$C_{12,13}^{7} = \begin{pmatrix}
0 & 0 & 0 & 0 & 0 & 0 & 1 & 0 & 0 & 0 & 0 & 0 & 0 \\
1 & 0 & 0 & 0 & 0 & 0 & 0 & 0 & 0 & 0 & 0 & 0 & 0 \\
0 & 0 & 0 & 0 & 0 & 0 & 0 & 1 & 0 & 0 & 0 & 0 & 0 \\
0 & 1 & 0 & 0 & 0 & 0 & 0 & 0 & 0 & 0 & 0 & 0 & 0 \\
0 & 0 & 0 & 0 & 0 & 0 & 0 & 0 & 1 & 0 & 0 & 0 & 0 \\
0 & 0 & 1 & 0 & 0 & 0 & 0 & 0 & 0 & 0 & 0 & 0 & 0 \\
0 & 0 & 0 & 0 & 0 & 0 & 0 & 0 & 0 & 1 & 0 & 0 & 0 \\
0 & 0 & 0 & 1 & 0 & 0 & 0 & 0 & 0 & 0 & 0 & 0 & 0 \\
0 & 0 & 0 & 0 & 0 & 0 & 0 & 0 & 0 & 0 & 1 & 0 & 0 \\
0 & 0 & 0 & 0 & 1 & 0 & 0 & 0 & 0 & 0 & 0 & 0 & 0 \\
0 & 0 & 0 & 0 & 0 & 0 & 0 & 0 & 0 & 0 & 0 & 1 & 0 \\
0 & 0 & 0 & 0 & 0 & 1 & 0 & 0 & 0 & 0 & 0 & 0 & 0
\end{pmatrix}
\qquad
C_{12,13}^{11} = \begin{pmatrix}
0 & 0 & 0 & 0 & 0 & 0 & 0 & 0 & 0 & 0 & 1 & 0 & 0 \\
0 & 0 & 0 & 0 & 0 & 0 & 0 & 0 & 1 & 0 & 0 & 0 & 0 \\
0 & 0 & 0 & 0 & 0 & 0 & 1 & 0 & 0 & 0 & 0 & 0 & 0 \\
0 & 0 & 0 & 0 & 1 & 0 & 0 & 0 & 0 & 0 & 0 & 0 & 0 \\
0 & 0 & 1 & 0 & 0 & 0 & 0 & 0 & 0 & 0 & 0 & 0 & 0 \\
1 & 0 & 0 & 0 & 0 & 0 & 0 & 0 & 0 & 0 & 0 & 0 & 0 \\
0 & 0 & 0 & 0 & 0 & 0 & 0 & 0 & 0 & 0 & 0 & 1 & 0 \\
0 & 0 & 0 & 0 & 0 & 0 & 0 & 0 & 0 & 1 & 0 & 0 & 0 \\
0 & 0 & 0 & 0 & 0 & 0 & 0 & 1 & 0 & 0 & 0 & 0 & 0 \\
0 & 0 & 0 & 0 & 0 & 1 & 0 & 0 & 0 & 0 & 0 & 0 & 0 \\
0 & 0 & 0 & 1 & 0 & 0 & 0 & 0 & 0 & 0 & 0 & 0 & 0 \\
0 & 1 & 0 & 0 & 0 & 0 & 0 & 0 & 0 & 0 & 0 & 0 & 0
\end{pmatrix}$$

Figure 11: Two code matrices for $y = 7$ and $y = 11$

3.3.1.2 Extended Quadratic Congruence TS with Prime WH (EQC/Prime)

The symmetric based TS/WH discussed in the previous section implemented a single prime number P as a basis for both hopping and spreading (Prime/Prime), or the ratio of hopping/spreading = 1, which is characterized by excellent cross- and autocorrelation properties [82]. A general model of the case of hopping/spreading > 1 (overcolored system) assumes different prime numbers for spreading and hopping patterns such that there are more wavelengths available in the hopping pattern than there are pulses in the spreading one (i.e., $n \geq l$). In this case, a critical factor is the correlation problems associated with this approach that can be much higher than 2, thereby calling upon a careful selection of the hopping pattern [82]. The approach to solving autocorrelation problems associated with two different primes was provided in [87] by using prime codes for hopping, while the spreading was based on EQC[19] in order to improve the correlation properties. The origin of EQC is the quadratic congruence codes (QCC) relation that was proposed in [86] as an almost ideal autocorrelation function at the expense of having a slightly increased number of coincidences in their cross-correlation functions. It was shown in [86] for QCC that P - 1 codes exist for every odd prime P and can serve as many as P - 1 different users in the shared fiber optic code division multiple access system. However, QCC suffered from high cross correlation that reached 4 [86], and EQC was introduced in [87] to further reduce the cross correlation to 1.

[19] Congruence relation is designated by ≡, and for a function $h(x) \equiv f(x)(\text{mod } g(x))$ means that h(x) and f(x) have the same remainder under division by g(x).

The EQC construction method uses congruent placement operator shown in (10), which has some differences from the Prime/Prime case placement operator in (9), and the code matrix C_{ml}^{y} shown in (8) has dimensions of $m = P$ rows and $l = (2P\text{-}1)$ columns [82][83]. The size of each row in (8) is increased as an extended prime code that uses (10) designed to reduce the maximum cross correlation value by padding code rows with trailing zeros [72].

$$a_y(m) \equiv y\frac{m(m+1)}{2} \ (\text{mod } P) \quad \begin{array}{l} 0 \le y \le P\text{-}1 \\ 0 \le m \le P\text{-}1 \end{array} \tag{10}$$

The relation in (10) places a pulse in a row m that has a size of $(2P\text{-}1)$ in code matrix y, which is part of maximum number of code matrices y ∈ $Y_{\max}$.

In [82], prime numbers were used as part of the dimension of the code matrix and designated for hopping as (P_h) and (P_s) for spreading. In the case that both numbers are equal $(P_h = P_s)$, this is labeled as symmetric TS/WH, which is the same as discussed in section 3.3.1.1. The symmetric TS/WH also is referred to in the literature as prime hop codes [82][83][88]. Otherwise, for $P_{\mathrm{h}} \neq P_{\mathrm{s}}$ it is labeled as asymmetric TS/WH, which is discussed in this section.

A prime number is used for and designated as P_h, which will be equal to one of the dimensions of wavelength grid matrix W_{mn}^{G} in (5), and used in (9) where it is based on prime numbers and not on EQC. On the other hand, the dimension of the code matrix C_{ml}^{y} will be different for TS/WH based on the EQC/Prime construction method. In this case, the prime number selected for the spreading (P_s) will be used in (10) for the pulse placement with an expression for the pulse placement operator expressed in (11).

$$a\ (m) = y\frac{m(m+1)}{2} \ (\text{mod } P_s) \quad \begin{array}{l} 0 \le y \le P_s\text{ -1} \\ 0 \le m \le P_s\text{ -1} \end{array} \tag{11}$$

The dimension of code matrix C_{ml}^{y} will have $m = P_s$ rows and $l = 2P_s$ - 1 columns, which leads to a maximum number of code matrices expressed as $Y_{\max}$ in (12) as:

$$Y_{\max} = P_s(2P_s\text{ -}1) \tag{12}$$

TS/WH based on EQC/Prime in (12) provides more code matrices than the TS/WH based on a symmetric prime number. The latter provided only P - 1 code matrices as was demonstrated in Appendix C for P = 13, which provided only 12 code matrices, while EQC/Prime provides a higher number of code matrices as using (12) for P_s = 11 provides a total of 231 code matrices.

Implementation of EQC provides low cross correlation properties [83]. The applicability of two different primes approach using TS/WH with EQC/Prime approach can be tailored to support security enhancement in PON in this dissertation by utilizing higher dimensions on the wavelength grid matrix W_{mn}^{G} where P_h can represent one of columns and be expressed as shown in (13).

$$(Ph) \geq (2Ps\text{-}1) \qquad (13)$$

Accordingly, the relation between the numbers of columns between the code matrix and the wavelength grid matrix can be expressed as:

$$l = (2P_s - 1) \leq m = P_h \qquad (14)$$

3.3.1.3 Prime for TS and EQC for WH (Prime/EQC)

It was suggested in [85] to reverse the function of the code implementation where the prime code is to be used for time spreads and EQC is to be used for wavelength hopping. Such implementation would increase overall cardinality to $P^2(P$ - 1), but cross correlation gets large up to 2, and therefore, this approach is not planned for implementation in this dissertation.

3.3.1.4 Multiple Wavelength Optical Orthogonal Codes (MW-OOC)

It is noticed that both cases of TS/WH (symmetric and asymmetric) based on prime numbers have a single pulse in every row of the code matrix in (8). In order to improve cardinality in wavelength hopping, an alternative method is to relax the maximum cross correlation value similar to the implementation in the frequency hopping (FH) use of Reed-Solomon codes in wireless systems [72]. However, such an approach would affect MAI, and ideally, cardinality needs to be a function of code length and not the preselected cross correlation [72].

MW-OOCs are *m x n* matrices 2-D codewords, where *m* is the number of rows (related to the number of available wavelengths) and *n* is the number of columns (related to the code length). Simply, MWOOCs are analogous to 1-D OOCs with multiple rows to support a much larger number of simultaneous users since the code cardinality is much larger [73], and are designed to meet autocorrelation and cross-correlation constraints in order to manage MAI.

MW-OOC matrices have fixed weight with $w > 1$ (w is number of 1's) in a single row m of the matrix, which is different from the case for TS/WH code matrices discussed in sections 3.3.1.1 and 3.3.1.2 for symmetric Prime/Prime and asymmetric EQC/Prime, respectively, where $w = 1$ in each row of the matrices.

Upper bounds on MW-OOC and its optimal cardinality are of interest, however, correlation properties are of concern also where careful implementation is required in order to control MAI. The cardinality of MW-OOC is expressed as $\Phi(mxn, w, A_c, X_c)$ where the upper bound of the MWOOC cardinality is derived as shown in (15) by multiplying the Johnson bound in [65] for a single wave as shown in (7) by available wavelengths [75].

$$\Phi(mxn, w, Ac, Xc) \leq \frac{m(mn-1)(mn-2)........(mn-Xc)Ac}{w(w-1)....(w-Xc)} \tag{15}$$

In access networks, OOCs are designed to be pseudo-orthogonal, i.e., the correlation (and therefore the interference) between pairs of codewords is constrained [74]. It is obvious in (15) that the upper bound (cardinality) is under the control of weight and allowed correlation as the system's constraints. Moreover, reducing the weight and increasing the size of the matrix in 2-D MW-OOCs provides a much larger number of simultaneous users [46].

There are various schemes for MW-OOC code constructions such as the 2-D TS/WH codes, which employ wavelength hopping algebraically under prime-sequence permutations on top of time-spreading OOCs as reported in [75]. In addition, another scheme for MW-OOC construction is proposed in [94] where the weight *w* has a fixed hamming[20] distance of (w + Q) for correlation Q, MW-OOC is expressed as *mn,w + Q,Q* and the same

[20] Hamming distance between two codewords, each with the same number of elements, is defined as the number of positions in which the corresponding elements differ.

cardinality provided in (15) is used, which assumes that both autocorrelation and cross correlation are equal in value ($A_x = A_c = Q$). The.findings of [94], that cardinality is increased where an example for using m = 61 wavelengths and codeword length n = 121 provides up to 75,030 MW-OOCs (simultaneous users). In [95], it is demonstrated that MW-OOCs perform better than both OOCs (by a factor of approximately 1.25) and asymmetric prime-hop codes (by a factor of approximately 3.5) over a wide range of offered loads.

In this dissertation, the focus is on the security aspect rather than trying to provide methods for construction of MW-OOCs or comparing them. More details about MW-OOCs are available in [46], [72], [85], and [95], which provide comparisons between the performances of different MW-OOC coding schemes.

3.3.1.5 Multiple Length Wavelength Hopping Prime Codes

It is expected that future systems will be required to support a large variety of services such as TPS (audio, video, and data) with multi rate multimedia services coexisting in the same network [97]. This implies simultaneous support for different signaling rates and quality of service (QoS) where constant codeword length may not be able to support such requirements [72]. The use of multi-length codewords rates and services can be matched to need, and in terms of security, such schemes enhance security by hiding patterns; however, this requires, for example, different dimensions of code matrices.

Careful selection and centralized control of the multiple length wavelength hopping prime codes is extremely needed due to the impact of such schemes on the system, which may cause poor correlation[72][93]. Some proposed designs in the literature [97] include multi-length OOC, however, the same study shows that performance of these multi-length OOCs worsen as the code length increases and the weight is still fixed but spread over a double length code word.

Analysis in [93] shows that performance with the use of multiple length codes improves as the code length decreases. Even though this unique characteristic allows “prioritization” and guarantees high QoS, reduction of code length provides less security due to fewer wavelengths.

The applicability of multiple lengths wavelength hopping prime codes to the proposed solution and in order to guarantee QoS at high data rates using fewer wavelengths as suggested in [93] results in a reduced security level due to less frames/packets diffusion among wavelengths. However, in the proposed solution in this dissertation, the multiple length wavelength hopping prime code matrices can be adopted easily such that the code matrices used in the mapping operation in (3) can be divided into sub matrices shared by users (ONUs). The result is that two or more actually share a wavelength sequence (λ_s) generated by (3) such as those shown in Appendix D.

In order not to affect security and reduce QoS degradation caused by reduction of wavelengths as mentioned [93], the proposed solution in this dissertation uses slow wavelength hopping with multiple wavelength sequences assignment per user (ONU). The analogy to multiple length wavelength hopping prime codes is actually based on having multiple sequences each shared by multiple ONUs at different proportions, with the alternate use of sequences among many users (ONUs) thus retaining a high number of wavelengths and not impacting QoS.

3.3.1.6 Code Words with Variable Weights (w)

In previous discussions for TS/WH MW-OOC and multiple length wavelength hopping primes codes, the weight *w*, which represents the non zero elements in each row (*m*) of code matrix, were fixed. Variable weight techniques have been discussed in the literature [79][96] and were intended originally for QoS or one way of providing different rates for different subscribers (ONUs) based on their applications and needs (multi-rate system).

The use of variable weights in the proposed solution actually enhances security where wavelength sequences generated by (3) in this case have different lengths from each other, and the security of a node (ONU) can be associated with number of sequences issued (*j* = 1 to *K*) for a single ONU and the summation of weights for each code matrix across all rows *m* as expressed in (16). Multiple security levels among ONUs can be defined based on the sum of weights as compared to other code matrices that had fixed weights in each row.

$$\text{Security Level} =(\sum_{j=1}^{i=K} \sum_{i=1}^{i=m} w_i) \qquad (16)$$

Of course, higher weight value impacts information transmission rate; for example, high weight codes will provide lower low rate information due to higher diffusion of Ethernet frames over several wavelengths, while low weight codes provide high rate information transfer due to less diffusion of Ethernet frames among wavelengths and still can impact QoS.

3.3.2 Code Matrices Implementation in this Dissertation

Various coding schemes were introduced and discussed, however, the focus of this dissertation is on security aspects of the proposed security enhancement based on mapping the two matrices, code matrix and wavelength sub grid matrices, as illustrated in Figure 8. The scope of the dissertation cannot cover all coding schemes in detail, and the intention is to have a higher number of code matrices that will provide better security rather than an access solution. The reason is based on the fact that current optical technology supports splitting the ratio of the passive optical coupler (PSC) up to N = 64 [35], which means that this dissertation sees that cardinality can be met easily for 64 ONUs in PON.

Wavelength matrices generation per (3) used in diffusing complete Ethernet frames/ packets and the different coding schemes discussed in section 3.3.1 with different fixed or variable weights w, all support data diffusion schemes when code matrices are mapped to wavelength grid matrices as shown in Figure 8 and (8). Each scheme may use more or less wavelengths in the hopping mode depending on the weight w, however, autocorrelation more than 1 necessitates synchronization of the use of wavelength sequences so that MAI is controlled.

Therefore, the scope of this dissertation is limited to one coding scheme, namely, TS/WH code matrices based on symmetric prime numbers as discussed in section 3.3.1.1, which appear to be most promising code types for generating code spaces that are large enough to prevent successful brute force code search attacks [68].

3.4 Wavelength Sequence λ_s Generation

The concept of security enhancement in PON starts with the basic PON architecture similar to that in Figure 2 and includes tailored OLTs and ONUs operation that require tunable laser transmitters and filters across C and L bands in addition to the necessary processing algorithm to enable a wavelength hopping scheme. The wavelength hopping sequence generation for a specific ONU is based on the mapping (indexing) of two matrices; wavelength sub grid matrices W_{mn}^{G} shown in Figure 10 with x being the designation of the specific wavelength sub grid matrix W_{mn}^{xG}, which can range from $x = 1$ to $x = n$.

Starting with the selected wavelength grid matrix W_{mn}^{G} from the available G_{max} formats in (6) and the wavelengths (channels) as a result of the relation in (4) over the band 191.0THz (1569.59 nm) to 195.975 THz (1529.75 nm) that covers both optical C and L bands, W_{mn}^{G} is constructed and W_{mn}^{xG} are derived from W_{mn}^{G}. For demonstration purposes, Appendix A shows the selected W_{mn}^{G} in this dissertation, which has a total of 192 unique, non-repeated wavelengths (channels) arranged in an mxn matrix with $m = 12$ rows and $n = 16$ columns. The columns complete cycle rotation per Figure 10 is carried out on W_{mn}^{G} producing a total of n W_{mn}^{xG} wavelength sub grid matrices as shown Appendix B.

The code matrices were already constructed as discussed in section 3.3.1.1 for TS/WH based on the symmetric prime number $P = 13$, with the results shown in Appendix C. The limited number of code matrices (P - 1) as dictated by equation (9) do not support a large number of nodes (ONUs) in PON, which can have up to 64 ONUs and plan for growth to 128 as indicated in ITU-T G984.1 for Giga PON (GPON). However, mapping in (3) provides sufficient wavelength sequences (λ_s) with each sequence unique and orthogonal to all other wavelength sequences generated by (3). Note that if higher code matrices will be required, the TS/WH based on EQC/Prime (asymmetric prime numbers) discussed in section 3.3.1.2 provide higher code matrices, but careful attention is needed to check on the correlation to avoid interference (MAI).

MATLAB® was used in the mapping operation (indexing) between the 16 sub grid matrices W_{mn}^{xG} in Appendx B and code matrices in Appendix C, and an example of such mapping results is shown as $W_x(C_y)$ in Table 2 for partial sequences representing 12 sequences in 9 hops. The complete results of the mapping operation, shown in Appendix D, has 192 unique wavelength sequences, with each wavelength in the sequence part of a single hop in the wavelength hopping scheme with good correlation such that no two wavelengths are alike in the same hop. This good zero autocorrelation guarantees the orthogonality between the wavelength sequences.

The duration for each hop in Table 1 is defined during the design, which is the time taken to transmit a fixed packet/frame length (T_w) and the budgeted guard time (T_g) for the system. The fact that there are no two wavelengths on the same frequency in the same hop in Appendix D is due to good orthogonal code matrices in Appendix C based on symmetric prime numbers, which exhibit autocorrelation of 0 and cross correlation of 1 [72][82]. The next step actually is to implement the wavelength sequences in a simulation model for PON with 64 wavelengths in each hop as discussed next.

Table 1: Hopping sequences for 8 hops with hop duration controlled by T_c+T_g

Mapping $W_x(C_y)$	**Hop #1**	**Hop #2**	**Hop #3**	**Hop #4**	**Hop #5**	**Hop #6**	**Hop #7**	**Hop #8**
W13(C3)	193	193.675	195.65	195.425	193.4	194.5	191.8	194.375
W2(C6)	195.1	191.8	192.6	194.675	193.8	192.1	191.825	195.2
W12(C7)	193.3	193.15	194.8	195.65	191.35	191.55	195.4	192.5
W13(C12)	194.925	195.55	194.85	194.7	191.7	195.525	192.5	191.975
W12(C4)	191.675	195.45	193.675	195.575	194.7	194.475	195.775	191.475
W1(C12)	191.25	195.25	193.5	194.275	192.175	192.725	192.275	193.175
W8(C7)	193.175	192.975	194.125	191.325	191.3	192.525	195.675	195.5
W7(C6)	193.95	191.65	191.1	194.6	192.025	191.3	194.9	194.8
W7(C12)	191.025	191.825	192.575	194.125	194.55	192.075	193	194.15
W13(C9)	193.15	195.7	193.225	195.625	194.475	194.975	192	194.35
W4(C12)	191.075	193.025	193.075	194.325	191.65	192.975	193.475	191.6
W9(C12)	191.125	193.65	194.425	192.25	195.125	194.65	195.5	195

3.5 DWDM Simulation Model in PON

One of the cornerstones of the proposed solution to security enhancement in PON in this dissertation is the feasibility of using a simultaneous high number of channels online in a (DWDM configuration. The maximum number of ONUs that can be supported in a typical PON topology, shown in Figure 4, is 64 ONUs [12][13], and the simulation model that is used in section 3.5.2.2 considers the worst case by having 64 wavelengths per hop selected from those in Appendix D coexisting simultaneously online.

The computer simulation software provides a high fidelity of DWDM simulation in shared fiber link by including solutions to various computations that are associated with loss, dispersion, and other fiber nonlinearities and impairments that can affect multiplexing capacity with their capability of impeding data flow. A representative model of PON architecture with 64 simultaneous wavelengths (channels) transmitted in the downstream direction (assuming the same effect in upstream) is shown in Figure 12, and additional simulated instrumentation included monitoring along the path of optical signals and at the receiving end of the simulated PON model performance analysis.

Simulation is necessary due to the fact that smaller channel spacing is being used (i.e., 25 GHz), and the effects of such spacing need to be examined due to fiber impairments, which includecCross-phase modulations (XPM) and four wave mixing (FWM) as discussed in sections 1.4.1.1.2 and 1.4.1.1.3, respectively.

The simulation model shown in Figure 12 consists of continuous wave (CW) laser transmitters' arrays where each transmitter provides 1 mw power at 0 degree phase angle on a single wavelength (channel) and all channels are selected from the ITU-T G694.1 wavelength grid based on 25 GHz channel spacing [26].

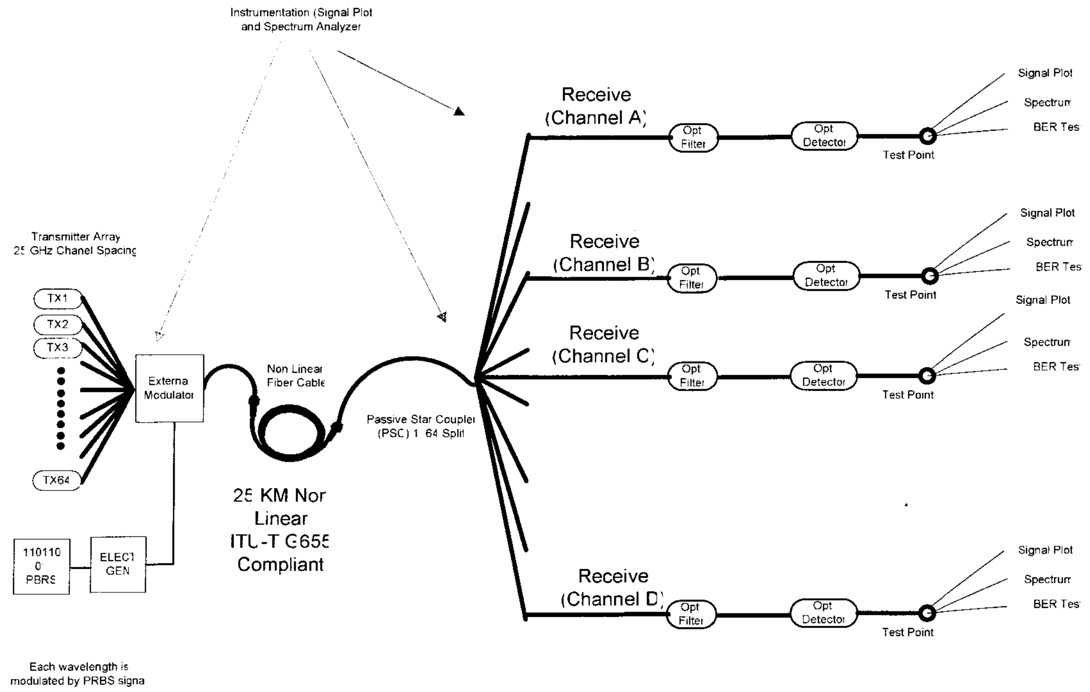

Figure 12: Top model of simulation model for 64 DWDM channels in PON

Each wavelength from the array is subjected to external (indirect) modulation by a pseudo random binary signal (PRBS), which is bit sequence of 0's and 1's representing typical digital traffic in a network and fed to an external modulator through the electrical generator as shown in Figure 12. The function of the electrical generator is to convert an input binary signal from PRBS into an output electrical signal. The PRBS is a single instance of the model used to provide multiple and similar pattern outputs used for modulating all 64 wavelengths at the same time in a single hop thus establishing a common baseline for evaluating all channels against one reference. Good channels should provide the same signal replica at the output of the monitored channels A, B, C, and D as shown in Figure 12.

The 64 channels in the simulation model shown in Figure 12 are transmitted simultaneously and carried over 25 km long non zero fispersion shifted fiber (NZ-DSF) compliant with the ITU-T G655 fiber cable standard. After the 25 km, the signal of each channel is passively split into 64 branches (1:64) without any amplification between the output of the modulator and the input of the optical filters on the receiving end of the PON simulation model as shown in Figure 12.

Selection of the ITU-T G655 fiber cable related to the cable being NZ-DSF, which has chromatic dispersion that is greater than the nonzero value through the C band (1500nm). Dispersion reduces the effect of fiber nonlinearities such as FWM, SPM, and XPM that are typically seen in DWDM, and this type of fiber cable is best suited and optimized to operate between 1500 and 1600 nm [8].

On the receiving end of the PON simulation model shown in Figure 12, each ONU has an optical tunable filter tuned to a single wavelength (channel) in each hop of the wavelength sequence specific to each ONU. Throughout the simulation model, signal spectrum and signal plot are monitored and instrumentation used for output of selected four channels (A, B, C, and D) is checked for certain performance parameters including eye pattern, BER, signal spectrum, and actual signal output as shown in Figure 12.

3.5.1 Performance Metrics for the Simulation Model

In a typical optical system design, fiber impairment such as FWM, SPM, and XPM and their effects can be seen in the signal quality and usability with tolerable noise level in the hopping mode. As a performance metric, BER, discussed in section 1.4.1.2.1, will be used to indicate the fitness of the shared link for multiple simultaneous sharing in the DWDM environment. The minimum, BER requirement for a typical end system will be in the range of 10^{-9} to 10^{-12}; in other words, for every 10^{9} bits transmitted, one corrupted bit is allowed. BER is a figure of merit for WDM networks and all designs in the industry usually adhere to that quality figure [8].

3.5.2 OptSim^{TM} 4.5 Simulation Software

The simulation software used in PON modeling is the OptSim^{TM} 4.5 provided by RSoft Design Group (www.RSoft.com). OptSim^{TM} 4.5 is an advanced simulation package used in designing optical communication systems and simulates them to determine their performance given various component parameters. OptSim^{TM} 4.5 provides an extensive component model library of the most commonly used components for the engineering of electro-optical systems; such components models used in this dissertation include for example the CW laser transmitters, optical filters, detectors, PSC, in addition to fiber cables modeling the nonlinearities and impairments in a typical physical fiber.

PON simulation model top level architecture shown in Figure 12 was constructed using simulated components from OptSim^{TM} 4.5 simulation software as shown in Figure 13 as an interconnected set of blocks, each block representing a component or subsystem in the communication system in the top level architecture in Figure 12. Similar to physical signals passed between components in a real world communication system, "signal" data is passed between Figure 13 components in the simulated model, and each block is simulated independently using the specified parameters settings summarized in Table 2.

Simulation results are extracted from the instrumentation provided, which includes, for example, signal waveform plots along a PON path, BER, a spectrum analyzer, a Q factor reader, and eye diagrams at the output of the four selected channels (A, B, C, and D) as shown in Figures 9 and 10.

Table 2: Parameters set for PON simulation architecture (Figure 13)

Component	Type	Parameter	Value
Transmitters Array	CW Laser	Peak Power	1 mW
		Channel Spacing	25 GHz
		Line Width	10 MHz
		Random Phase	Included
		Number of Channels	64
		Force polarization	Yes
		Wavelengths	1529.75nm to 1569.59nm
		Relative Intensity Noise (RIN)	-150 dB/Hz
PRBS		Bit Rate	10 Gbps
		Pattern Length	2^7 bits
		Offset between channels	5 bits
Electrical Generator	ON_OFF	Modulation Type	NRZ
		Signal Type	Voltage
		V_{max}	1 V
		V_{min}	0 V
		Time Jitter	1x 10^{-18} Sec
External Modulator		Modulation Type	External/Amplitude
Fiber Cable		Length	25 KM
		Loss Model	Constant
		Loss	.35dB/KM
		Optimization Level	3
		DispersionLambda0	1.565e-6 m
		Dispersion S0	0.1686e3 s/m^3
		Dispersion Offset	6.0e-6 s/m^2
		Include Dispersion	Yes
		Nonlinearity Model	Constant
		Diameter	8.8e-6 m
		affect	1.0522
		Include self-phase modulation (SPM)	Yes
		Include cross-hase modulation (XPM)	Yes
		PMD Method	Coarse step: 1.58e-14 s/m^0.5
		Include SBS	Yes
Splitter	Passive	Passive Star Splitter	1:64
		Polarization	Combination X& Y
		Spectrum noise	Yes
Optical Filters		Type	Gaussian
		Bandwidth	.2 nm
		Drop Threshold	10^{-9} Watts
		Show noise	Yes
		Polarization	Separate X & Y

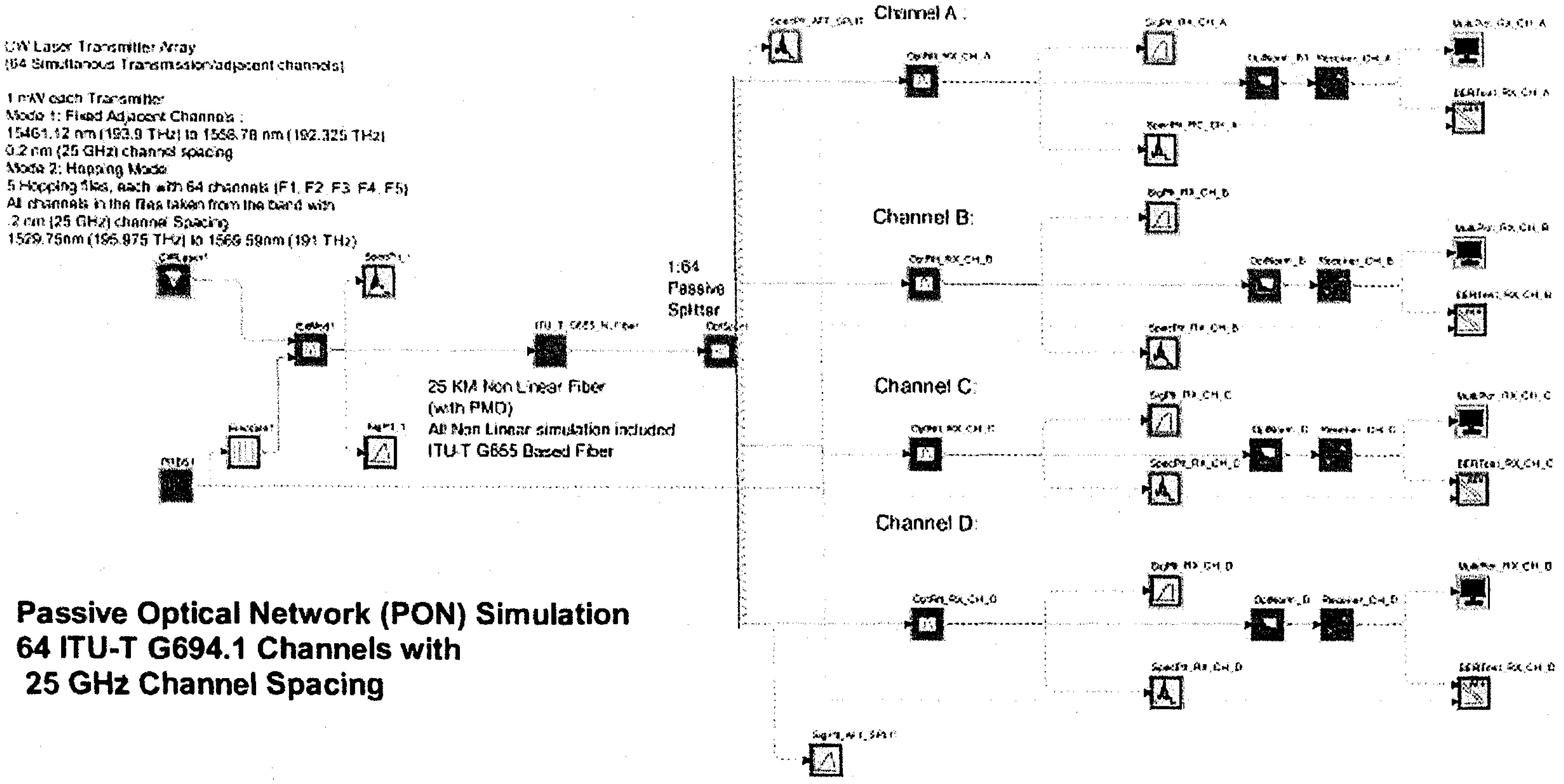

CW Laser Transmitter Array
(64 Simultanous Transmission/adjacent channels)

1 mW each Transmitter
Mode 1: Fixed Adjacent Channels :
15461.12 nm (193.9 THz) to 1558.78 nm (192.325 THz)
0.2 nm (25 GHz) channel spacing
Mode 2: Hopping Mode
5 Hopping files, each with 64 channels (F1, F2, F3, F4, F5)
All channels in the files taken from the band with
.2 nm (25 GHz) channel Spacing
1529.75nm (195.875 THz) to 1569.59nm (191 THz)

25 KM Non Linear Fiber
(with PMD)
All Non Linear simulation included
ITU-T G655 Based Fiber

Passive Optical Network (PON) Simulation
64 ITU-T G694.1 Channels with
25 GHz Channel Spacing

Figure 13: PON simulated model with components of OptSim^{TM} 4.5 software

The simulation in this dissertation is used to provide a proof of concept for the DWDM in PON, and consists of two parts: the first is used to establish a baseline using 64 adjacent channels with equal spacing of 25 GHz, and the second is in the hopping mode where the channels are selected from files prepared specifically for this simulation.

3.5.2.1 64Adjacent Channels Simulation

This part of the simulation is used to establish a baseline for performance metrics, which includes having simultaneous transmission of 64 adjacent channels taken from the ITU-T G694.1 wavelength grid within the band 15461.12 nm (193.9 THz) to 1558.78 nm (192.325 THz) with 0.2 nm (25 GHz) channel spacing and using a data rate of 10 Gbps.

The combined signals are monitored before entry to the 25 km fiber link, after the 1:64 splitters, after the coarse optical filter to check on channel impairments, and at the selected four channels A, B, C, and D on the receiving end of PON architecture shown in Figures 12 and 13. Table 3 lists the frequencies of the four adjacent monitored channels A, B, C, and D that represent a sample of all 64 channels. This part of the simulation is important due to channel cross talk and impairments such as FWM, which is usually more apparent in equally spaced channels in a WDM system and operating at high power [8][45]. A fixed power level of 1mW is applied from each laser transmitter in the array and the focus will be on investigating the channels' impairments. The same physical parameters listed in Table 2 used in every hop across in simulation efforts are reused except for the channel tuning (both transmitters and filters) changed for each hop.

The spectrum of the 64 adjacent channels with 0.2 nm spacing before entering the 25 km long fiber shown in Figure 14 with combined wavelengths (channels) coexisting on the shared fiber link are captured after the 1:64 passive splitter as shown in Figure 15. All channels exhibit the same power level, which is considered a good feature in terms of security against eavesdropping and tapping that uses isolation of channels based on power level screening.

Table 3: Four adjacent channels used in monitoring in Figure 13

Channel Designation	**Frequency**	Wavelength	**Data Rate**	**Parameters Monitored**
A	193.125 THz	1552.32 nm	10 Gbps	BER, Eye , Q factor, Signal, spectrum
B	193.15 THz	1552.12 nm	10 Gbps	BER, Eye , Q factor, Signal, spectrum
C	193.175 THz	1551.92 nm	10 Gbps	BER, Eye , Q factor, Signal, spectrum
D	193.2 THz	1551.72 nm	10 Gbps	BER, Eye , Q factor, Signal, spectrum

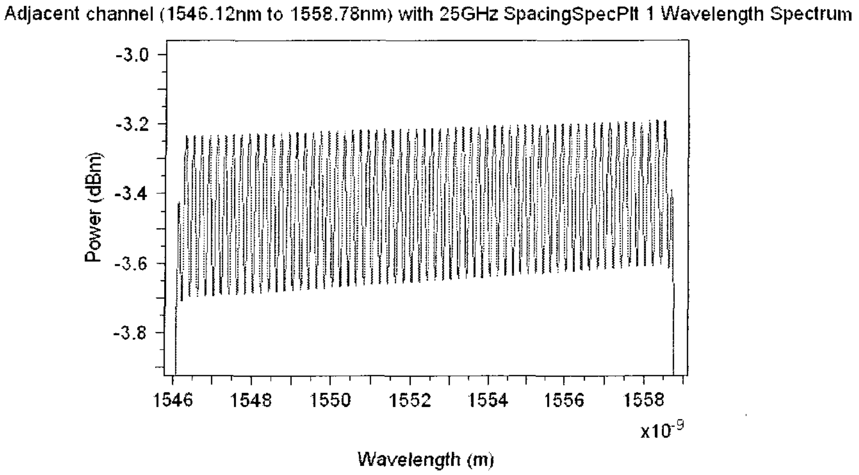

Figure 14: Spectrum of 64 adjacent channels provided by laser transmitter array.

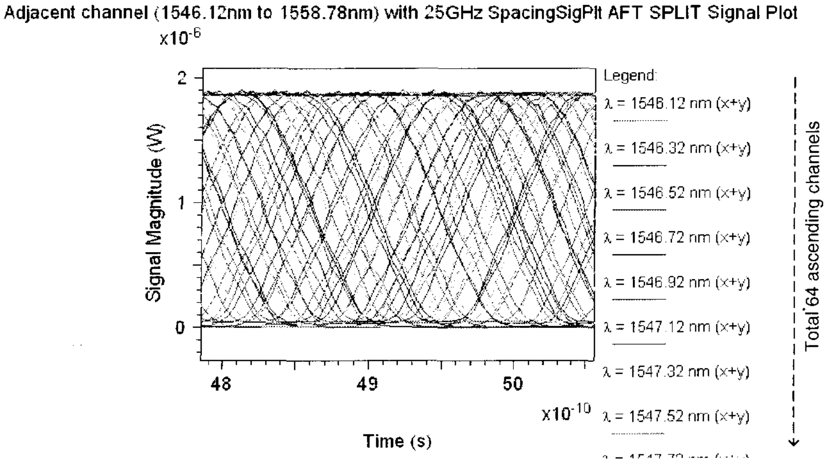

Figure 15: 64 channels in ascending order coexisting on shared fiber link of PON

The eye pattern provides an indication of good system performance by inspecting the opening of the eye in Figure 16, with minor distortions shown as result of the parameters settings in simulation model such as noise sources, jitter, dispersion, and others as shown in Table 2.

Since the same source PRBS signal is used to modulate all 64 wavelengths, all channels are set to the same evaluation criteria, and they are expected on the receiving end to provide a similar common original signal in terms of shape with minimal distortion such as that illustrated for the four monitored channels in Figure 17.

For confidence in the network, other parameters that are related to quality of signal are used, which include performance metrics such as BER and Q factor, discussed in sections 1.4.1.2.1 and 1.4.1.2.2, respectively. BER readings for the four monitored A, B, C, and D channels are shown in Figure 18. The four channels actually performed better than typical minimum benchmarks for the BER standard (between the rates of 10^{-9} and 10^{-12} as an industry minimum standard [8]), which were set in section 1.4.1.2.1. In addition, monitored channels met objective error rates required for optical components that should be better than 10^{-10} in the environment conditions as defined in recommendation ITU-T G.957.

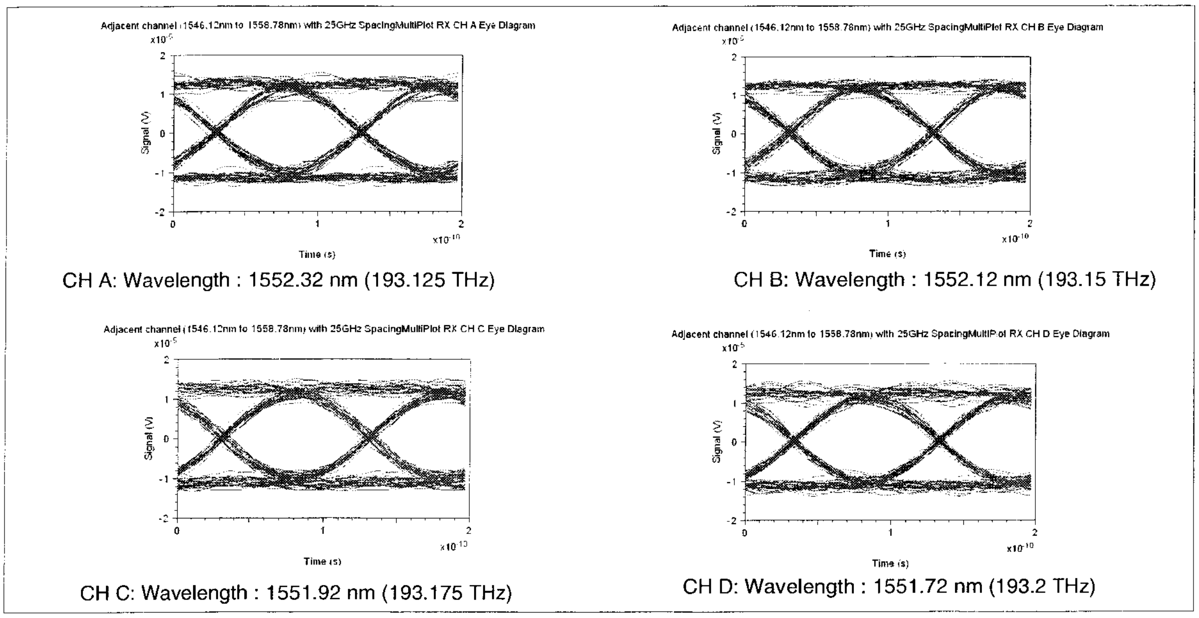

CH A: Wavelength : 1552.32 nm (193.125 THz)

CH B: Wavelength : 1552.12 nm (193.15 THz)

CH C: Wavelength : 1551.92 nm (193.175 THz)

CH D: Wavelength : 1551.72 nm (193.2 THz)

Figure 16: Eye patterns for A, B, C, and D channels of Figure 13 and Table 3

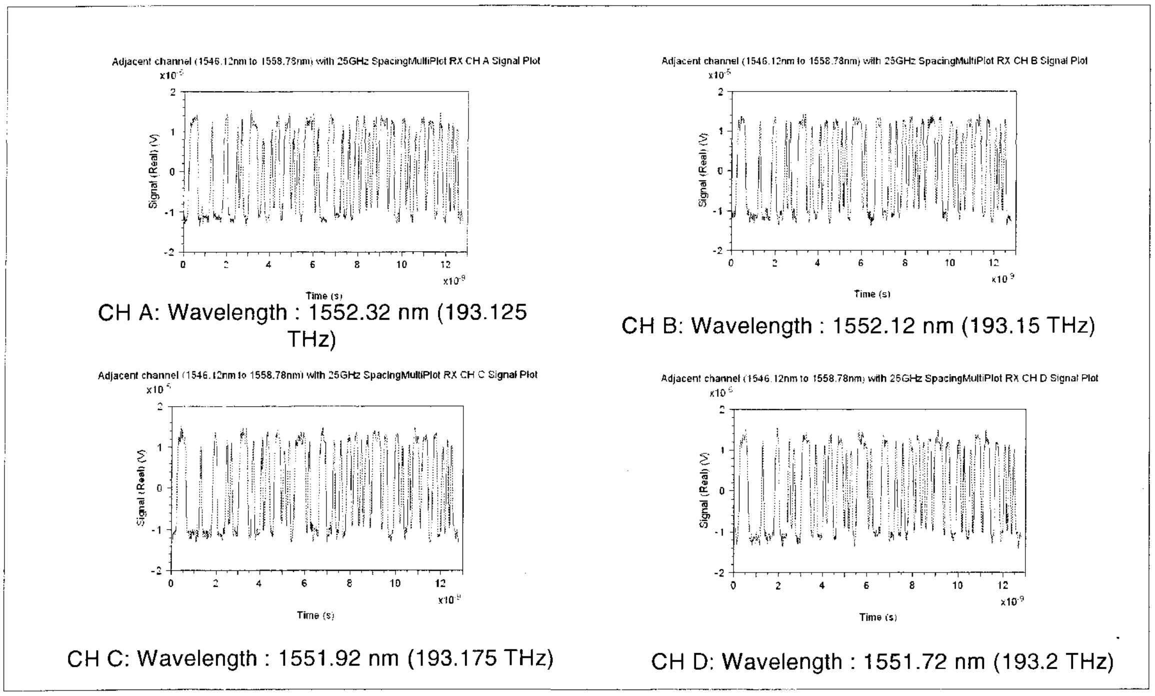

CH A: Wavelength : 1552.32 nm (193.125 THz)

CH B: Wavelength : 1552.12 nm (193.15 THz)

CH C: Wavelength : 1551.92 nm (193.175 THz)

CH D: Wavelength : 1551.72 nm (193.2 THz)

Figure 17: Signal output at A, B, C, and D channel output

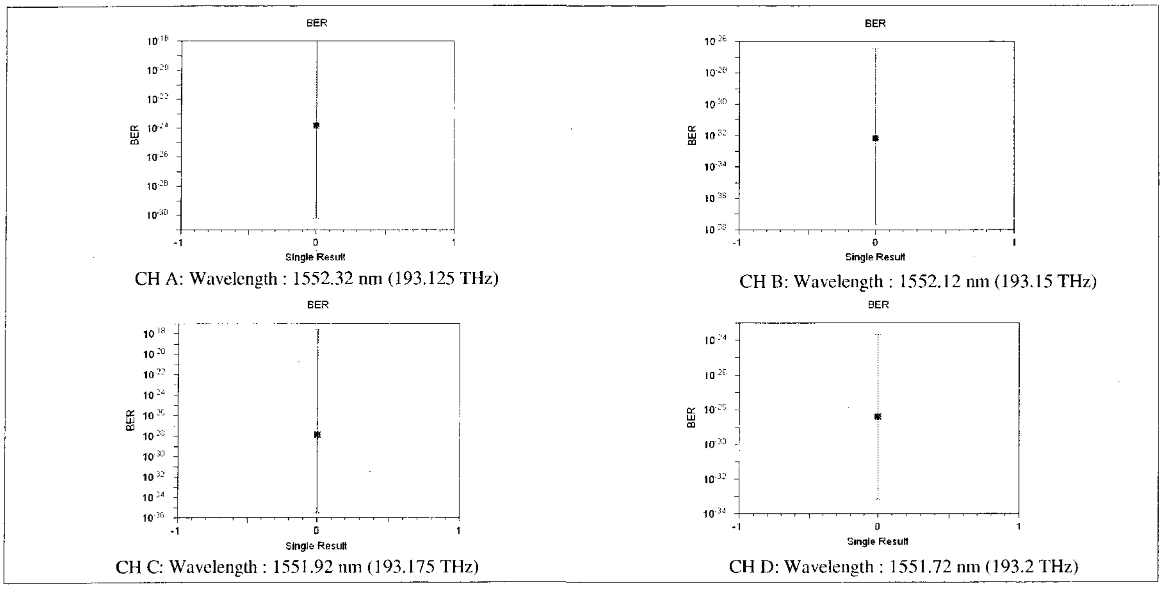

CH A: Wavelength : 1552.32 nm (193.125 THz)

CH B: Wavelength : 1552.12 nm (193.15 THz)

CH C: Wavelength : 1551.92 nm (193.175 THz)

CH D: Wavelength : 1551.72 nm (193.2 THz)

Figure 18: BER for A,B,C, and D channels in Figure 13

The Q factor readings for the four monitored channels in Figure 13 are shown in Figure 19. It was mentioned in section 1.4.1.2.4 that FEC is a technique that adds overhead bits to the signal in order to make it easy for receiver detection, and when implemented, much lower rates of BER can be accepted. The eye patterns, along with the BER and Q factors, indicate that FEC will not be required in PON with the 25 GHz channel spacing. The summary of the performance parameters with and without using the FEC are listed in Table 4 to show the margin provided and to indicate the system improvements with FEC.

Table 4 shows that the simulation model for PON system performance meets the minimum standards of 10^{-9} for BER where the system has some system margins for the Q factor[21], and accordingly, FEC will not be required in the proposed solution in this dissertation for PON security enhancement.

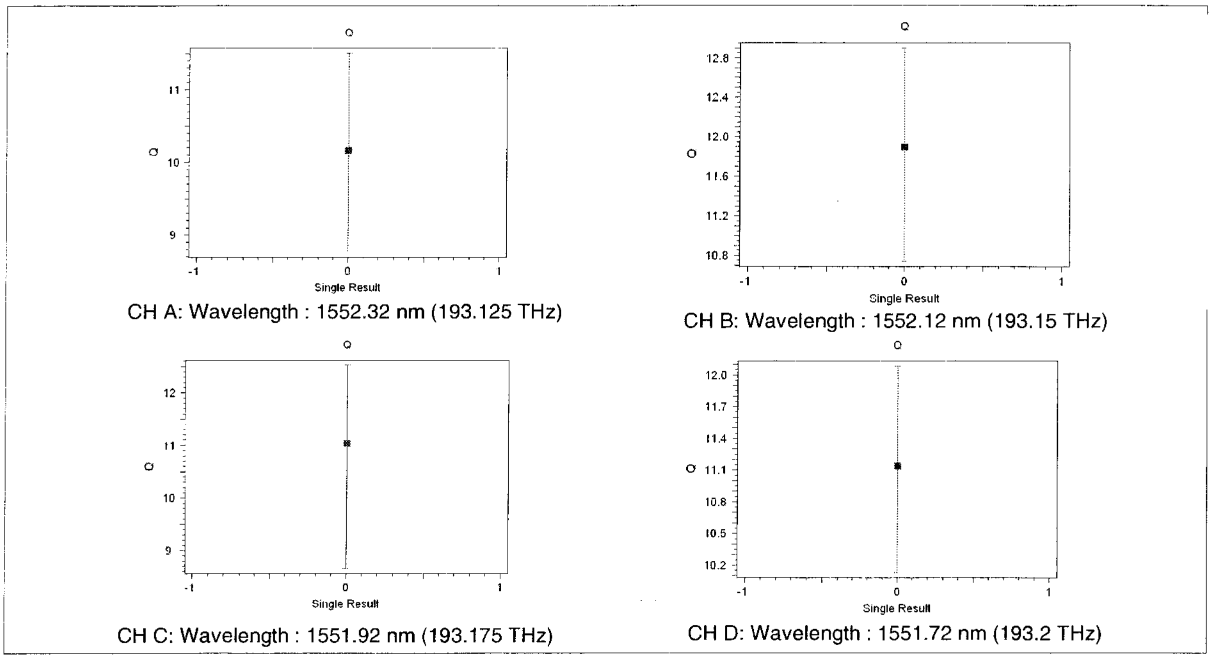

CH A: Wavelength : 1552.32 nm (193.125 THz)

CH B: Wavelength : 1552.12 nm (193.15 THz)

CH C: Wavelength : 1551.92 nm (193.175 THz)

CH D: Wavelength : 1551.72 nm (193.2 THz)

Figure 19: Q-factor for channels A, B, C, and D channels of Figure 13

[21] Margin for Q factor is an expression for the simulation Q (dB) less the required Q before FEC (dB).

Table 4: BER and Q factors readings for A, B, C, and D channesl of Figure 13

Performance Budget	Channel A	Channel B	Channel C	Channel D
1. Simulation Q (dB)	20.14	21.51	20.86	20.94
2. Simulation BER	1.43E-24	6.41E-33	1.29E-28	4.09E-29
3. BER Requirement	1.00E-09	1.00E-09	1.00E-09	1.00E-09
4. Required Q (dB)	15.56	15.56	15.56	15.56
5. Required Q before FEC (dB)	10.44	10.44	10.44	10.44
6. Required BER before FEC	4.41E-04	4.41E-04	4.41E-04	4.41E-04
7. Q factor System Margin (dB)	9.7	11.07	10.42	10.5

In addition to the previous plots for performance parameters and metrics, a check for the spectrum around channel center frequency used for assessment of channel stability as required is discussed in section 1.3. Each absolute wavelength supports operating with small channels spacing in DWDM operation requires good stability and to be confined around the base frequency for each channel. Using the simulated spectrum analysis, the stability of the monitored channels around their center frequency shown in Figure 20 illustrates the maximum variation around 5 GHz to each side of the channel center frequency, which is less than the channel spacing used between all channels (25 GHz).

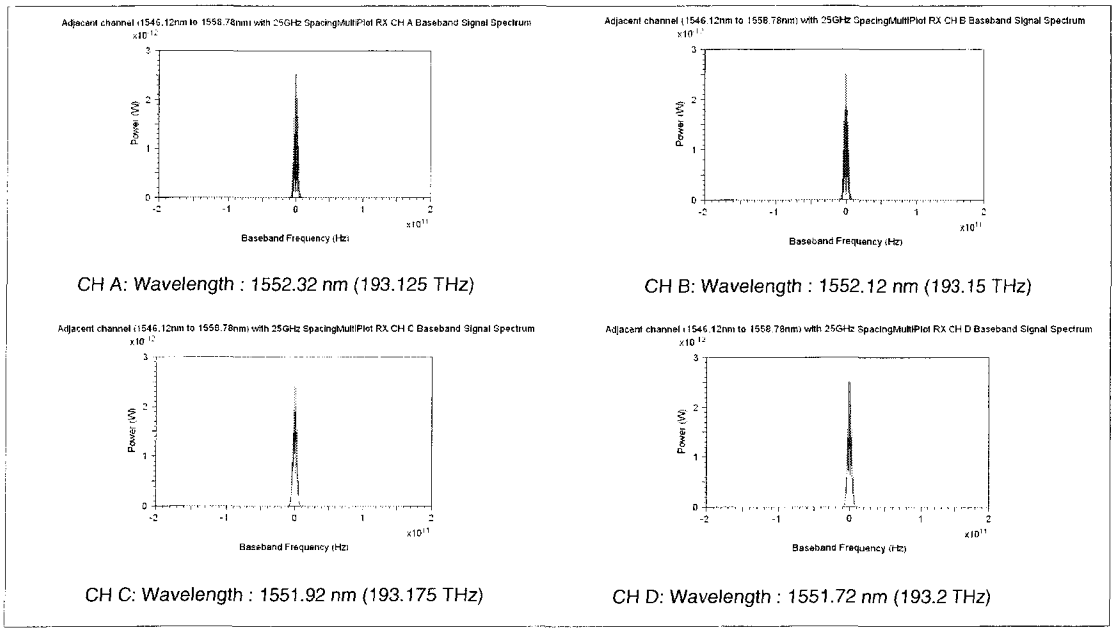

CH A: Wavelength : 1552.32 nm (193.125 THz)

CH B: Wavelength : 1552.12 nm (193.15 THz)

CH C: Wavelength : 1551.92 nm (193.175 THz)

CH D: Wavelength : 1551.72 nm (193.2 THz)

Figure 20: Stability A, B, C, and D channles in Figure 13 around center frequency

The discussions in section 1.4.1.1 included the problems associated with impairment in a WDM system, especially for small and equal spacing between channels in DWDM networks. The signal magnitudes recorded for the four monitored channels are shown in Figure 21 with monitoring taken immediately after the coarse optical filtering for each channel (A, B, C, and D). The signal plots show a low level of interference from adjacent channels, however, their effects are minimal, which confirms that fiber non linearities are minimal for short distances specially if dispersion is managed through the use of NZ-DSF.

In order to demonstrate the level of interference for lower channel spacing, the same simulation model in Figure 13 subjected DWDM to smaller channel spacing along with the proper frequency grid based on 12.5 GHz (.1 nm) using (4). The interference for the 12.5 GHz channel spacing is higher, as shown in Figure 22, for a single channel monitored channel, and this can influence higher cross talk between adjacent channels as compared to the case of 25GHz channel spacing in Figure 21.

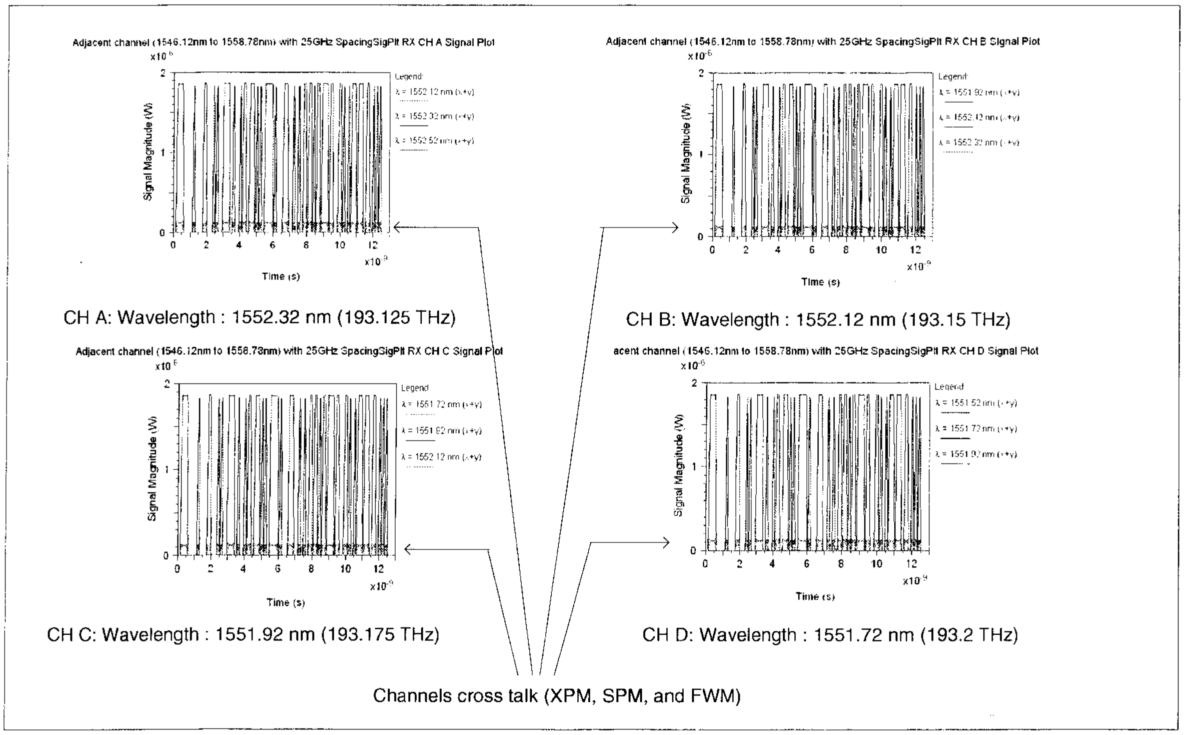

CH A: Wavelength : 1552.32 nm (193.125 THz)

CH B: Wavelength : 1552.12 nm (193.15 THz)

CH C: Wavelength : 1551.92 nm (193.175 THz)

CH D: Wavelength : 1551.72 nm (193.2 THz)

Channels cross talk (XPM, SPM, and FWM)

Figure 21: Cross talk between adjacent channels in Figure 13

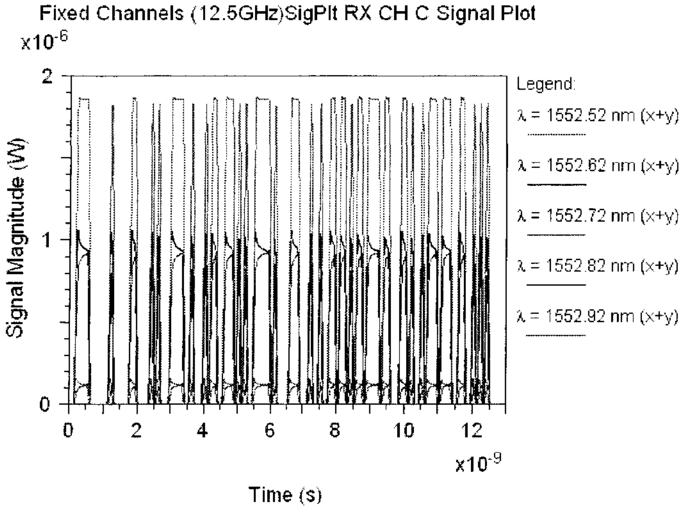

Figure 22: Increased cross talk with 12.5 GHz spacing in Figure 13

The implementation of lower channel spacing, such as 12.5 GHz, enhances proposed security due to the double wavelengths provided (≅ 400 wavelengths), and this makes the wavelength grid matrix in (5) larger such that wavelength sequences are longer.

The feasibility of using 12.5 GHz channel spacing and minimizing cross channel interferences as shown in Figure 22 is possible, however, the solution will be expensive since FEC is required in this case. Also, there are stringent requirements on optical components in terms of technical specifications, in addition to operational requirements in terms of the way wavelengths are arranged in the grid matrices in (5) to avoid adjacent wavelengths. This dissertation continues to implement 25 GHz channel spacing, while 12.5 GHZ is left for future research work.

3.5.2.2 Simulation of Wavelength Hopping Mode in PON

The approach to simulation of wavelength hopping is based on statistically assigned 63 wavelengths to each hop allocated in a single file (Fx) with each hop using a different file from the five files (F1–F5) representing five hops. Wavelengths in each file are used to tune optical transmitters and filters, and the same approach is used in monitoring four channels (A, B, C, and D). The wavelengths of each file are extracted from available wavelength sequences generated per equation (3) and listed in Appendix D, and the frequency of each channel (wavelength) shown for F1, F2, F3, and F4 is in Appendix E.

The same PON simulation model in Figure 13 is used to run the simulation for wavelength hopping input files for each hop with a data rate of 10 Gbps (similar to the adjacent channels simulation). The setup for the four monitoring channels (A, B, C, and D) will be arbitrary from the specific file used in the simulation and not adjacent channels. The channels monitored in both adjacent channels and hopping channels are shown in Table 5.

The wavelength hopping simulation is more open to all C and L bands 1529.75 nm (195.975 THz) to 1569.59 nm (191.0 THz), which is different from the case for the simulation of the adjacent channels, however, the source of the hopping sequences are from those established by (3) and documented in Appendix D. The simulation results for a single first hop in the sequence of file F1 in Appendix E will be shown here, while the results of the simulation from running the other files, the F3, F4, and F5 files, are documented in Appendix F. The simulation of the hopping mode starts similar to the adjacent channels simulation and the spectrum of the channels from running file F1 monitored after the 1:64 splitter is shown in Figure 23, which is different from the case for adjacent channels in Figure 14.

In addition, Figure 24 shows the signal plot for the wavelengths (channels) on the shared wavelength. The hopping channels simulation shows that all channels exhibit the same power level for all channels on the shared fiber link as shown in both Figures 23 and 24.

The eye patterns monitored on channels in the hopping mode simulation using wavelengths in file F1 are shown in Figure 25, which indicates wide eye opening and is considered a good preliminary sign of good quality of signals received.

Table 5: Channels A, B, C, and D monitored hopping wavelengths simulation in Figure 13

CH	**Adjacent Channels** Wavelength (Frequency)	**File F1 Channels** Wavelength (Frequency)	**File F2 Channels** Wavelength (Frequency)	**File F3 Channels** Wavelength (Frequency)	**File F4 Channels** Wavelength (Frequency)	**File F5 Channels** Wavelength (Frequency)
A	1553.32nm (193.125THz)	1544.13nm (194.5THZ)	1552.12nm (193.15THz)	1546.72nm (193.825THz)	1534.05nm (195.425THz)	1548.71 (193.575THz)
B	1552.12nm (193.15THz)	1559.39nm (192.25THz)	1557.36nm (192.5THz)	1547.92nm (193.675THz)	1566.52nm (191.375THz)	1560.00nm (192.175THz)
C	1551.92nm (193.175THz)	1548.91nm (193.55THz)	1568.16nm (191.175THz)	1545.32nm (194.0THz)	1541.13nm (194.425THz)	1539.57nm (194.725nm)
D	1551.72nm (193.2THz)	1565.50nm (191.5THz)	1561.01nm (192.05THz)	1562.23nm (191.9THz)	1537.20nm (195.025THz)	1537.40nm (195.0THz)

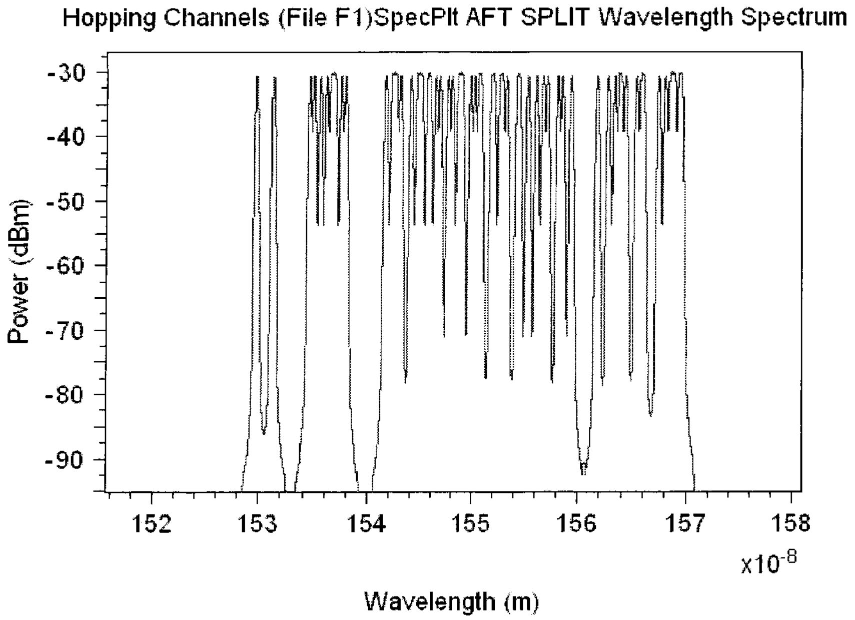

Figure 23: Spectrum of simulation channels in File 1

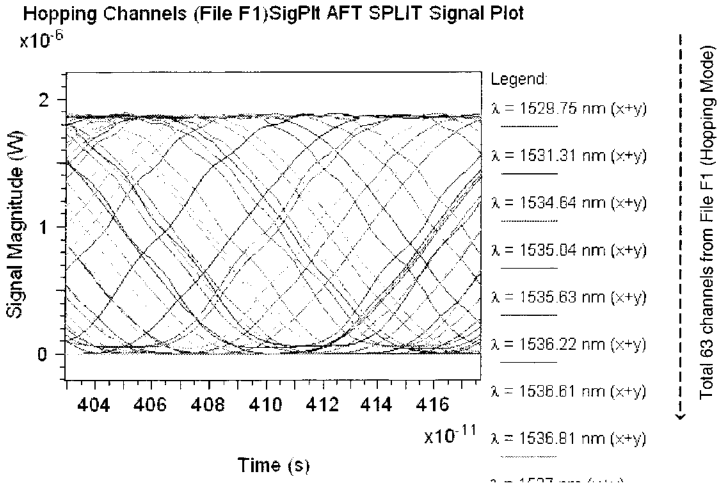

Figure 24: Wavelengths used from file Fl after the 1:64 splitter of Figure 13

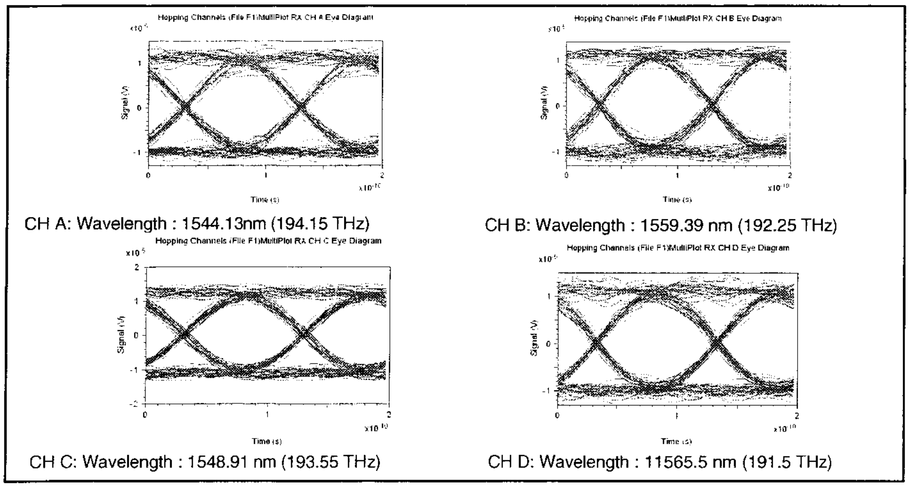

CH A: Wavelength : 1544.13nm (194.15 THz)

CH B: Wavelength : 1559.39 nm (192.25 THz)

CH C: Wavelength : 1548.91 nm (193.55 THz)

CH D: Wavelength : 11565.5 nm (191.5 THz)

Figure 25: Eye patterns for A, B, C, and D channels of Figure 13

Similar to the simulation of adjacent channels, the same PRBS signal is used to modulate the 63 wavelengths in the F1 file of hopping wavelengths as a common input source to all channels, and the same signal is reproduced at the four monitored channels A, B, C, and D of Figure 13 as shown in Figure 26.

Figure 27 and Figure 28 show BER and Q factors, respectively, as does Table 6, for the hopping mode simulation running under channels in file F1. There is no impact on channel frequency stability as shown in Figure 29 compared to the adjacent channel frequency stability shown in Figure 20.

The simulation model running under wavelengths hopping using channels from file F1 provides 63 channels with unequal spacing between channels on the shared fiber link as shown in Figure 23. This helps in reducing channel cross talk where it was found that channel interference due to cross talk and fiber impairment is reduced to one channel out of the four on one of the monitored channels, as shown in Figure 30, while in the case of adjacent channels all channels had cross talk on all channels, as shown in Figure 21. This is an improvement, but even though the impact was minimal for the cross talk in either case, careful assignments of wavelengths in the master wavelength grid matrix in (5) is still a good practice that helps reduce cross talk between channels.

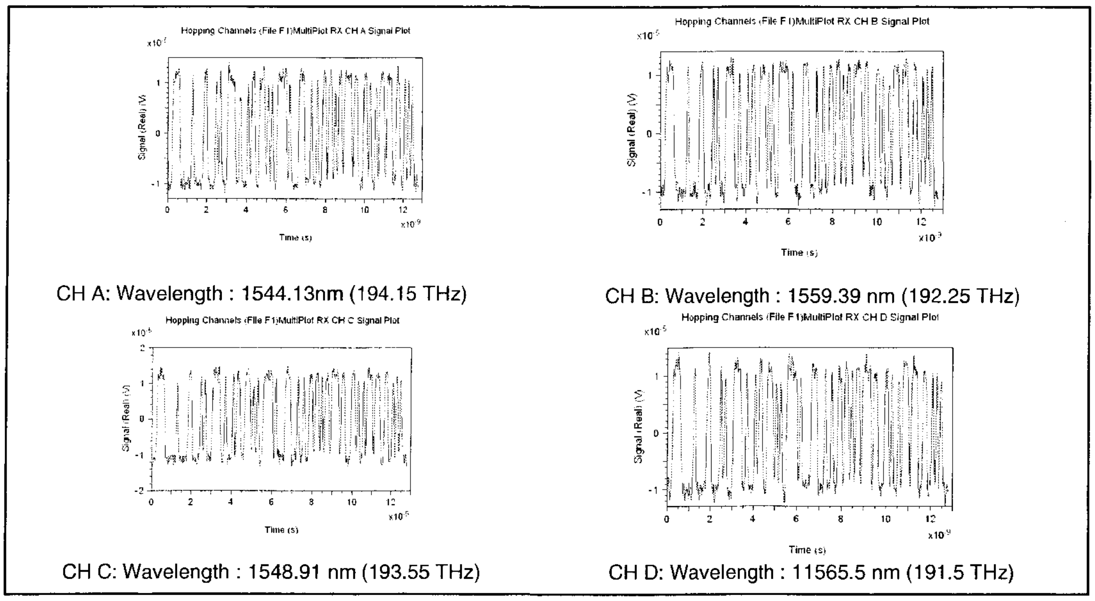

CH A: Wavelength : 1544.13nm (194.15 THz)

CH B: Wavelength : 1559.39 nm (192.25 THz)

CH C: Wavelength : 1548.91 nm (193.55 THz)

CH D: Wavelength : 11565.5 nm (191.5 THz)

Figure 26: Signal at A,B,C, and D channels output in Figure 13 using F1

Table 6: BER and Q factors readings for hopping channels A, B, C, and D of Figure 13

Performance Budget	Channel A	Channel B	Channel C	Channel D
1. Simulation Q (dB)	19.15	2.10E+01	20.12	20.56
2. Simulation BER	6.16E-20	1.12E-29	1.92E-24	7.50E-27
3. BER Requirement	1.00E-09	1.00E-09	1.00E-09	1.00E-09
4. Required Q (dB)	15.56	15.56	15.56	15.56
5. Required Q before FEC (dB)	10.44	10.44	10.44	10.44
6. Required BER before FEC	4.41E-04	4.41E-04	4.41E-04	4.41E-04
7. System Margin (dB)	8.71	1.06E+01	9.68	10.12

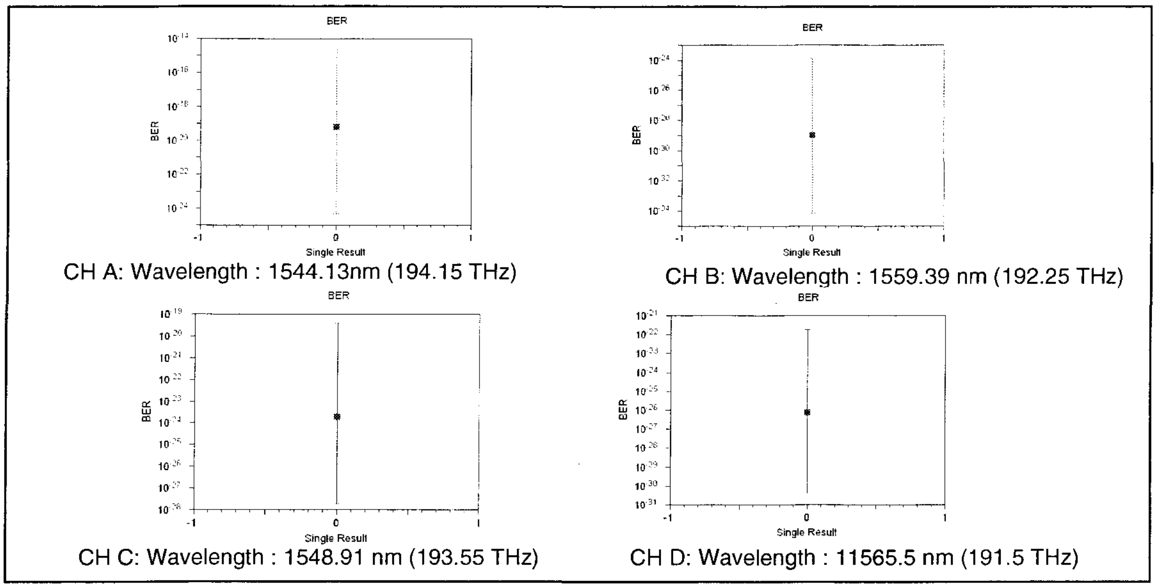

CH A: Wavelength : 1544.13nm (194.15 THz)

CH B: Wavelength : 1559.39 nm (192.25 THz)

CH C: Wavelength : 1548.91 nm (193.55 THz)

CH D: Wavelength : 11565.5 nm (191.5 THz)

Figure 27: BER readings at channels A, B, C, and D of Figure 13

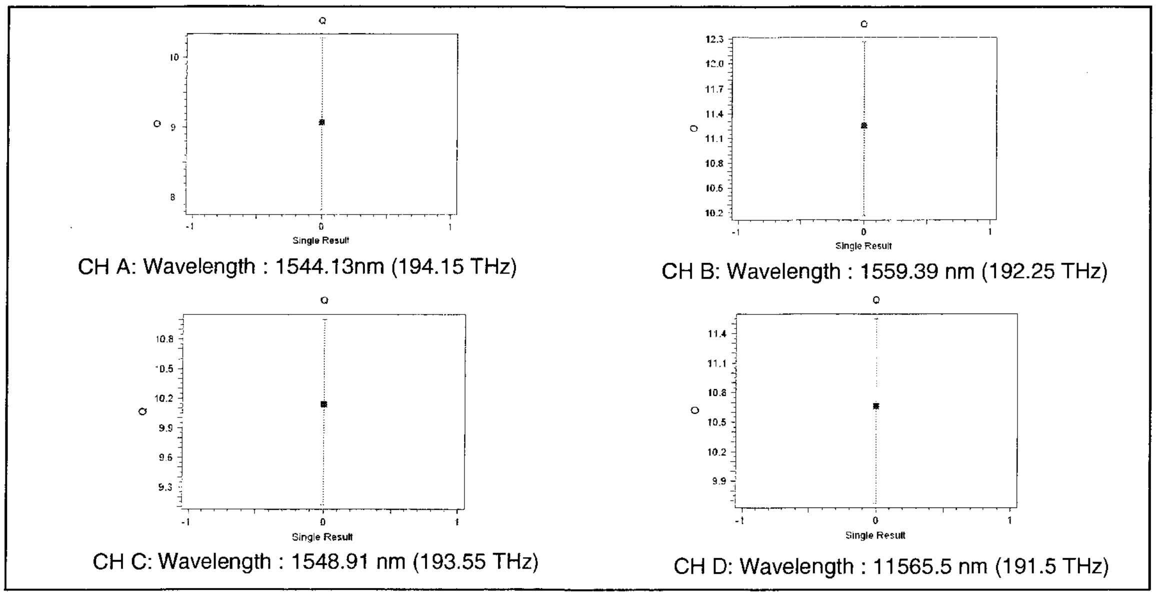

CH A: Wavelength : 1544.13nm (194.15 THz)

CH B: Wavelength : 1559.39 nm (192.25 THz)

CH C: Wavelength : 1548.91 nm (193.55 THz)

CH D: Wavelength : 11565.5 nm (191.5 THz)

Figure 28: Q-Factor at channels A, B, C, and D of Figure 13

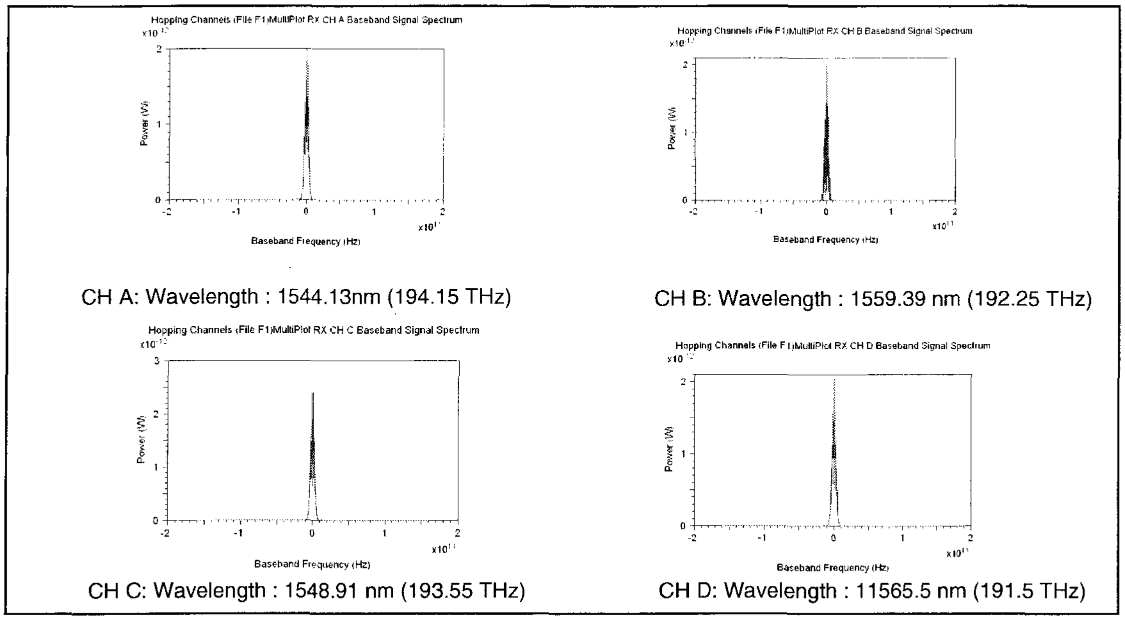

CH A: Wavelength : 1544.13nm (194.15 THz)

CH B: Wavelength : 1559.39 nm (192.25 THz)

CH C: Wavelength : 1548.91 nm (193.55 THz)

CH D: Wavelength : 11565.5 nm (191.5 THz)

Figure 29: Frequency stability of channels A, B, C, and D of Figure 13

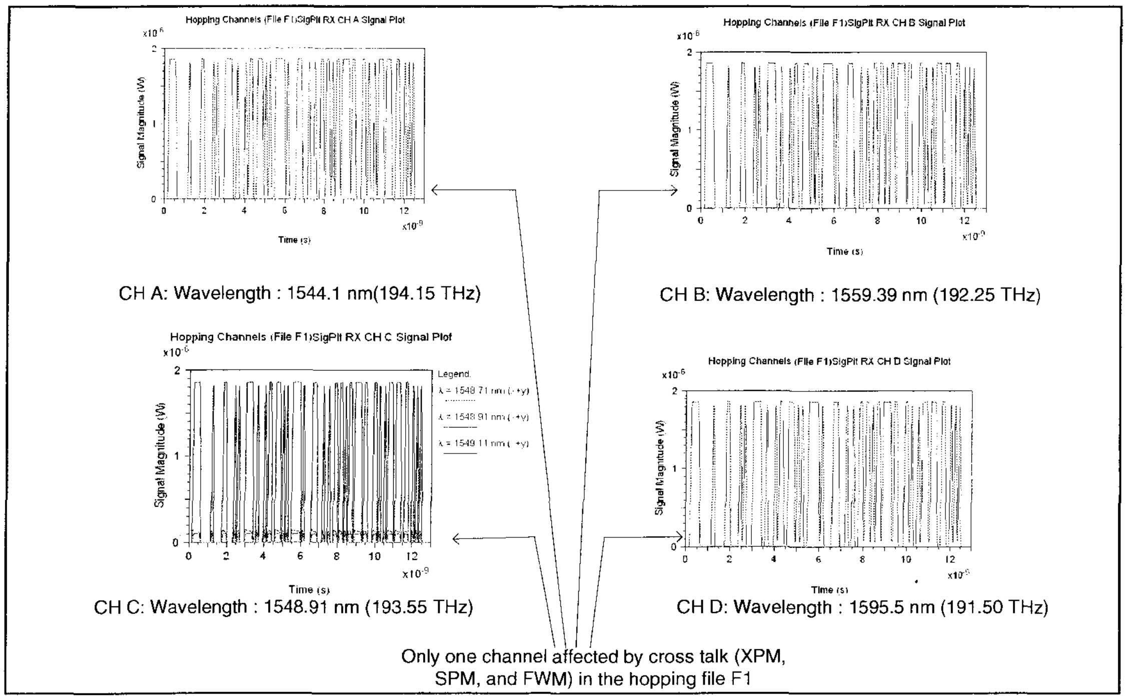

CH A: Wavelength : 1544.1 nm(194.15 THz)

CH B: Wavelength : 1559.39 nm (192.25 THz)

CH C: Wavelength : 1548.91 nm (193.55 THz)

CH D: Wavelength : 1595.5 nm (191.50 THz)

Only one channel affected by cross talk (XPM, SPM, and FWM) in the hopping file F1

Figure 30: Cross talk reduction for channels A, B, C, and D of Figure 13

3.6 Implementation and Deployment Considerations

The results in section 3.5 provided proof that the concept for using DWDM in a hopping mode is feasible in the proposed solution in this dissertation and provides foundation for a total solution toward a secure PON. This is considered a big step in the conceptual approach to security enhancement, however, there are many other nontechnical requirements that need to be addressed and will be mentioned in this section; details of those requirements and the solution to them are outside the scope of this dissertation.

3.6.1 The Role of Cryptography in the Proposed Security Enhancement

The function of cryptography is to provide protection of data in the presence of an adversary, and the approach to security enhancement in this dissertation is built on a system that has all traffic encrypted in both directions of the PON topology shown in Figure 2. In cryptography, it is important to determine how immune the signals are to eavesdropping, and determining the reliability of the network is also crucial, since without satisfactory QoS guarantees, cryptographic issues may be moot [52].

The approach is similar to any other security implementation in the sense that in the absence of cryptographic techniques, the solution may still provide other weak security measures including identification through a password or implicitly through the use of a network port. However, the assumption in the proposed solution to security enhancement in PON is that any cryptographic implementation needs to be part of the network security by using the cryptography in the first and second layers of the OSI model (physical and data link layers), which will make it transparent to the applications and other layers above it. This approach for cryptography at lower levels is intended for authentication, integrity, and confidentiality between the OLT and ONUs.

It is established that there are cost advantages with Ethernet-based access networks as opposed to ITU-T G983.1 standards that uses ATM, and there have been new demands for security features in the Ethernet switches [89]. The cryptography at lower layers as proposed in this dissertation conceals SA and DA that are part of Ethernet frames where they are no longer exposed. The system will require buffers and encryption/decryption functional modules before OLT and after each ONU, and the keys for each ONU will be different from the keys for others.

For a user's application program, applications security can be used as additional security mechanisms that may be deployed at higher layers of the OSI reference model.

The encryption of the upstream transmission prevents interception of the upstream traffic when a tap is added at the PON splitter and minimizes the problems that are currently considered as security vulnerabilities as discussed in section 2.1. For example, it is possible to encrypt upstream traffic since the wavelength sequences provided by (3) is considered as a signature and shared secret between the OLT and ONU, and this signature provides protection against ONU impersonation discussed in section 2.1.2 where protected registration data arrives from ONUs.

The type of encryption is left to specific implementations and is to be decided in the design details depending on the type of PON, whether it is used by a service provider and residential users, or the PON belongs to a financial, government, or any other form of institution. In some cases, OLT may need to accommodate different types of encryption types in order to support different granularity of encryptions of specific ONUs, which adds cost to the PON infrastructure.

Some of the encryption standards that can be used include AES, which provides an encryption standard used to protect confidential information like financial data for government and commercial use. An alternative is the data encryption standard (DES) and triple DES encryption algorithm. DES is arguably the most important and widely used cryptographic algorithm. However, even though it has been reported in numerous literature that usefulness of DES is now quite limited because of the fact that the DES key can now be easily cracked after several hours of number crunching, the approach in this dissertation is intended to make it difficult for an eavesdropper to capture a good sample of the traffic that can be used to crack the key of the cryptographic system.

With slow wavelength hopping and the size of transmission being Ethernet frames or complete packets, keys of any cryptographic standard are not impacted since various keys to support block sizes of 128-bit and key sizes of 128-bit, 192-bit, 256-bit, or even the future key sizes as large as 1,024 bits can be easily accommodated. The length of keys affects the processing power of the end machines, and encrypted material in PON is simply treated as data being transmitted.

3.6.1.1 Combining Wavelength Hopping with Block Cipher Encryption

A block cipher encryption technique, such as AES discussed in [69], encrypts a block of data using a secret, symmetric key. For an attacker to start cryptanalysis of an encrypted block to try to discover the key, the attacker must have the entire encrypted block. Using our wavelength hopping system, an attacker can be listening on one or more wavelength channels, eavesdropping on transmissions. If a block encryption algorithm is used with a block consisting of M slots, then cryptanalysis will be unsuccessful unless the attacker successfully acquires M consecutive slots, which are encrypted as a block. Therefore, using wavelength hopping together with block cipher encryption presents the attacker with the following obstacles that have to be overcome, which makes it harder for the attacker to launch a potentially successful attack:

- The attacker must listen to M successive transmissions on M channels (wavelengths), which are chosen according to equation (3).
- The attacker must determine the beginning of the block, which can be any wavelength in λ_s expressed in (3) as the beginning of the block.
- The attacker must launch cryptanalysis on the acquired block.

Therefore, the difficulty of a cryptanalysis attack is increased by including the first two factors above, and the probability of a successful cryptanalysis is now reduced significantly

3.6.2 Keys Distribution

Traditional cryptosystems are based on the secret key or symmetric model, and they have been the focus in the world of cryptography where keys are generated by a mathematical algorithm that generally involves very large prime numbers. With a public key system, information encrypted with a particular public key can be decrypted only by using the corresponding private key. Cryptography where implementation takes place in the higher layers of OSI models is not impacted in the proposed approach for security enhancement in this dissertation.

However, new keys are added as part of the proposed approach for the security enhancement as discussed in section 2.5, namely, the wavelength grid matrix selected for operation (W_{mn}^{G}), the wavelength sequences assigned to each ONU (λ_s), and the order of sequencing the wavelength sequences assigned to a single ONU. Those are small files and can be made transparent to the application layers since they affect interfaces at both ends of PON, namely the OLT and ONUs. There are many ways to distribute the keys, and the distribution mechanism can be left to design and implementation, which is not the focus of this dissertation.

3.6.3 ONUs Authentication

Cryptographic techniques to identify the source of data and to protect data from unauthorized modification have been used as a mechanism of authentication. Already the IEEE 802.1X specification offers an effective framework for authentication and controlling user traffic to a protected network[89]. A security model and security protocol to support authentication in an IEEE 802.3ah (EPON) based network proposed in [59], is based on encryption services in the lower layers using public key exchange and a key establishment protocol with authentication of the ONU and user made separately. This is similar to the approach in the proposed solution, where user identification is based on other means and ONU authentication is based on the wavelength sequence assigned to the ONU.

IEEE 802.1X can be implemented as a user authentication mechanism in the proposed approach to security enhancement in PON since it is involved mostly with the higher layers of OSI models. Authenticity on the other hand can be also in the form of group authenticity or source authenticity [53], which means that it is possible in the proposed solution to identify a particular sender ONU based on the wavelength sequences assigned to the ONU and be capable of synchronizing with the OLT based on the hopping pattern in the wavelength sequence. This allows only authorized ONUs with the correct signature to be able to follow reception or transmission to or from the OLT. This is considered as an OSI lower layer authentication scheme between the OLT and ONUs, which is transparent to the higher levels of the OSI mode.

The various granularities of security levels and authentication of ONUs dictates the mechanisms to be deployed focused on having the OLT recognize the correct ONU with proper authentication and source identification against an eavesdropper.

3.6.4 Timing and Synchronization

The current IEEE 802.ah standard for EPON in [13] includes multi-point control protocol MPCP, which specifies P2MP communication between PON OLT and ONUs. MPCP is a MAC layer protocol supported by bridging elements with functions that provide ONT/ONU timing synchronization, implementation of auto discovery, and bandwidth/timeslot assignments to ONUs, in addition to ranging[22], which is required to be done frequently for measurement of round trip time (RTT) to all ONUs.

The proposed solution in this dissertation handles data rates at 10 Gbps even though previously the technical hurdle of achieving synchronization at speeds higher than 622 Mbit/s (upstream) was quite high given the physical layer specification of BPON based on ITU-T G983.1 standard [90]. Speeds of 1 Gbps is already the standard in the IEEE 802.3ah EPON [13] and 2.4 Gbps in standards such as GPON ITU-T G.984.1.

The proposed security enhancement for PON in this dissertation requires that functions of PMCP be modified to handle synchronization requirements, with imposing restrictions on the size of frames/packet by making them all equal to a fixed length to guarantee orthogonal operation between wavelength sequences without any overlapping. In addition, requirements for synchronization include retaining the preceding and trailing of frames/packets by the IGP shown in Figure 5.

It is absolutely required that all ONUs use a slave clock to the OLT master clock in order to guarantee synchronization of wavelength hopping, and that master clock data be extracted by ONUs similar to the current clock data recovery (CDR) used in the physical medium layer in ITU-T G983.1 [12], or clock recovery unit (CRU) in IEEE 802.3ah [13]. The assumption made in this dissertation is that solving the requirements for clock and synchronization are part of the detailed system design and outside the scope of this dissertation.

[22] Ranging is the process of finding the round trip time to each ONU where the time is updated to maintain synchronization of PON operation.

Other considerations in the synchronization process must account for timing related to other parameters including those in Table 7 and additional parameters that are part of the final network architecture and topology.

Other important factors for all wavelength sequences, shown for example in Appendix D, are synchronized and no overlapping allowed, and it is not practical for an ONU to wait until the end of sequence is executed in order to start transmission or reception. Any ONU can join and start at the time slot coinciding with the next hop in the wavelength sequence in (3), and this is a good reason for requiring ONUs and the OLT to have a common reference clock that is controlled and updated by the OLT.

Table 7: Examples of timings that need to be considered in the synchronization

Ethernet frame time	T_E	This is the time required to pass one Ethernet frame across the network To/From ONU Ethernet frame
Ranging time	$T_{R(K)}$	This is used in the measurement of distances to the individual ONUk, which will be a factor for the complete system synchronization. and decides the ranging time, This is also heavily dependent on the topology, and during system installation or new ONUs installed for example, delay lines ma be used to support timing for the system in case one or more ONUs very close to OLT than others.
Guard time	T_g	This is a safety margin time left between messages in order to account for any system latencies no accounted for in other timing schemes.
Laser transmitter tuning speed	T_{LD}	This is the maximum time required for a laser transmitter to switch from one end to the other extreme end of the ITU-T G694.1 wavelength grid.
Laser filter switching speed	T_{FL}	This is the maximum time required for a laser transmitter to switch from one end to the other extreme end of the ITU-T G694.1 wavelength grid.
Tuning (settling) time	Ts	The tuning (settling) time of a tunable optical devices, which is defined as the time-duration from the start of frequency tuning to the time when the tunable transmitter/filter loss converges to within (ffs) dB of its final value at the demanded centre frequency ± half of the 3 dB pass band width.

3.6.5 Physical and Other Forms of Security Measures

The proposed security enhancement for PON in this dissertation does not substitute for other security schemes such as authentication, digital signatures, and encryption to prevent corruption of information, or physical security that could include preventive measures and detection systems at the CO where the OLT is located: personnel access control, security guards, CCTV, alarm systems, etc. In most cases where the threat is generated from within the organization, this is extremely costly in the case cryptography and provided keys, and it is recommended that the keys are set and accessible by, for example, the service provider.

3.6.6 Assignments of Wavelength Sequences and Security Level

Depending on the access network and the type of service provided, assignment of wavelength code matrices must follow the security levels as keys for secure operation. It can be also advantageous for two or three ONUs to share some of the sequences that will provide higher diffusion of data. However, centralized control and a proper algorithm will be required.

3.6.7 Changing Network Wavelength Matrix

The wavelength grid matrix selected for the PON network is the starting point for providing security, and frequent changes protect data against time. The most convenient changes are carried over online and with synchronized clocks in all locations, so it is possible to command all nodes when the change happens.

3.7 Chapter Summary

In this chapter, an approach to provide security enhancement in PON based on the concept of data diffusion through wavelength hopping was presented. Figure 8 provided the top level illustration of a conceptual system that was a process of mapping two matrices, wavelength grid matrices and code matrices, where the outcome was wavelength sequences that are orthogonal to each other in the case of time spreading and wavelength hopping based on the same prime code (symmetric TS/WH) and have excellent correlation properties. In addition, the wavelength sequences increased for the case of pseudo orthogonal where TS/WH uses a different basis for prime numbers and for other coding schemes. Wavelength sequences provide a good source for secure wavelength hopping when assigned to ONUs based on their security levels.

The details of the approach started by establishing an industry standard ITU-T G694.1 wavelength grid as the source for selecting wavelength, followed by formulation of sub grid wavelength matrices. Different coding schemes along with the construction basis TS/WH based on symmetric (Prime/Prime) and asymmetric (EQC/Prime) was presented, in addition to a review of other coding schemes for MW-OOC. It was found that the best code matrices that provide good correlation properties with autocorrelation of 0 and cross correlation of 1 as the desirable properties are those based on TS/WH and symmetric prime numbers (Prime/Prime) where actual wavelengths sequences generated are proved to be orthogonal.

Even though wavelength sequences are generated mathematically, an important part in the proposed security enhancement is to provide proof that the approach is feasible and achievable. A simulation model for a PON was established and DWDM was used with simultaneous transmission of 64 wavelengths in 25 km shared fiber links. Four channels were set up for monitoring purposes in the simulation model with encouraging results about the feasibility obtained using performance metrics such as the BER, which exceeded the minimum requirements for BER of 10^{-9}. All channels showed good quality of signals and BER better than 10^{-20}, and the eye pattern showed a wide opening providing confirmation of good signal characteristics.

Additional brief discussions about implementation and deployment topics were provided that included, for example, the role of cryptography, keys distribution, and timing considerations, however, the details of those topics are outside the scope of this dissertation since they are specific to the implementation and detailed design of projects' unique requirements.

The results of wavelength sequences generation and results of simulations provided foundations to move to the next chapter, which discusses performance evaluation of the proposed approach to PON security enhancement.

CHAPTER 4: SECURITY PERFORMANCE EVALUATION

4.1 Background and Motivation

As mentioned in section 2.4, high bandwidth offered by fiber cables is seen as the media of choice to meet demand for bandwidth where optical network designers are not concerned about electromagnetic emissions, for example. However, demand for high bit-rate in fiber cables is driving WDM technology toward DWDM where multiplexing capacity increases and careful design calls for avoidance of inter channel interference within the optical network itself, as well as tapping and eavesdropping by outsiders.

The importance of PON as low cost and capable of meeting high bandwidth at the Giga bits rates makes them the choice for applications in many areas such as storage area network (SAN) and network area storage (NAS). Both SAN and NAS are beginning to converge as NAS file managers become more specialized and use managed SANs for back-end storage. A NAS head with a SAN back end is functionally identical to a SAN using a metadata controller to provide file-based access [99], and PON provide the high bandwidth required for such storage networks.

In the multimedia services, using B&S features PON as a massive distribution tool by service providers that can potentially replace coaxial cable in the future. Current practices using encryption techniques, applied to IP over LAN include video-digital encoding techniques such as motion picture expertise group (MPEG2), which is a family of standards used for coding audio-visual information (e.g., movies, video, and music). MPEG is a digital compressed format used to provide reductions in bandwidth, which was not intended for security of transmission in the first place [100]. The use of wavelength hopping as a way to provide protection for downstream traffic in PON provides an approach for protection against theft of service. One application can be, for example, providing protection to digital video broadcast (DVB) standard based systems that have an enhanced transport stream structure defined in MPEG, which provides a very robust transmission system that is capable of supporting broadband constant bit-rate traffic such as high quality video in the same carrier or multiplex that carries computer data.

The low cost of passive devices and reliability of fiber connectivity compels many services to merge into one connectivity such as TPS (audio, video, data) in addition to mass storage networks, etc., where security concerns become of paramount importance due to dependency for multiple services in one connection.

4.2 Assumptions about Attackers

The objectives of attackers/eavesdropper were discussed in section 2.1, and in this dissertation, it is assumed that an attacker is monitoring the shared fiber link as shown in Figure 6 with the major objective of deducing the order of specific ONUs' wavelength sequences generated by (3) (similar to deducing the key in cryptography). Learning the contents of messages intercepted from eavesdropping on the shared fiber link of Figure 6 requires additional cryptanalysis that is outside the scope of this dissertation, but the proposed solution provides difficulty in collecting that sample. The strength of the proposed security enhancement in PON resides entirely in the difficulty in determining the sequence specific to an ONU and not in the algorithm used to generate the wavelength sequence in (3).

Assumptions are made that no collaborations between nodes exist since the nature of data transmitted could be "personal" or sensitive to the organization in some cases. In addition, assumptions are made that attackers are technologically sophisticated and know a great deal about signals being transmitted in PON, and in particular, know what types of signals are being exchanged between an OLT and ONUs. The knowledge about the signal includes technical information such as data rates, type of encoding, structure of codes, synchronization, beginning and ending of the bits/messages, and basically the basis of the operation of the secure system being attacked, but do not have the particular codes being used by the OLT and ONUs. The assumptions are based on the well-known Kerckhoffs' principle in cryptography [69], which essentially states that one should assume that the eavesdropper knows everything about the cryptographic algorithm except for the key that each user employs.

4.3 Performance Evaluation for the Proposed Security Enhancement

Simulation of DWDM with 25 GHz channel spacing in a shared fiber link was provided in section 3.5 with results in Figures 14 and 15 for 64 adjacent channels, in addition to results in Figures 23 and 24 for wavelength hopping mode that showed equal power level across all channels. Simulation accounted for impairment factors such as time jitter, fiber non linearities, cross channel interferences, dispersion, noise, etc., which are factors in the power level and signal quality degradation, and the result of simulation provided required proof of the concept that the PON supports DWDM. However, this dissertation discusses the security approach for PON where performance analysis is still required to provide proof about the protection level provided against brute force attack type external to PON.

In order to evaluate the strength of the security enhancement against malicious attacks on PON such as eavesdropping, an analysis considers the situation where an attacker managed to get some wavelength sequences recorded online from the B&S traffic. The job of the attacker is to run an analysis on the collected sample in order to deduce wavelength sequences or the three new keys introduced in the proposed approach for security enhancement that include: the wavelength grid matrix W_{mn}^{G} selected for PON operation, code matrices, C_{ml}^{y}, and the order of implementing the wavelength sequences λ_s introduced in the contribution section 2.5. The three keys are required to deduce the wavelength sequence, and full independency exists between the selection of any key from each other, which means that there are no restrictions of assignment of certain wavelength sequences to certain ONUs and no restrictions on combining certain wavelength matrices with certain code matrices.

Start with the selected wavelength grid matrix $\mathrm{W}_{\mathrm{mn}}^{\mathrm{G}}$ in (5) for PON operation, which is one of many available formats expressed in (6) as $G_{max}= (n!)^m$. However, n out of G_{max} from selected $\mathrm{W}_{\mathrm{mn}}^{\mathrm{G}}$ will be subjected to columns cycling to produce a total of n sub grid matrices $\mathrm{W}_{\mathrm{mn}}^{\mathrm{xG}}$ as shown in Figure 10. This means that the probability of guessing the correct grid matrix $\mathrm{W}_{\mathrm{mn}}^{\mathrm{G}}$ can be expressed as $P_C(W)$ as shown in (17).

$$P_c(W) = \frac{1}{(G_{\max} - n)} = \frac{1}{((n!)^m - n)} \tag{17}$$

The probability of finding the second key, which is the correct wavelength sequence assigned to a single ONUk (λ_s^k) generated by equation (3) requires the knowledge of two components, namely, the wavelength sub grid matrices W_{mn}^{xG} and code matrix C_{ml}^{y} used from those available by the specific coding scheme, which can be symmetric or asymmetric TS/WH, MW-OOC, etc. Each coding scheme provides its own maximum available code matrices designated as Y_{max}. For example, the maximum codes provided by the prime placement operator with prime number *P* as shown in (9) is *(P - 1)*, which represents the lowest code set among other coding schemes as compared to asymmetric TS/WH (EQC/Prime) in (12), which provides $Y_{\max} = P_s(2P_s - 1)$, or the different MW-OOC used, which provide various degrees of cardinality as expressed in (15), which depends on *m, n* and weight *w* and allows cross correlations. It is important to note that because of the correlation control in (15), this implies that there is exclusivity in the selection of codes, and accordingly, there is no independence in MW-OOC codes selection for simultaneous operation as compared to TS/WH codes.

The maximum number of set sub grid matrices (W_{mn}^{xG}) is equivalent to the number of columns (*n*) as shown in Figure 10. Taking the two components of the second key, this implies that the single probability of finding the correct wavelength sequence is expressed as $P_c(\lambda_s)$ as shown in (18).

$$P_C(\lambda_s) = (\frac{1}{Y_{\max}})(\frac{1}{n}) \qquad (18)$$

The probability of finding the third key, which is the sequencing order of wavelength sequences assigned to a single ONU out of the maximum available sequences generated by (3) starts with the expression for maximum wavelength sequences provided by (3) expressed as S_{max} similar to those shown in Appendix D, with a total of 192 generated by (3) for the TS/WH (Prime/Prime) case. Out of S_{max}, the number of sequences assigned to a single ONU is expressed as S_a, where the number of assigned $S_a < S_{max}$ and is based on the security levels of the ONUs.

The number of combinations of S_a that can be selected from S_{max} can be expressed as a combination set (CS_s) of sequences shown in (19).

$$\text{CSs} = \begin{pmatrix} S_{\max} \\ S_a \end{pmatrix} . S_a\,! = \left(\frac{S_{\max}\,!}{(S_{\max} - S_A)\,!} \right) \tag{19}$$

The single probability of capturing a single wavelength sequence is *$P_C(\lambda s)$*, which is the probability of breaking the hopping pattern with correct wavelengths in the sequence out of the combination set in (19) for a single ONU as expressed as in (20).

$$\text{PC}\ (\lambda\text{s}) = \left(\frac{(S_{\max} - S_a)!}{S_{\max}\,!} \right) . (\frac{1}{S_a}) \tag{20}$$

However, a single ONU can have a set of sequences S_a where they can be cycled in a different order, which is the third shared secret key between the OLT and the specific ONU. The order of cycling (executing) assigned wavelength sequences (S_a) can be one of S_a!. The probability in (20) is supplemented with an additional factor ($1/S_a$!) to show the impact of the third secret key and is expressed in (21).

$$\text{PC}\ (\lambda\text{s}) = \left(\frac{(S_{\max} - S_a)!}{S_{\max}\,!} \right) . (\frac{1}{S_a}) . (\frac{1}{S_a\,!}) \tag{21}$$

The effect of cycling order for assigned wavelength sequences when added in (20) is dependent on the number of assigned wavelength sequences (S_a) per ONU, and this is illustrated in Figure 31, which shows the logarithmic relation in (21) for the case of code matrix and wavelength grid matrices used to generate wavelength sequences in Appendix D ($m = l = 12$, $n = 16$).

The contribution of single probabilities expressed (17), (18), and (21), along with the number of users on line (U), can be used to find the overall probability of capturing the correct wavelength sequence $P_C(\lambda_s^k)$ for a single ONU$_\text{k}$ as expressed in (22).

$$\text{P}_\text{C}\ (\lambda_s^k) = \frac{1}{((n!)^m - n)} (\frac{1}{Y_{\max}})(\frac{1}{n}) \left(\frac{(S_{\max} - S_a)!}{S_{\max}!} \right) . (\frac{1}{S_a}) . (\frac{1}{S_a!})\ (\frac{1}{U}) \tag{22}$$

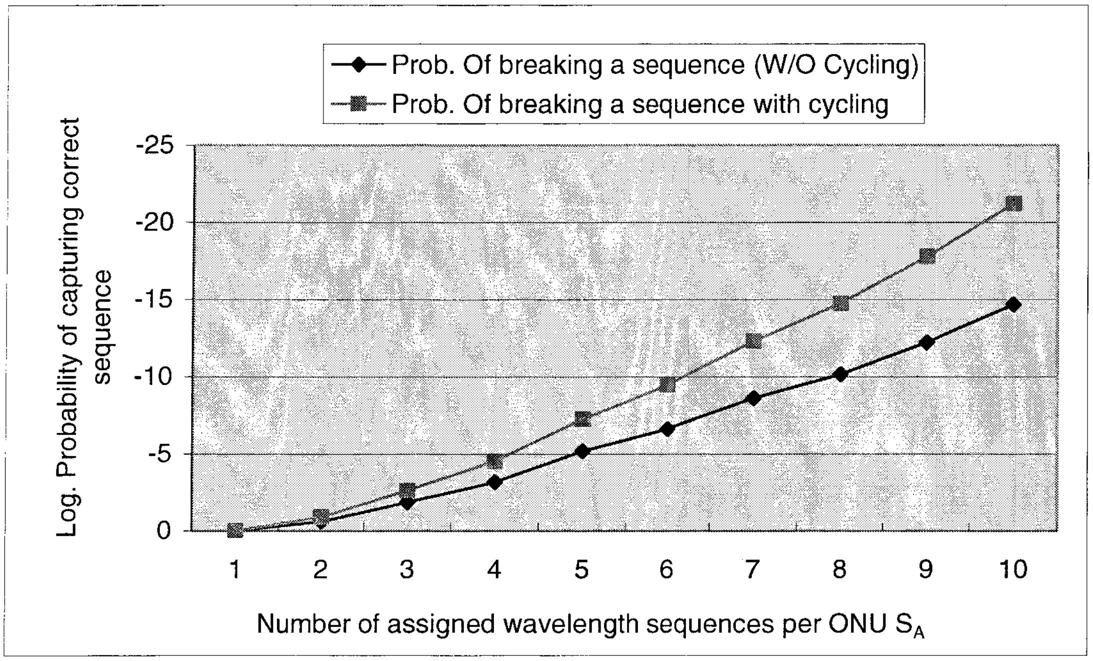

Figure 31: Effect cycling on capturing a sequence for single ONU

The probability expression in (22) provides a foundation to use for the evaluation of the robustness of coding schemes discussed in section 3.3. For example, the effect of the number of wavelength assignments for the case of TS/WH is based on multiple symmetric prime numbers (n), and the number of columns in wavelength grid W^{G}_{mn} matrix $m = 16$ for single user $U = 1$ is shown in Figure 32. The probability of capturing a specific wavelength sequence via an exhaustive shows that in Figure 32 it takes only a few assigned wavelengths (S_a) and small prime numbers to reach the negative mathematical infinity ($-\infty$) of MATLAB®, which is in the order of 10^{-300}.

One important note to (22) is considered in the next section where the analysis for synchronized detection is presented.

In the following analysis, the same assumptions are made about eavesdropper(s) being sophisticated with background as discussed in section 4.2, and managing to get the proper synchronization by exploiting the CDR/CRU discussed in section 3.6.4, with the exact start and end for each single hop and the complete wavelength sequences. The question arises if there is a way to reconstruct specific wavelengths sequences assigned to a single ONU.

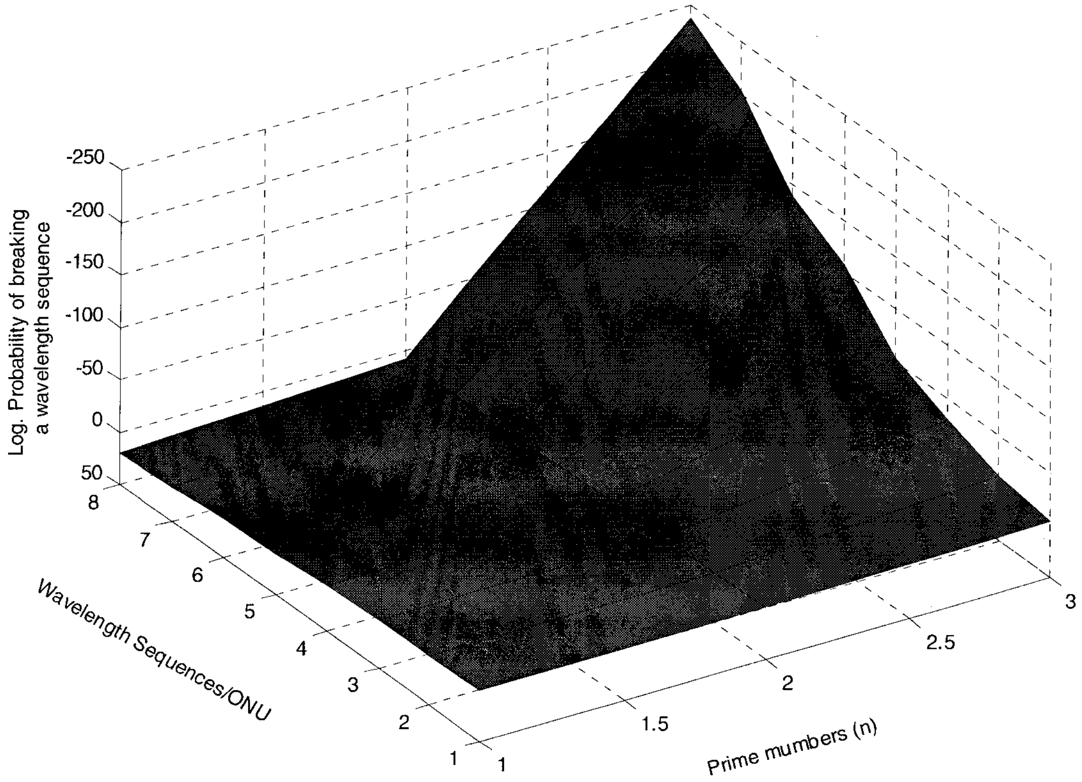

Figure 32: Effect of multiple wavelength assignment per ONU with cycling

4.4 Capturing Wavelength Sequences Via Reverse Analysis

The proposed approach should follow the same philosophy as in cryptography where the strength should be in the key and not the algorithm, and assumes that the eavesdropper has managed to mathematically generate or have access to the complete code matrices C_{ml}^{y} used by the PON such as those in Appendix C. This is the case where independence of probabilities is required for the relation in (18), and the impact on (22) for any conditional probabilities with independent terms leaves the strength of the algorithm in the other two terms of (22), namely, the probabilities of two independent terms for the selected wavelength grid matrix, and the way that wavelength sequences are assigned to ONUs. The contribution of knowing code matrices beforehand depends on the coding scheme, and actually, the effect is minimal for the case of TS/WH based on a symmetric prime number (Prime/Prime).

It is known that each hop in a wavelength sequence is generated by row mapping in (3) between code matrices C^{y}_{ml} and W^{xG}_{mn}. Starting with hop number 1 in wavelength sequences shown in Table 1, total wavelengths in the hop are equal to the number of users *U* (i.e., *U* wavelengths) on the shared fiber link shown in Figure 6.

Starting with the first row of wavelength sub grid matrix W^{xG}_{mn} shown in Figure 10, the position of each wavelength (λ_i) recorded in hop 1 can be in any of the *n* slots (columns) of each one of the *n* sub grid matrices W^{xG}_{mn}. There are *m* rows, and the process is repeated for each hop row, which implies that the probability of a single wavelength (λ_i) to be in the right position in any of the multiple wavelength grid matrices W^{xG}_{mn} can be expressed as $P_C(\lambda_i)$ as shown in (23).

$$P_c(\lambda_i) = (\frac{1}{n^2})^m (\frac{1}{U}) \tag{23}$$

For the case of a single user online (i.e., $U = 1$) (23), this is a situation where recommendations for additional security measures need to be in place as discussed in section 4.5. Figure 33 provides an illustration of how it is difficult to reconstruct the wavelength sub grid matrix from recording the wavelengths on line.

Assuming an hourly change of master wavelength grid matrix W^{G}_{mn} as discussed in section 3.2 and an eavesdropper with powerful computing resources to process each possible combination, it will take time to process where each wavelength is placed in the correct position in the master gird matrix W^{G}_{mn}. This can be illustrated for a single user ($U = 1$) in the case of TS/WH with symmetric prime numbers (Prime/Prime) in (8), with $m = l = 13$ for code matrices C^{y}_{ml} in Appendix C and the master wavelength grid matrix W^{G}_{mn} and its derivatives W^{xG}_{mn} shown in Appendix A and Appendix B. The probability of placement of a single wavelength *PC(λi)* per (23) is equal to 2.58 x 10^{-36}. This result of low probability can be compared against the processing capabilities of the world's fastest computer, the IBM Blue Gene/L supercomputer as reported in 2005 [101][102]. The IBM Blue Gene/L supercomputer has broken its own previous record and reached 280.6 teraflops[23] (280.6 trillion calculations a second), so it would take 4.38 x 10^{15} hours (5 x 10^{11} years) of

[23] FLOPS, floating point operations per second, is a measure of computer performance in calculation speed, which is in the trillion operations per second for current computer technologies.

processing to find the correct wavelength sub grid matrix W_{mn}^{xG}. This is a long time, especially when considering the master wavelength grid matrix W_{mn}^{G} is changed on an hourly basis.

The relation in (23) did not use the code matrices and assumed that the right code matrix C_{ml}^{y} will be found when the wavelengths in the hop and the mapping in (3) agree; the code matrix will be used for confirmation purpose.

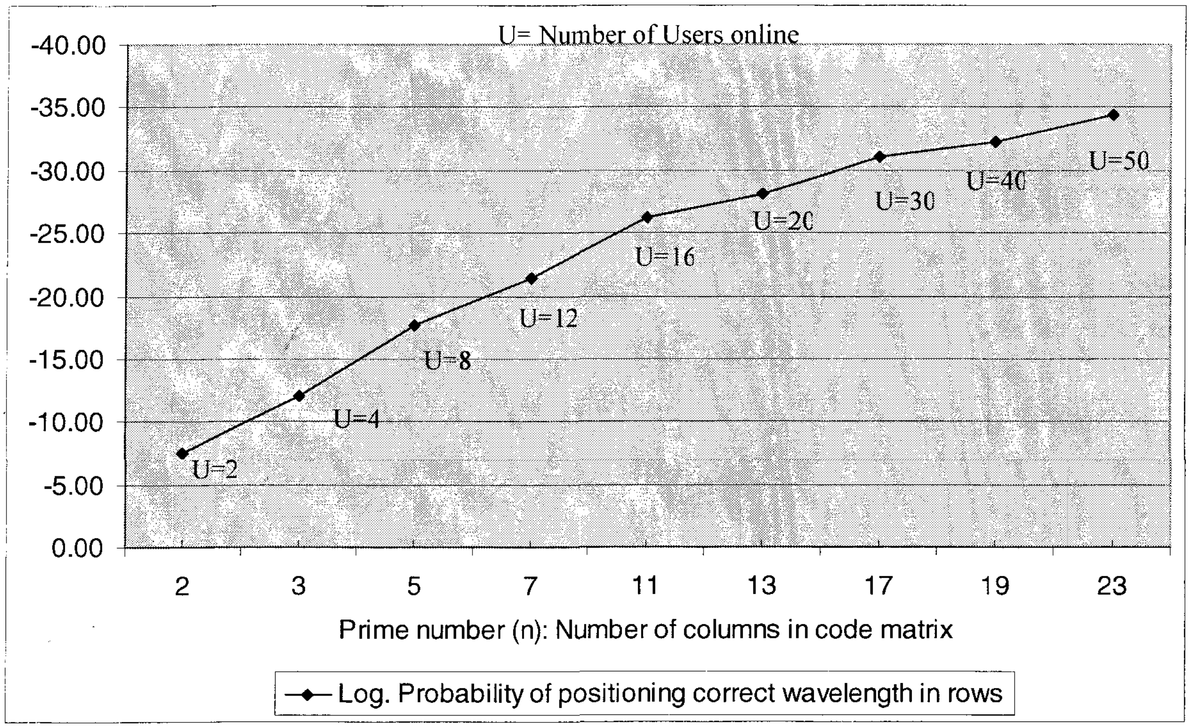

Figure 33: Probability of placing the correct wavelength in master grid matrix

The basic relation derived in (22) is very dependent on the coding scheme used, and the following sections provide some comments about how robust the probability is when (22) is applied to different coding schemes.

4.5 Additional Security Practices for a Single Online User

It is noticed that in (22) the number of online users at any instant (U) is part of the security measures that can be implemented. It is good practice to maintain the shared fiber link in PON busy to certain levels of online users. The number of users as shown in (23) does not provide great help to support probability figures as shown in Figure 34 for different users' levels. However, the number of users required to avoid the case of a single online user where the hopping pattern of a single sequence can be exploited, and in such case, the difficulty of identifying the specific ONU lies in the power of the cryptography used to encrypt the data. It is recommended that the network load be monitored by the OLT and information updated to each ONU. In a situation where the load dropping below a certain level is determined by the security policy of the organization, the available resources at the OLT and ONUs start to transmit dummy traffic that can be identified as normal traffic, which means that the dummy traffic requires encryption without necessarily carrying any destination information. For example, the ONUs can have a minimum of three laser transmitters where, when those are not used, it will be commanded by OLT to transmit dummy traffic in order to avoid exploiting a single online user.

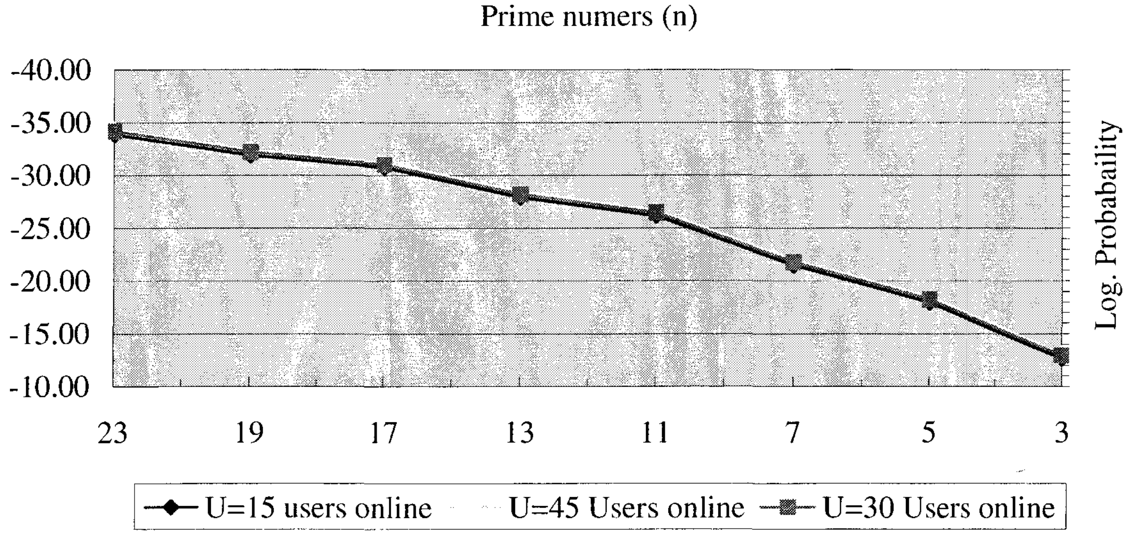

Figure 34 Log. prob. of breaking a sequence for symmetric TS/WH (Prime/Prime)

4.5.1 Attacks on TS/WH Scheme Using Symmetric Prime Numbers (Prime/Prime)

The TS/WH based on a symmetric prime number and related wavelength sequences generated in Appendix D illustrates that this coding scheme is excellent in terms of meeting ideal correlation properties. The limitation on available wavelengths based on 25 GHz limited the generation to only 192 wavelength sequences as shown in Appendix D, and those are more than enough when considering that the number of ONUs in PON can reach 64 and, with growth, 128 ONUs. Previous computations showed, for example, that it takes 5 x 10^{11} years to reconstruct a master wavelength grid matrix.

The major disadvantage of wavelength sequences generated by TS/WH based on single symmetric prime number is its simple arrangement and symmetry of matrices, which provides fixed and relatively simple relations between code sequences, which could greatly facilitate the process of breaking the system. However, even though the computation is still hard to achieve, once a certain sequence in a symmetric system is deciphered, all the sequences can be deduced by simply applying the prime algorithm to that sequence (set of wavelengths).

4.5.2 Attacks on Asymmetric TS/WH Scheme (EQC/Prime)

In the case of TS/WH using two different asymmetric prime numbers such as P_s for spreading and P_h for hopping, greater security is provided via the random relations between code sequences. Asymmetric systems offer additional protection in this sense since in order to deduce the relation between sequences in the system, the column selection function should be known[88]. Considering an overcolored system ($P_h > P_s$), the difference between the prime numbers provides additional security against an attack on a TS/WH asymmetric scheme.

Considering the probability for capturing the correct wavelength sequence in (22), the code matrices have different dimensions (asymmetric), and the number of columns l in C^{y}_{ml} is less than number of columns n in the wavelength grid matrix W^{G}_{mn} ($l<n$). The placement operator for EQC was discussed in section 3.3.1.2 with a restriction on the dimensions on the matrices, and the relation of the asymmetric prime numbers P_h and P_s is expressed in (12), (13), and (14).

The total wavelengths available for hopping are those in the master grid matrix W^{G}_{mn}, or simply mn. In the hopping mode, every time the number of wavelengths used from total available wavelength equal to P_h, which had minimum value restriction placed at m per the relation in (14). In addition, the number of columns in the code matrix C^{y}_{ml} is expressed, as shown in (14), to be $l = 2P_s - 1$. The possible selections of combination sets (CS_a) in the asymmetric case can be expressed similar to that discussed in [92], with modifications to suit the approach in this dissertation as shown in (24), which is different from that for the symmetric TS/WH (Prime/Prime) shown in (19) expressed for the combination set of sequences.

$$CS_a = \binom{mn}{m}.(m!).\binom{m}{l}.(l!) \tag{24}$$

The available combination set expressed in (24) is used to provide the single probability for the correct sequence for the asymmetric TS/WH sequence expressed as P_{CSa} (λ_{as}) shown in (25). The relation in (25) provides additional complexity to the overall probability of breaking a wavelength sequence using the asymmetric TS/WH, which replaces (20) and expresses the overall probability with the new dimensions that are related to two asymmetric prime ($P_{h,}$ P_s) indirectly by using m, n, and l.

It is interesting to note that in (25) the term related to the order of cycling of assigned wavelength sequences assigned to a single ONU is retained since it is independent from the combination set, and wavelength sequences can be arbitrarily assigned and cycled.

$$P_{CSa}(\lambda_{as}) = \frac{(mn-l)}{mn!}(\frac{1}{l})(\frac{1}{m}) \tag{25}$$

$$\text{PC}\ (\lambda_s^k) = \frac{1}{((n!)^m - n)}\ (\frac{1}{C_{\max}})(\frac{1}{n})\frac{(mn-l)}{mn!}(\frac{1}{l})(\frac{1}{m})\ .(\frac{1}{S_a!})\ (\frac{1}{U}) \tag{26}$$

4.5.3 Attacks on MWOOC Codes

The MW-OOC constructions with its varieties as discussed in section 3.3.1.4 present various degrees of challenges to attackers, specifically, the multi lengths multi weights MW-OOC that were discussed in sections 3.3.1.5 and 3.3.1.6, respectively.

MWWC with fixed length and weight tend to have known patterns, however, when both lengths and weights are changing for different ONUs depending on the security level, the challenges for attackers (eavesdroppers) become greater and more challenges are faced by systems designers in terms of technical complexities to manage synchronizations, timing, cross channels, and an overall management of correlations.

Part of the discussion in the motivation section 2.4.2 for cost vs. value of security included the recommendation that there must be a balance between security, cost, and usability. Though security must be a prime design consideration, it is not necessarily the overriding one, and benefits must be weighed against costs to achieve a balanced, cost-effective system [70]. Accordingly, implementation of MW-OOC with its various schemes poses technical complexities and justification of cost is a big item for consideration.

The discussion in section 3.3.1.4 about MW-OOC was brief, and so this section follows in terms of investigation of attacks on MW-OOC-based security, which is limited to a brief discussion in this dissertation.

4.6 Chapter Summary

In this chapter, completion of the performance evaluation of the novel security enhancement in terms of robustness of the proposed solution provided various scenarios used for the evaluation of the security aspect of the proposed solution. The evaluation basis included assumptions about the attacker's background and sophistication, and assumptions were made that the attacker knows great technical details about the timing and synchronization, including the messages and encryption standards. In addition, the system was subjected to different attacks, and probability equations of capturing correct wavelength sequences were derived for the TS/WH, while attacks against MW-OOC sequences were discussed pointing out their advantages and various schemes available to provide MW-OOCs, especially those with multi-lengths and multi-weights that pose technical complexities in addition to a high level of protection.

The focus in this chapter was on the novel approach to enhance security in PON, which involves the mapping of the two matrices, wavelength grid matrices and code matrices. In addition to the advantage of issuing multiple wavelength sequences and the cycle order, how the sequence is used between an OLT and ONUs shows the improvement and is used as an additional key to security.

The TS/WH based on symmetric prime numbers (Prime/Prime) exhibits the lowest number in terms of generating wavelengths sequences as demonstrated in Appendix D, however, it provides superior correlation properties compared to all other coding schemes. In addition, symmetric TS/WH performed well against brute force types of attacks such that it is a potential for use and provides excellent security level and simplicity of implementation.

In case the security requirement is actually higher and requires introducing higher levels of security against capturing a wavelength sequence, the TS/WH with a basis using two dissimilar numbers was evaluated against brute force types of attackers, and actually provides higher security, although it does introduce a level of cross correlation that needs to be managed.

A brief discussion about MW-OOCs was included. Even though they provide a higher level of security compared to TS/WH, technical difficulty and the impact on synchronization can be costly.

In addition to the evaluation of coding schemes against attacks by eavesdroppers, a recommendation is that when the shared fiber link in PON is not loaded, it is required to have supplementary transmitters in some or all ONUs to provide dummy transmission to void the case of a single online user in which the wavelength sequence can be exploited.

CHAPTER 5: CONCLUSIONS AND FUTURE WORK

Security is a complex field in terms of needs and their justifications; however, it is at the end considered a risk management problem with optimization between risk reduction and complexity/cost increase. Risk exposure to a certain extent is accepted in some cases where allowed in the organization's security policy, however, security is a competition factor among service providers when it comes to residential subscribers and part of their expectations in a new service.

The trend in increasing demand for bandwidth is an indication of increasing customer dependency on access networks for daily transactions, and the emergence of low cost passive optical components and networks facilitates the extension of fiber connectivity and solves the increasing demand for bandwidth. For example, emerging networks such as Fiber-to-the-X (FTTX) where X can be Home, Building, or Curb fiber based on PON provide the solution to fiber connectivity at high speeds, and a significant amount of research in recent years is aiming at providing solutions to increasing cardinality in access networks via various coding schemes.

The main question remains: What about security? It is known that optical networking technologies such as WDM provide the solution, and it is time to determine which direction in research activities to focus on security rather than solving the access schemes in access networks. For example, PON implements B&S type of traffic in which ONUs select their traffic based on time slots and all operate at the same wavelength. This security vulnerability in terms of confidentiality and privacy will not be sufficient to provide protection against sophisticated eavesdroppers and their advanced tools. It is required that additional protection be provided at the network level against eavesdroppers, who can be attackers tapping into a shared fiber link or simply one of the ONUs operating in a promiscuous mode providing the time to eavesdrop without being detected. It is a fact that there is no absolute security, however, protection should be based on making it difficult for attackers to collect good samples useful for cryptanalysis.

The work presented in this dissertation provides a novel solution to security enhancement in PON using wavelength hopping with implementation in physical and data link layers of the OSI model. The technique uses slow wavelength hopping in order to make it feasible to implement with existing optical components technology and provides diffusion of data packets into separate wavelengths so that it can be difficult to trace traffic with destination to a single ONU by an eavesdropper.

The proof of concept provided through the PON simulation model was subjected to 64 channels in a DWDM implementation, and analysis of the brute force trial of capturing the correct wavelength sequence that belongs to a single ONU had encouraging results that support confidentiality and privacy at the network level.

The novel solution to security enhancement in PON introduced the idea of using ITU-T based wavelengths grid as the base for construction of keys, in addition to using multiple assignments of wavelength sequences to a single ONU based on their security level. In addition, the cycling order for execution of the assigned wavelengths sequences are two additional keys to provide robustness to secure operation in PON.

More specifically, the following is a summary of the work presented in this dissertation.

- In Chapter 1, discussions included the increasing demand for bandwith supported by measured data and charts showing global market depending on PON, in addition to current recommendation standards that cover PON. In order to lay out the background for discussions about the novel solution to security enamncement in PON, discussions included enabling technologies for optical componenets used in PON, and introduced PON as the solution and potential candidate for FTTH in its ability to meet the increasing demand on bandwidth. Since the novel solution is based on DWDM implementations, the investigation of channel impairmanets with DWDM application requires also providing discussions about the established performance paramaters that are used in the evaluation of the proposed solution. The chapter also presented the organization of the dissertation.
- In Chapter 2, security vulnerabilty of optical networks was covered, especially those related to PONs, and a review of types of attacks on PONs and the current practices used to provide security for the traffic was included as part of establishing and highlighting current problems with PONs. In addition, the chapter covered the literature review for previous work and reports that addressed providing security to

optical networks, and comments were provided about each approach in the cited literature. The motivation section discussed the basis for the evaluation of the needs for security and addressed cost vs. security where security was related to the value of the asset being protected.

- In Chapter 3, the chapter started by introducing the novel solution via a conceptual approach to security enhancement in PON at the top level, which involved mapping two matrices, the wavelength grid matrix and the code matrix, and generating wavelength sequences that are assigned in multiples to ONUs based on their security levels. The novel approach introduced three keys for secure operations that are not available in current practices or even reported in the open literature for PON or optical system security. The three keys are: (1) the format of the wavelength grid matrix that can be changed on hourly (or more frequent) basis, (2) the multiple assignments of wavelength sequences, and (3) the use of cycling order to assigned wavelength sequences. In this context, the novelty of the proposed concepts is due to the techniques used in the generation of wavelengths sequences via the mapping process, and multiple assignment of wavelength sequences to a single ONU in addition to using the cycling order wavelength sequences to boost the security level in PON. Various coding techniques and their code construction methods were discussed, and proof of the concept was provided through a PON model simulation running 64 channels of DWDM. Performance measurements were made to provide a confirmation of the feasibility of the technical approach to security enhancements in PON as proposed in this dissertation. The chapter ends with implementation and deployment considerations that need to be addressed in an operational system, including the role of cryptography, timing and synchronization, physical security, in addition to wavelength matrix assignment and changes.
- In Chapter 4, evaluation of the effectiveness of the proposed system against brute force attack by an eavesdropper, and by reverse construction of wavelength grid matrices from monitored data online revealed that the proposed security enhancement in PON actually performed very well even with TS/WH based on a symmetric prime number, which is the coding scheme that generates the least wavelength sequences.

This is due mainly to the maximum limitation on ONUs up to 64, and with growth to 128, there are enough sequences that, when assigned in multiples to a single ONU and using pre-arranged cycling order for assigned wavelength sequences, the probability of capturing the correct wavelength sequence actually reached the negative infinity. The result was evaluated by using the world's fastest computer to check the time required to try all possible combinations to break the wavelength sequence hopping order, and it was found that the time required is in the order 10^{11} years, which is secure when considering that the wavelength grid matrix can be changed on hourly basis. Other coding schemes actually provide a higher level of security, however, they will require a higher level of correlation management.

Despite the significant amount of research that has been made in the area of optical access networks with a focus on increasing cardinality, security is of paramount importance to all users of networks, of course at a justifiable cost. There is no real evidence of the magnitude of eavesdropping in PON because it is just becoming available due to the reduced cost of passive optical components in the past few years. It is a new technology and its fate is similar to older networking technologies where it will be a victim to eavesdropping, and the problem of eavesdropping will not disappear with the optical networking technologies.

The work presented in this dissertation represents an important step toward providing security at the network level in PON. However, several issues still need to be investigated, and in particular, the following issues open up new research directions in the security of PON:

- Providing centralized control that monitors the loading of the network, and the protocol used to command ONUs to transmit dummy data in the event the number of users drop below a certain level.
- The symmetric TS/WH based on a single prime number (Prime/Prime) are the best in terms of correlation properties and ease of implentation; however, more work is required in order to support various data rates and supporting different QoS requiremnts.

- Providing the best mechanism for commanding the ONUs to switch, for example, on an hourly basis to a different wavelength grid matrix, or simply transmit the hopping sequence encoded on several channels, requires an investigation of keys distribution.
- Multi level security support (MLS) based on wavelength sequences, and finding a framework and guidance for relating the number of wavelengths for each level of security.
- Investigation of providing a mechanism whereby all ONUs can be notified of ongoing tapping, preferably if it includes eavesdropping by external attackers as well as internal ones to the network by one or more ONUs, and use of a defense startegy in case of such attacks.
- Designing hardware and software that can be modular and open in their operation and with the strength to reside in the keys and not in the equipment design and algorithm.
- Exploring the synchrionization mechanizm, specifically for the MW-OOC that supports multi lengths and multi variable weights, and at the same managing the correlation issues where this coding scheme could be the hardest to break when monitored online.

In summary, we presented an approach to provide protection to PON via slow wavelength hopping techniques, and it would be interesting to investigate the above related topics, since it is the potential access network to answer the increasing demand for bandwidth and still meet cost limitations.

APPENDIX A: ITU -T G694.1 BASED W_{mn}^{G} WAVELENGTH GRID

(m = 12, n = 16)

The wavelength grid matrix below represents W_{mn}^{G} that is used in this dissertation as baseline grid matrix to provide proof of the of concept dense wave division multiplexing (DWDM) in passive optical networks (PON), and the same matrix is subject to complete columns cyclic to generate sub grid matrices W_{mn}^{xG} that are shown in Appendix B.

193.125	191.55	192.4	194.25	194.35	194.075	193.8	195.225	194.05	193.575	194.175	192.025	191.05	192.525	193.675	194.775
195.625	193.4	195.775	193.925	194	194.625	192.9	191.375	191.925	192.475	194.95	191.275	192.875	191.175	193.375	194.875
194.2	195.175	195.4	191.775	194.375	194.675	193.875	193.975	193.275	193.45	194.6	194.575	191.45	195.075	195.675	195.475
195	191.525	195.375	192.15	191.975	192.125	192.325	192.625	193.175	193.05	193.85	191.6	193.3	195.45	194.15	194.825
193.2	194.475	195.15	192.5	192.6	192.675	192.45	192.275	193.725	191.1	193.475	192.425	193.825	193	195.325	195.5
195.425	193.6	195.525	192.925	191	192.3	192.725	192.55	192.825	192.975	193.35	192.95	192.075	193.15	194.65	195.6
194.3	191.7	195.35	191.8	191.575	192.175	191.9	191.95	191.65	193.425	192.85	194.55	191.675	195.125	194.525	192.7
194.7	193.75	194.975	192.05	194.275	193.55	194.025	194.325	192.8	195.2	194.125	191.725	192.25	194.225	194.8	194.75
194.725	192.375	195.1	193.5	195.3	193.7	193.075	193.95	191.75	192.575	192.75	194.425	191.225	194.45	195.7	194.85
191.15	191.2	195.25	193.25	192.65	193.025	191.875	193.525	191.825	192.225	193.65	191.325	195.975	194.9	195.55	195.65
193.625	191.25	194.5	192	191.075	191.85	191.4	191.025	191.625	191.125	192.775	193.1	192.35	194.925	195.725	195.575
191.35	194.4	195.275	191.475	194.1	193.325	191.425	192.1	191.5	193.775	195.025	192.2	191.3	195.05	193.9	193.225

APPENDIX B: W_{mn}^{xG} SUB GRID MATRICES

W_{mn}^{xG} Wavelength Sub Grid Matrix (x=1)

193.125	191.55	192.4	194.25	194.35	194.075	193.8	195.225	194.05	193.575	194.175	192.025	191.05	192.525	193.675	194.775
195.625	193.4	195.775	193.925	194	194.625	192.9	191.375	191.925	192.475	194.95	191.275	192.875	191.175	193.375	194.875
194.2	195.175	195.4	191.775	194.375	194.675	193.875	193.975	193.275	193.45	194.6	194.575	191.45	195.075	195.675	195.475
195	191.525	195.375	192.15	191.975	192.125	192.325	192.625	193.175	193.05	193.85	191.6	193.3	195.45	194.15	194.825
193.2	194.475	195.15	192.5	192.6	192.675	192.45	192.275	193.725	191.1	193.475	192.425	193.825	193	195.325	195.5
195.425	193.6	195.525	192.925	191	192.3	192.725	192.55	192.825	192.975	193.35	192.95	192.075	193.15	194.65	195.6
194.3	191.7	195.35	191.8	191.575	192.175	191.9	191.95	191.65	193.425	192.85	194.55	191.675	195.125	194.525	192.7
194.7	193.75	194.975	192.05	194.275	193.55	194.025	194.325	192.8	195.2	194.125	191.725	192.25	194.225	194.8	194.75
194.725	192.375	195.1	193.5	195.3	193.7	193.075	193.95	191.75	192.575	192.75	194.425	191.225	194.45	195.7	194.85
191.15	191.2	195.25	193.25	192.65	193.025	191.875	193.525	191.825	192.225	193.65	191.325	195.975	194.9	195.55	195.65
193.625	191.25	194.5	192	191.075	191.85	191.4	191.025	191.625	191.125	192.775	193.1	192.35	194.925	195.725	195.575
191.35	194.4	195.275	191.475	194.1	193.325	191.425	192.1	191.5	193.775	195.025	192.2	191.3	195.05	193.9	193.225

W_{mn}^{xG} Wavelength Sub Grid Matrix (x=2)

191.55	192.4	194.25	194.35	194.075	193.8	195.225	194.05	193.575	194.175	192.025	191.05	192.525	193.675	194.775	193.125
193.4	195.775	193.925	194	194.625	192.9	191.375	191.925	192.475	194.95	191.275	192.875	191.175	193.375	194.875	195.625
195.175	195.4	191.775	194.375	194.675	193.875	193.975	193.275	193.45	194.6	194.575	191.45	195.075	195.675	195.475	194.2
191.525	195.375	192.15	191.975	192.125	192.325	192.625	193.175	193.05	193.85	191.6	193.3	195.45	194.15	194.825	195
194.475	195.15	192.5	192.6	192.675	192.45	192.275	193.725	191.1	193.475	192.425	193.825	193	195.325	195.5	193.2
193.6	195.525	192.925	191	192.3	192.725	192.55	192.825	192.975	193.35	192.95	192.075	193.15	194.65	195.6	195.425
191.7	195.35	191.8	191.575	192.175	191.9	191.95	191.65	193.425	192.85	194.55	191.675	195.125	194.525	192.7	194.3
193.75	194.975	192.05	194.275	193.55	194.025	194.325	192.8	195.2	194.125	191.725	192.25	194.225	194.8	194.75	194.7
192.375	195.1	193.5	195.3	193.7	193.075	193.95	191.75	192.575	192.75	194.425	191.225	194.45	195.7	194.85	194.725
191.2	195.25	193.25	192.65	193.025	191.875	193.525	191.825	192.225	193.65	191.325	195.975	194.9	195.55	195.65	191.15
191.25	194.5	192	191.075	191.85	191.4	191.025	191.625	191.125	192.775	193.1	192.35	194.925	195.725	195.575	193.625
194.4	195.275	191.475	194.1	193.325	191.425	192.1	191.5	193.775	195.025	192.2	191.3	195.05	193.9	193.225	191.35

W_{mn}^{xG} Wavelength Sub Grid Matrix (x=3)

192.4	194.25	194.35	194.075	193.8	195.225	194.05	193.575	194.175	192.025	191.05	192.525	193.675	194.775	193.125	191.55
195.775	193.925	194	194.625	192.9	191.375	191.925	192.475	194.95	191.275	192.875	191.175	193.375	194.875	195.625	193.4
195.4	191.775	194.375	194.675	193.875	193.975	193.275	193.45	194.6	194.575	191.45	195.075	195.675	195.475	194.2	195.175
195.375	192.15	191.975	192.125	192.325	192.625	193.175	193.05	193.85	191.6	193.3	195.45	194.15	194.825	195	191.525
195.15	192.5	192.6	192.675	192.45	192.275	193.725	191.1	193.475	192.425	193.825	193	195.325	195.5	193.2	194.475
195.525	192.925	191	192.3	192.725	192.55	192.825	192.975	193.35	192.95	192.075	193.15	194.65	195.6	195.425	193.6
195.35	191.8	191.575	192.175	191.9	191.95	191.65	193.425	192.85	194.55	191.675	195.125	194.525	192.7	194.3	191.7
194.975	192.05	194.275	193.55	194.025	194.325	192.8	195.2	194.125	191.725	192.25	194.225	194.8	194.75	194.7	193.75
195.1	193.5	195.3	193.7	193.075	193.95	191.75	192.575	192.75	194.425	191.225	194.45	195.7	194.85	194.725	192.375
195.25	193.25	192.65	193.025	191.875	193.525	191.825	192.225	193.65	191.325	195.975	194.9	195.55	195.65	191.15	191.2
194.5	192	191.075	191.85	191.4	191.025	191.625	191.125	192.775	193.1	192.35	194.925	195.725	195.575	193.625	191.25
195.275	191.475	194.1	193.325	191.425	192.1	191.5	193.775	195.025	192.2	191.3	195.05	193.9	193.225	191.35	194.4

W_{mn}^{xG} Wavelength Sub Grid Matrix (x=4)

194.25	194.35	194.075	193.8	195.225	194.05	193.575	194.175	192.025	191.05	192.525	193.675	194.775	193.125	191.55	192.4
193.925	194	194.625	192.9	191.375	191.925	192.475	194.95	191.275	192.875	191.175	193.375	194.875	195.625	193.4	195.775
191.775	194.375	194.675	193.875	193.975	193.275	193.45	194.6	194.575	191.45	195.075	195.675	195.475	194.2	195.175	195.4
192.15	191.975	192.125	192.325	192.625	193.175	193.05	193.85	191.6	193.3	195.45	194.15	194.825	195	191.525	195.375
192.5	192.6	192.675	192.45	192.275	193.725	191.1	193.475	192.425	193.825	193	195.325	195.5	193.2	194.475	195.15
192.925	191	192.3	192.725	192.55	192.825	192.975	193.35	192.95	192.075	193.15	194.65	195.6	195.425	193.6	195.525
191.8	191.575	192.175	191.9	191.95	191.65	193.425	192.85	194.55	191.675	195.125	194.525	192.7	194.3	191.7	195.35
192.05	194.275	193.55	194.025	194.325	192.8	195.2	194.125	191.725	192.25	194.225	194.8	194.75	194.7	193.75	194.975
193.5	195.3	193.7	193.075	193.95	191.75	192.575	192.75	194.425	191.225	194.45	195.7	194.85	194.725	192.375	195.1
193.25	192.65	193.025	191.875	193.525	191.825	192.225	193.65	191.325	195.975	194.9	195.55	195.65	191.15	191.2	195.25
192	191.075	191.85	191.4	191.025	191.625	191.125	192.775	193.1	192.35	194.925	195.725	195.575	193.625	191.25	194.5
191.475	194.1	193.325	191.425	192.1	191.5	193.775	195.025	192.2	191.3	195.05	193.9	193.225	191.35	194.4	195.275

W_{mn}^{xG} Wavelength Sub Grid Matrix (x=5)

194.35	194.075	193.8	195.225	194.05	193.575	194.175	192.025	191.05	192.525	193.675	194.775	193.125	191.55	192.4	194.25
194	194.625	192.9	191.375	191.925	192.475	194.95	191.275	192.875	191.175	193.375	194.875	195.625	193.4	195.775	193.925
194.375	194.675	193.875	193.975	193.275	193.45	194.6	194.575	191.45	195.075	195.675	195.475	194.2	195.175	195.4	191.775
191.975	192.125	192.325	192.625	193.175	193.05	193.85	191.6	193.3	195.45	194.15	194.825	195	191.525	195.375	192.15
192.6	192.675	192.45	192.275	193.725	191.1	193.475	192.425	193.825	193	195.325	195.5	193.2	194.475	195.15	192.5
191	192.3	192.725	192.55	192.825	192.975	193.35	192.95	192.075	193.15	194.65	195.6	195.425	193.6	195.525	192.925
191.575	192.175	191.9	191.95	191.65	193.425	192.85	194.55	191.675	195.125	194.525	192.7	194.3	191.7	195.35	191.8
194.275	193.55	194.025	194.325	192.8	195.2	194.125	191.725	192.25	194.225	194.8	194.75	194.7	193.75	194.975	192.05
195.3	193.7	193.075	193.95	191.75	192.575	192.75	194.425	191.225	194.45	195.7	194.85	194.725	192.375	195.1	193.5
192.65	193.025	191.875	193.525	191.825	192.225	193.65	191.325	195.975	194.9	195.55	195.65	191.15	191.2	195.25	193.25
191.075	191.85	191.4	191.025	191.625	191.125	192.775	193.1	192.35	194.925	195.725	195.575	193.625	191.25	194.5	192
194.1	193.325	191.425	192.1	191.5	193.775	195.025	192.2	191.3	195.05	193.9	193.225	191.35	194.4	195.275	191.475

W_{mn}^{xG} Wavelength Sub Grid Matrix (x=6)

194.075	193.8	195.225	194.05	193.575	194.175	192.025	191.05	192.525	193.675	194.775	193.125	191.55	192.4	194.25	194.35
194.625	192.9	191.375	191.925	192.475	194.95	191.275	192.875	191.175	193.375	194.875	195.625	193.4	195.775	193.925	194
194.675	193.875	193.975	193.275	193.45	194.6	194.575	191.45	195.075	195.675	195.475	194.2	195.175	195.4	191.775	194.375
192.125	192.325	192.625	193.175	193.05	193.85	191.6	193.3	195.45	194.15	194.825	195	191.525	195.375	192.15	191.975
192.675	192.45	192.275	193.725	191.1	193.475	192.425	193.825	193	195.325	195.5	193.2	194.475	195.15	192.5	192.6
192.3	192.725	192.55	192.825	192.975	193.35	192.95	192.075	193.15	194.65	195.6	195.425	193.6	195.525	192.925	191
192.175	191.9	191.95	191.65	193.425	192.85	194.55	191.675	195.125	194.525	192.7	194.3	191.7	195.35	191.8	191.575
193.55	194.025	194.325	192.8	195.2	194.125	191.725	192.25	194.225	194.8	194.75	194.7	193.75	194.975	192.05	194.275
193.7	193.075	193.95	191.75	192.575	192.75	194.425	191.225	194.45	195.7	194.85	194.725	192.375	195.1	193.5	195.3
193.025	191.875	193.525	191.825	192.225	193.65	191.325	195.975	194.9	195.55	195.65	191.15	191.2	195.25	193.25	192.65
191.85	191.4	191.025	191.625	191.125	192.775	193.1	192.35	194.925	195.725	195.575	193.625	191.25	194.5	192	191.075
193.325	191.425	192.1	191.5	193.775	195.025	192.2	191.3	195.05	193.9	193.225	191.35	194.4	195.275	191.475	194.1

W_{mn}^{xG} Wavelength Sub Grid Matrix (x=7)

193.8	195.225	194.05	193.575	194.175	192.025	191.05	192.525	193.675	194.775	193.125	191.55	192.4	194.25	194.35	194.075
192.9	191.375	191.925	192.475	194.95	191.275	192.875	191.175	193.375	194.875	195.625	193.4	195.775	193.925	194	194.625
193.875	193.975	193.275	193.45	194.6	194.575	191.45	195.075	195.675	195.475	194.2	195.175	195.4	191.775	194.375	194.675
192.325	192.625	193.175	193.05	193.85	191.6	193.3	195.45	194.15	194.825	195	191.525	195.375	192.15	191.975	192.125
192.45	192.275	193.725	191.1	193.475	192.425	193.825	193	195.325	195.5	193.2	194.475	195.15	192.5	192.6	192.675
192.725	192.55	192.825	192.975	193.35	192.95	192.075	193.15	194.65	195.6	195.425	193.6	195.525	192.925	191	192.3
191.9	191.95	191.65	193.425	192.85	194.55	191.675	195.125	194.525	192.7	194.3	191.7	195.35	191.8	191.575	192.175
194.025	194.325	192.8	195.2	194.125	191.725	192.25	194.225	194.8	194.75	194.7	193.75	194.975	192.05	194.275	193.55
193.075	193.95	191.75	192.575	192.75	194.425	191.225	194.45	195.7	194.85	194.725	192.375	195.1	193.5	195.3	193.7
191.875	193.525	191.825	192.225	193.65	191.325	195.975	194.9	195.55	195.65	191.15	191.2	195.25	193.25	192.65	193.025
191.4	191.025	191.625	191.125	192.775	193.1	192.35	194.925	195.725	195.575	193.625	191.25	194.5	192	191.075	191.85
191.425	192.1	191.5	193.775	195.025	192.2	191.3	195.05	193.9	193.225	191.35	194.4	195.275	191.475	194.1	193.325

W_{mn}^{xG} Wavelength Sub Grid Matrix (x=8)

195.225	194.05	193.575	194.175	192.025	191.05	192.525	193.675	194.775	193.125	191.55	192.4	194.25	194.35	194.075	193.8
191.375	191.925	192.475	194.95	191.275	192.875	191.175	193.375	194.875	195.625	193.4	195.775	193.925	194	194.625	192.9
193.975	193.275	193.45	194.6	194.575	191.45	195.075	195.675	195.475	194.2	195.175	195.4	191.775	194.375	194.675	193.875
192.625	193.175	193.05	193.85	191.6	193.3	195.45	194.15	194.825	195	191.525	195.375	192.15	191.975	192.125	192.325
192.275	193.725	191.1	193.475	192.425	193.825	193	195.325	195.5	193.2	194.475	195.15	192.5	192.6	192.675	192.45
192.55	192.825	192.975	193.35	192.95	192.075	193.15	194.65	195.6	195.425	193.6	195.525	192.925	191	192.3	192.725
191.95	191.65	193.425	192.85	194.55	191.675	195.125	194.525	192.7	194.3	191.7	195.35	191.8	191.575	192.175	191.9
194.325	192.8	195.2	194.125	191.725	192.25	194.225	194.8	194.75	194.7	193.75	194.975	192.05	194.275	193.55	194.025
193.95	191.75	192.575	192.75	194.425	191.225	194.45	195.7	194.85	194.725	192.375	195.1	193.5	195.3	193.7	193.075
193.525	191.825	192.225	193.65	191.325	195.975	194.9	195.55	195.65	191.15	191.2	195.25	193.25	192.65	193.025	191.875
191.025	191.625	191.125	192.775	193.1	192.35	194.925	195.725	195.575	193.625	191.25	194.5	192	191.075	191.85	191.4
192.1	191.5	193.775	195.025	192.2	191.3	195.05	193.9	193.225	191.35	194.4	195.275	191.475	194.1	193.325	191.425

W_{mn}^{xG} Wavelength Sub Grid Matrix (x=9)

194.05	193.575	194.175	192.025	191.05	192.525	193.675	194.775	193.125	191.55	192.4	194.25	194.35	194.075	193.8	195.225
191.925	192.475	194.95	191.275	192.875	191.175	193.375	194.875	195.625	193.4	195.775	193.925	194	194.625	192.9	191.375
193.275	193.45	194.6	194.575	191.45	195.075	195.675	195.475	194.2	195.175	195.4	191.775	194.375	194.675	193.875	193.975
193.175	193.05	193.85	191.6	193.3	195.45	194.15	194.825	195	191.525	195.375	192.15	191.975	192.125	192.325	192.625
193.725	191.1	193.475	192.425	193.825	193	195.325	195.5	193.2	194.475	195.15	192.5	192.6	192.675	192.45	192.275
192.825	192.975	193.35	192.95	192.075	193.15	194.65	195.6	195.425	193.6	195.525	192.925	191	192.3	192.725	192.55
191.65	193.425	192.85	194.55	191.675	195.125	194.525	192.7	194.3	191.7	195.35	191.8	191.575	192.175	191.9	191.95
192.8	195.2	194.125	191.725	192.25	194.225	194.8	194.75	194.7	193.75	194.975	192.05	194.275	193.55	194.025	194.325
191.75	192.575	192.75	194.425	191.225	194.45	195.7	194.85	194.725	192.375	195.1	193.5	195.3	193.7	193.075	193.95
191.825	192.225	193.65	191.325	195.975	194.9	195.55	195.65	191.15	191.2	195.25	193.25	192.65	193.025	191.875	193.525
191.625	191.125	192.775	193.1	192.35	194.925	195.725	195.575	193.625	191.25	194.5	192	191.075	191.85	191.4	191.025
191.5	193.775	195.025	192.2	191.3	195.05	193.9	193.225	191.35	194.4	195.275	191.475	194.1	193.325	191.425	192.1

W_{mn}^{xG} Wavelength Sub Grid Matrix (x=10)

193.575	194.175	192.025	191.05	192.525	193.675	194.775	193.125	191.55	192.4	194.25	194.35	194.075	193.8	195.225	194.05
192.475	194.95	191.275	192.875	191.175	193.375	194.875	195.625	193.4	195.775	193.925	194	194.625	192.9	191.375	191.925
193.45	194.6	194.575	191.45	195.075	195.675	195.475	194.2	195.175	195.4	191.775	194.375	194.675	193.875	193.975	193.275
193.05	193.85	191.6	193.3	195.45	194.15	194.825	195	191.525	195.375	192.15	191.975	192.125	192.325	192.625	193.175
191.1	193.475	192.425	193.825	193	195.325	195.5	193.2	194.475	195.15	192.5	192.6	192.675	192.45	192.275	193.725
192.975	193.35	192.95	192.075	193.15	194.65	195.6	195.425	193.6	195.525	192.925	191	192.3	192.725	192.55	192.825
193.425	192.85	194.55	191.675	195.125	194.525	192.7	194.3	191.7	195.35	191.8	191.575	192.175	191.9	191.95	191.65
195.2	194.125	191.725	192.25	194.225	194.8	194.75	194.7	193.75	194.975	192.05	194.275	193.55	194.025	194.325	192.8
192.575	192.75	194.425	191.225	194.45	195.7	194.85	194.725	192.375	195.1	193.5	195.3	193.7	193.075	193.95	191.75
192.225	193.65	191.325	195.975	194.9	195.55	195.65	191.15	191.2	195.25	193.25	192.65	193.025	191.875	193.525	191.825
191.125	192.775	193.1	192.35	194.925	195.725	195.575	193.625	191.25	194.5	192	191.075	191.85	191.4	191.025	191.625
193.775	195.025	192.2	191.3	195.05	193.9	193.225	191.35	194.4	195.275	191.475	194.1	193.325	191.425	192.1	191.5

W_{mn}^{xG} Wavelength Sub Grid Matrix (x=11)

194.175	192.025	191.05	192.525	193.675	194.775	193.125	191.55	192.4	194.25	194.35	194.075	193.8	195.225	194.05	193.575
194.95	191.275	192.875	191.175	193.375	194.875	195.625	193.4	195.775	193.925	194	194.625	192.9	191.375	191.925	192.475
194.6	194.575	191.45	195.075	195.675	195.475	194.2	195.175	195.4	191.775	194.375	194.675	193.875	193.975	193.275	193.45
193.85	191.6	193.3	195.45	194.15	194.825	195	191.525	195.375	192.15	191.975	192.125	192.325	192.625	193.175	193.05
193.475	192.425	193.825	193	195.325	195.5	193.2	194.475	195.15	192.5	192.6	192.675	192.45	192.275	193.725	191.1
193.35	192.95	192.075	193.15	194.65	195.6	195.425	193.6	195.525	192.925	191	192.3	192.725	192.55	192.825	192.975
192.85	194.55	191.675	195.125	194.525	192.7	194.3	191.7	195.35	191.8	191.575	192.175	191.9	191.95	191.65	193.425
194.125	191.725	192.25	194.225	194.8	194.75	194.7	193.75	194.975	192.05	194.275	193.55	194.025	194.325	192.8	195.2
192.75	194.425	191.225	194.45	195.7	194.85	194.725	192.375	195.1	193.5	195.3	193.7	193.075	193.95	191.75	192.575
193.65	191.325	195.975	194.9	195.55	195.65	191.15	191.2	195.25	193.25	192.65	193.025	191.875	193.525	191.825	192.225
192.775	193.1	192.35	194.925	195.725	195.575	193.625	191.25	194.5	192	191.075	191.85	191.4	191.025	191.625	191.125
195.025	192.2	191.3	195.05	193.9	193.225	191.35	194.4	195.275	191.475	194.1	193.325	191.425	192.1	191.5	193.775

W_{mn}^{xG} Wavelength Sub Grid Matrix (x=12)

192.025	191.05	192.525	193.675	194.775	193.125	191.55	192.4	194.25	194.35	194.075	193.8	195.225	194.05	193.575	194.175
191.275	192.875	191.175	193.375	194.875	195.625	193.4	195.775	193.925	194	194.625	192.9	191.375	191.925	192.475	194.95
194.575	191.45	195.075	195.675	195.475	194.2	195.175	195.4	191.775	194.375	194.675	193.875	193.975	193.275	193.45	194.6
191.6	193.3	195.45	194.15	194.825	195	191.525	195.375	192.15	191.975	192.125	192.325	192.625	193.175	193.05	193.85
192.425	193.825	193	195.325	195.5	193.2	194.475	195.15	192.5	192.6	192.675	192.45	192.275	193.725	191.1	193.475
192.95	192.075	193.15	194.65	195.6	195.425	193.6	195.525	192.925	191	192.3	192.725	192.55	192.825	192.975	193.35
194.55	191.675	195.125	194.525	192.7	194.3	191.7	195.35	191.8	191.575	192.175	191.9	191.95	191.65	193.425	192.85
191.725	192.25	194.225	194.8	194.75	194.7	193.75	194.975	192.05	194.275	193.55	194.025	194.325	192.8	195.2	194.125
194.425	191.225	194.45	195.7	194.85	194.725	192.375	195.1	193.5	195.3	193.7	193.075	193.95	191.75	192.575	192.75
191.325	195.975	194.9	195.55	195.65	191.15	191.2	195.25	193.25	192.65	193.025	191.875	193.525	191.825	192.225	193.65
193.1	192.35	194.925	195.725	195.575	193.625	191.25	194.5	192	191.075	191.85	191.4	191.025	191.625	191.125	192.775
192.2	191.3	195.05	193.9	193.225	191.35	194.4	195.275	191.475	194.1	193.325	191.425	192.1	191.5	193.775	195.025

W_{mn}^{xG} Wavelength Sub Grid Matrix (x=13)

191.05	192.525	193.675	194.775	193.125	191.55	192.4	194.25	194.35	194.075	193.8	195.225	194.05	193.575	194.175	192.025
192.875	191.175	193.375	194.875	195.625	193.4	195.775	193.925	194	194.625	192.9	191.375	191.925	192.475	194.95	191.275
191.45	195.075	195.675	195.475	194.2	195.175	195.4	191.775	194.375	194.675	193.875	193.975	193.275	193.45	194.6	194.575
193.3	195.45	194.15	194.825	195	191.525	195.375	192.15	191.975	192.125	192.325	192.625	193.175	193.05	193.85	191.6
193.825	193	195.325	195.5	193.2	194.475	195.15	192.5	192.6	192.675	192.45	192.275	193.725	191.1	193.475	192.425
192.075	193.15	194.65	195.6	195.425	193.6	195.525	192.925	191	192.3	192.725	192.55	192.825	192.975	193.35	192.95
191.675	195.125	194.525	192.7	194.3	191.7	195.35	191.8	191.575	192.175	191.9	191.95	191.65	193.425	192.85	194.55
192.25	194.225	194.8	194.75	194.7	193.75	194.975	192.05	194.275	193.55	194.025	194.325	192.8	195.2	194.125	191.725
191.225	194.45	195.7	194.85	194.725	192.375	195.1	193.5	195.3	193.7	193.075	193.95	191.75	192.575	192.75	194.425
195.975	194.9	195.55	195.65	191.15	191.2	195.25	193.25	192.65	193.025	191.875	193.525	191.825	192.225	193.65	191.325
192.35	194.925	195.725	195.575	193.625	191.25	194.5	192	191.075	191.85	191.4	191.025	191.625	191.125	192.775	193.1
191.3	195.05	193.9	193.225	191.35	194.4	195.275	191.475	194.1	193.325	191.425	192.1	191.5	193.775	195.025	192.2

W_{mn}^{xG} Wavelength Sub Grid Matrix (x=14)

192.525	193.675	194.775	193.125	191.55	192.4	194.25	194.35	194.075	193.8	195.225	194.05	193.575	194.175	192.025	191.05
191.175	193.375	194.875	195.625	193.4	195.775	193.925	194	194.625	192.9	191.375	191.925	192.475	194.95	191.275	192.875
195.075	195.675	195.475	194.2	195.175	195.4	191.775	194.375	194.675	193.875	193.975	193.275	193.45	194.6	194.575	191.45
195.45	194.15	194.825	195	191.525	195.375	192.15	191.975	192.125	192.325	192.625	193.175	193.05	193.85	191.6	193.3
193	195.325	195.5	193.2	194.475	195.15	192.5	192.6	192.675	192.45	192.275	193.725	191.1	193.475	192.425	193.825
193.15	194.65	195.6	195.425	193.6	195.525	192.925	191	192.3	192.725	192.55	192.825	192.975	193.35	192.95	192.075
195.125	194.525	192.7	194.3	191.7	195.35	191.8	191.575	192.175	191.9	191.95	191.65	193.425	192.85	194.55	191.675
194.225	194.8	194.75	194.7	193.75	194.975	192.05	194.275	193.55	194.025	194.325	192.8	195.2	194.125	191.725	192.25
194.45	195.7	194.85	194.725	192.375	195.1	193.5	195.3	193.7	193.075	193.95	191.75	192.575	192.75	194.425	191.225
194.9	195.55	195.65	191.15	191.2	195.25	193.25	192.65	193.025	191.875	193.525	191.825	192.225	193.65	191.325	195.975
194.925	195.725	195.575	193.625	191.25	194.5	192	191.075	191.85	191.4	191.025	191.625	191.125	192.775	193.1	192.35
195.05	193.9	193.225	191.35	194.4	195.275	191.475	194.1	193.325	191.425	192.1	191.5	193.775	195.025	192.2	191.3

W_{mn}^{xG} Wavelength Sub Grid Matrix (x=15)

193.675	194.775	193.125	191.55	192.4	194.25	194.35	194.075	193.8	195.225	194.05	193.575	194.175	192.025	191.05	192.525
193.375	194.875	195.625	193.4	195.775	193.925	194	194.625	192.9	191.375	191.925	192.475	194.95	191.275	192.875	191.175
195.675	195.475	194.2	195.175	195.4	191.775	194.375	194.675	193.875	193.975	193.275	193.45	194.6	194.575	191.45	195.075
194.15	194.825	195	191.525	195.375	192.15	191.975	192.125	192.325	192.625	193.175	193.05	193.85	191.6	193.3	195.45
195.325	195.5	193.2	194.475	195.15	192.5	192.6	192.675	192.45	192.275	193.725	191.1	193.475	192.425	193.825	193
194.65	195.6	195.425	193.6	195.525	192.925	191	192.3	192.725	192.55	192.825	192.975	193.35	192.95	192.075	193.15
194.525	192.7	194.3	191.7	195.35	191.8	191.575	192.175	191.9	191.95	191.65	193.425	192.85	194.55	191.675	195.125
194.8	194.75	194.7	193.75	194.975	192.05	194.275	193.55	194.025	194.325	192.8	195.2	194.125	191.725	192.25	194.225
195.7	194.85	194.725	192.375	195.1	193.5	195.3	193.7	193.075	193.95	191.75	192.575	192.75	194.425	191.225	194.45
195.55	195.65	191.15	191.2	195.25	193.25	192.65	193.025	191.875	193.525	191.825	192.225	193.65	191.325	195.975	194.9
195.725	195.575	193.625	191.25	194.5	192	191.075	191.85	191.4	191.025	191.625	191.125	192.775	193.1	192.35	194.925
193.9	193.225	191.35	194.4	195.275	191.475	194.1	193.325	191.425	192.1	191.5	193.775	195.025	192.2	191.3	195.05

W_{mn}^{xG} Wavelength Sub Grid Matrix (x=16)

194.775	193.125	191.55	192.4	194.25	194.35	194.075	193.8	195.225	194.05	193.575	194.175	192.025	191.05	192.525	193.675
194.875	195.625	193.4	195.775	193.925	194	194.625	192.9	191.375	191.925	192.475	194.95	191.275	192.875	191.175	193.375
195.475	194.2	195.175	195.4	191.775	194.375	194.675	193.875	193.975	193.275	193.45	194.6	194.575	191.45	195.075	195.675
194.825	195	191.525	195.375	192.15	191.975	192.125	192.325	192.625	193.175	193.05	193.85	191.6	193.3	195.45	194.15
195.5	193.2	194.475	195.15	192.5	192.6	192.675	192.45	192.275	193.725	191.1	193.475	192.425	193.825	193	195.325
195.6	195.425	193.6	195.525	192.925	191	192.3	192.725	192.55	192.825	192.975	193.35	192.95	192.075	193.15	194.65
192.7	194.3	191.7	195.35	191.8	191.575	192.175	191.9	191.95	191.65	193.425	192.85	194.55	191.675	195.125	194.525
194.75	194.7	193.75	194.975	192.05	194.275	193.55	194.025	194.325	192.8	195.2	194.125	191.725	192.25	194.225	194.8
194.85	194.725	192.375	195.1	193.5	195.3	193.7	193.075	193.95	191.75	192.575	192.75	194.425	191.225	194.45	195.7
195.65	191.15	191.2	195.25	193.25	192.65	193.025	191.875	193.525	191.825	192.225	193.65	191.325	195.975	194.9	195.55
195.575	193.625	191.25	194.5	192	191.075	191.85	191.4	191.025	191.625	191.125	192.775	193.1	192.35	194.925	195.725
193.225	191.35	194.4	195.275	191.475	194.1	193.325	191.425	192.1	191.5	193.775	195.025	192.2	191.3	195.05	193.9

APPENDIX C: ORTHOGONAL SYMMETRIC CODE MATRICES FOR P= 13

$$C^{1}_{12,13}=\begin{pmatrix}
1&0&0&0&0&0&0&0&0&0&0&0&0\\
0&1&0&0&0&0&0&0&0&0&0&0&0\\
0&0&1&0&0&0&0&0&0&0&0&0&0\\
0&0&0&1&0&0&0&0&0&0&0&0&0\\
0&0&0&0&1&0&0&0&0&0&0&0&0\\
0&0&0&0&0&1&0&0&0&0&0&0&0\\
0&0&0&0&0&0&1&0&0&0&0&0&0\\
0&0&0&0&0&0&0&1&0&0&0&0&0\\
0&0&0&0&0&0&0&0&1&0&0&0&0\\
0&0&0&0&0&0&0&0&0&1&0&0&0\\
0&0&0&0&0&0&0&0&0&0&1&0&0\\
0&0&0&0&0&0&0&0&0&0&0&1&0
\end{pmatrix}
\quad
C^{2}_{12,13}=\begin{pmatrix}
0&1&0&0&0&0&0&0&0&0&0&0&0\\
0&0&0&1&0&0&0&0&0&0&0&0&0\\
0&0&0&0&0&1&0&0&0&0&0&0&0\\
0&0&0&0&0&0&0&1&0&0&0&0&0\\
0&0&0&0&0&0&0&0&0&1&0&0&0\\
0&0&0&0&0&0&0&0&0&0&0&1&0\\
1&0&0&0&0&0&0&0&0&0&0&0&0\\
0&0&1&0&0&0&0&0&0&0&0&0&0\\
0&0&0&0&1&0&0&0&0&0&0&0&0\\
0&0&0&0&0&0&1&0&0&0&0&0&0\\
0&0&0&0&0&0&0&0&1&0&0&0&0\\
0&0&0&0&0&0&0&0&0&0&1&0&0
\end{pmatrix}$$

$$C^{k3}_{12,13}=\begin{pmatrix}
0&0&1&0&0&0&0&0&0&0&0&0&0\\
0&0&0&0&0&1&0&0&0&0&0&0&0\\
0&0&0&0&0&0&0&0&1&0&0&0&0\\
0&0&0&0&0&0&0&0&0&0&0&1&0\\
0&1&0&0&0&0&0&0&0&0&0&0&0\\
0&0&0&0&1&0&0&0&0&0&0&0&0\\
0&0&0&0&0&0&0&1&0&0&0&0&0\\
0&0&0&0&0&0&0&0&0&0&1&0&0\\
1&0&0&0&0&0&0&0&0&0&0&0&0\\
0&0&0&1&0&0&0&0&0&0&0&0&0\\
0&0&0&0&0&0&1&0&0&0&0&0&0\\
0&0&0&0&0&0&0&0&0&1&0&0&0
\end{pmatrix}
\quad
C^{4}_{12,13}=\begin{pmatrix}
0&0&0&1&0&0&0&0&0&0&0&0&0\\
0&0&0&0&0&0&0&1&0&0&0&0&0\\
0&0&0&0&0&0&0&0&0&0&0&1&0\\
0&0&1&0&0&0&0&0&0&0&0&0&0\\
0&0&0&0&0&0&1&0&0&0&0&0&0\\
0&0&0&0&0&0&0&0&0&0&1&0&0\\
0&1&0&0&0&0&0&0&0&0&0&0&0\\
0&0&0&0&0&1&0&0&0&0&0&0&0\\
0&0&0&0&0&0&0&0&0&1&0&0&0\\
1&0&0&0&0&0&0&0&0&0&0&0&0\\
0&0&0&0&1&0&0&0&0&0&0&0&0\\
0&0&0&0&0&0&0&0&1&0&0&0&0
\end{pmatrix}$$

$$C^{5}_{12,13}=\begin{pmatrix}
0&0&0&0&1&0&0&0&0&0&0&0&0\\
0&0&0&0&0&0&0&0&0&1&0&0&0\\
0&1&0&0&0&0&0&0&0&0&0&0&0\\
0&0&0&0&0&0&1&0&0&0&0&0&0\\
0&0&0&0&0&0&0&0&0&0&0&1&0\\
0&0&0&1&0&0&0&0&0&0&0&0&0\\
0&0&0&0&0&0&0&0&1&0&0&0&0\\
1&0&0&0&0&0&0&0&0&0&0&0&0\\
0&0&0&0&0&1&0&0&0&0&0&0&0\\
0&0&0&0&0&0&0&0&0&0&1&0&0\\
0&0&1&0&0&0&0&0&0&0&0&0&0\\
0&0&0&0&0&0&0&1&0&0&0&0&0
\end{pmatrix}
\quad
C^{6}_{12,13}=\begin{pmatrix}
0&0&0&0&0&1&0&0&0&0&0&0&0\\
0&0&0&0&0&0&0&0&0&0&0&1&0\\
0&0&0&0&1&0&0&0&0&0&-0&0&0\\
0&0&0&0&0&0&0&0&0&0&1&0&0\\
0&0&0&1&0&0&0&0&0&0&0&0&0\\
0&0&0&0&0&0&0&0&0&1&0&0&0\\
0&0&1&0&0&0&0&0&0&0&0&0&0\\
0&0&0&0&0&0&0&0&1&0&0&0&0\\
0&1&0&0&0&0&0&0&0&0&0&0&0\\
0&0&0&0&0&0&0&1&0&0&0&0&0\\
1&0&0&0&0&0&0&0&0&0&0&0&0\\
0&0&0&0&0&0&1&0&0&0&0&0&0
\end{pmatrix}$$

$$C^{7}_{12,13}=\begin{pmatrix}
0&0&0&0&0&0&1&0&0&0&0&0&0\\
1&0&0&0&0&0&0&0&0&0&0&0&0\\
0&0&0&0&0&0&0&1&0&0&0&0&0\\
0&1&0&0&0&0&0&0&0&0&0&0&0\\
0&0&0&0&0&0&0&0&1&0&0&0&0\\
0&0&1&0&0&0&0&0&0&0&0&0&0\\
0&0&0&0&0&0&0&0&0&1&0&0&0\\
0&0&0&1&0&0&0&0&0&0&0&0&0\\
0&0&0&0&0&0&0&0&0&0&1&0&0\\
0&0&0&0&1&0&0&0&0&0&0&0&0\\
0&0&0&0&0&0&0&0&0&0&0&1&0\\
0&0&0&0&0&1&0&0&0&0&0&0&0
\end{pmatrix}
\quad
C^{8}_{12,13}=\begin{pmatrix}
0&0&0&0&0&0&0&1&0&0&0&0&0\\
0&0&1&0&0&0&0&0&0&0&0&0&0\\
0&0&0&0&0&0&0&0&0&0&1&0&0\\
0&0&0&0&0&1&0&0&0&0&0&0&0\\
1&0&0&0&0&0&0&0&0&0&0&0&0\\
0&0&0&0&0&0&0&0&1&0&0&0&0\\
0&0&0&1&0&0&0&0&0&0&0&0&0\\
0&0&0&0&0&0&0&0&0&0&0&1&0\\
0&0&0&0&0&0&1&0&0&0&0&0&0\\
0&1&0&0&0&0&0&0&0&0&0&0&0\\
0&0&0&0&0&0&0&0&0&1&0&0&0\\
0&0&0&0&1&0&0&0&0&0&0&0&0
\end{pmatrix}$$

$$C^{9}_{12,13}=\begin{pmatrix}
0&0&0&0&0&0&0&0&1&0&0&0&0\\
0&0&0&0&1&0&0&0&0&0&0&0&0\\
1&0&0&0&0&0&0&0&0&0&0&0&0\\
0&0&0&0&0&0&0&0&0&1&0&0&0\\
0&0&0&0&0&1&0&0&0&0&0&0&0\\
0&1&0&0&0&0&0&0&0&0&0&0&0\\
0&0&0&0&0&0&0&0&0&0&1&0&0\\
0&0&0&0&0&0&1&0&0&0&0&0&0\\
0&0&1&0&0&0&0&0&0&0&0&0&0\\
0&0&0&0&0&0&0&0&0&0&0&1&0\\
0&0&0&0&0&0&0&1&0&0&0&0&0\\
0&0&0&1&0&0&0&0&0&0&0&0&0
\end{pmatrix}
\quad
C^{10}_{12,13}=\begin{pmatrix}
0&0&0&0&0&0&0&0&0&1&0&0&0\\
0&0&0&0&0&0&1&0&0&0&0&0&0\\
0&0&0&1&0&0&0&0&0&0&0&0&0\\
1&0&0&0&0&0&0&0&0&0&0&0&0\\
0&0&0&0&0&0&0&0&0&0&1&0&0\\
0&0&0&0&0&0&0&1&0&0&0&0&0\\
0&0&0&0&1&0&0&0&0&0&0&0&0\\
0&1&0&0&0&0&0&0&0&0&0&0&0\\
0&0&0&0&0&0&0&0&0&0&0&1&0\\
0&0&0&0&0&0&0&0&1&0&0&0&0\\
0&0&0&0&0&1&0&0&0&0&0&0&0\\
0&0&1&0&0&0&0&0&0&0&0&0&0
\end{pmatrix}$$

$$C^{11}_{12,13}=\begin{pmatrix}
0&0&0&0&0&0&0&0&0&0&1&0&0\\
0&0&0&0&0&0&0&0&1&0&0&0&0\\
0&0&0&0&0&0&1&0&0&0&0&0&0\\
0&0&0&0&1&0&0&0&0&0&0&0&0\\
0&0&1&0&0&0&0&0&0&0&0&0&0\\
1&0&0&0&0&0&0&0&0&0&0&0&0\\
0&0&0&0&0&0&0&0&0&0&0&1&0\\
0&0&0&0&0&0&0&0&0&1&0&0&0\\
0&0&0&0&0&0&0&1&0&0&0&0&0\\
0&0&0&0&0&1&0&0&0&0&0&0&0\\
0&0&0&1&0&0&0&0&0&0&0&0&0\\
0&1&0&0&0&0&0&0&0&0&0&0&0
\end{pmatrix}
\quad
C^{12}_{12,13}=\begin{pmatrix}
0&0&0&0&0&0&0&0&0&0&0&1&0\\
0&0&0&0&0&0&0&0&0&0&1&0&0\\
0&0&0&0&0&0&0&0&0&1&0&0&0\\
0&0&0&0&0&0&0&0&1&0&0&0&0\\
0&0&0&0&0&0&0&1&0&0&0&0&0\\
0&0&0&0&0&0&1&0&0&0&0&0&0\\
0&0&0&0&0&1&0&0&0&0&0&0&0\\
0&0&0&0&1&0&0&0&0&0&0&0&0\\
0&0&0&1&0&0&0&0&0&0&0&0&0\\
0&0&1&0&0&0&0&0&0&0&0&0&0\\
0&1&0&0&0&0&0&0&0&0&0&0&0\\
1&0&0&0&0&0&0&0&0&0&0&0&0
\end{pmatrix}$$

APPENDIX D: WAVELENGTH SEQUENCES FOR SYMMETRIC TS/WH, P= 13

The following wavelength sequences were generated by mapping the wavelength matrices to symmetric time spreading/ wavelength hopping matrices using the relation in $\lambda_{mn}^{ks} = C_{mn}^{ks_s} \odot \mathrm{W}_{\mathrm{mn}}^{\mathrm{SG}}$, where mapping is indicated as $\mathrm{W}_{\mathrm{x}}(\mathrm{C}_{\mathrm{y}})$ and where x and y indicate the wavelength sub grid (1 to 16) and code matrices (1 to 12), respectively.

Mapping	Hop1	Hop2	Hop3	Hop4	Hop5	Hop6	Hop7	Hop8	Hop9	Hop10	Hop11	Hop12
W1(C1)	193.125	193.4	195.4	192.15	192.6	192.3	191.9	194.325	191.75	192.225	192.775	192.2
W1(C2)	194.3	191.55	194.975	193.925	195.3	194.675	191.875	192.625	191.625	191.1	195.025	192.95
W1(C3)	194.725	194.475	192.4	193.25	191	194.625	191.4	191.95	193.275	193.775	194.125	191.6
W1(C4)	191.15	191.7	195.375	194.25	191.075	193.55	192.45	191.375	191.5	192.575	193.35	194.575
W1(C5)	194.7	195.175	194.5	192.925	194.35	193.7	192.325	192.1	191.65	192.475	193.65	192.425
W1(C6)	193.625	192.375	195.35	192.5	194.375	194.075	191.425	193.525	192.8	192.975	193.85	191.275
W1(C7)	195.625	191.525	195.525	192.05	192.65	193.325	193.8	193.975	193.725	193.425	192.75	193.1
W1(C8)	193.2	191.2	195.775	191.8	194.1	192.125	193.075	195.225	192.825	191.125	194.6	191.725
W1(C9)	194.2	193.6	195.1	191.475	194	192.675	194.025	191.025	194.05	193.05	192.85	191.325
W1(C10)	195	193.75	195.275	191.775	191.575	191.85	192.9	192.55	191.825	193.575	193.475	194.425
W1(C11)	195.425	194.4	195.15	192	191.975	193.025	193.875	193.95	191.925	195.2	194.175	194.55
W1(C12)	191.35	191.25	195.25	193.5	194.275	192.175	192.725	192.275	193.175	193.45	194.95	192.025
W2(C1)	191.55	195.775	191.775	191.975	192.675	192.725	191.95	192.8	192.575	193.65	193.1	191.3
W2(C2)	191.7	192.4	192.05	194	193.7	193.875	193.525	193.175	191.125	193.475	192.2	192.075
W2(C3)	192.375	195.15	194.25	192.65	192.3	192.9	191.025	191.65	193.45	195.025	191.725	193.3
W2(C4)	191.2	195.35	192.15	194.35	191.85	194.025	192.275	191.925	193.775	192.75	192.95	191.45
W2(C5)	193.75	195.4	192	191	194.075	193.075	192.625	191.5	193.425	194.95	191.325	193.825
W2(C6)	191.25	195.1	191.8	192.6	194.675	193.8	192.1	191.825	195.2	193.35	191.6	192.875
W2(C7)	193.4	195.375	192.925	194.275	193.025	191.425	195.225	193.275	191.1	192.85	194.425	192.35
W2(C8)	194.475	195.25	193.925	191.575	193.325	192.325	193.95	194.05	192.975	192.775	194.575	192.25
W2(C9)	195.175	195.525	193.5	194.1	194.625	192.45	194.325	191.625	193.575	193.85	194.55	195.975
W2(C10)	191.525	194.975	191.475	194.375	192.175	191.4	191.375	192.825	192.225	194.175	192.425	191.225
W2(C11)	193.6	195.275	192.5	191.075	192.125	191.875	193.975	191.75	192.475	194.125	192.025	191.675
W2(C12)	194.4	194.5	193.25	195.3	193.55	191.9	192.55	193.725	193.05	194.6	191.275	191.05
W3(C1)	192.4	193.925	194.375	192.125	192.45	192.55	191.65	195.2	192.75	191.325	192.35	195.05
W3(C2)	195.35	194.25	194.275	194.625	193.075	193.975	191.825	193.05	192.775	192.425	191.3	193.15
W3(C3)	195.1	192.5	194.35	193.025	192.725	191.375	191.625	193.425	194.6	192.2	192.25	195.45
W3(C4)	195.25	191.8	191.975	194.075	191.4	194.325	193.725	192.475	195.025	194.425	192.075	195.075

Mapping	Hop1	Hop2	Hop3	Hop4	Hop5	Hop6	Hop7	Hop8	Hop9	Hop10	Hop11	Hop12
W3(C5)	194.975	191.775	191.075	192.3	193.8	193.95	193.175	193.775	192.85	191.275	195.975	193
W3(C6)	194.5	193.5	191.575	192.675	193.875	195.225	191.5	192.225	194.125	192.95	193.3	191.175
W3(C7)	195.775	192.15	191	193.55	191.875	192.1	194.05	193.45	193.475	194.55	191.225	194.925
W3(C8)	195.15	193.25	194	192.175	191.425	192.625	191.75	193.575	193.35	193.1	191.45	194.225
W3(C9)	195.4	192.925	195.3	193.325	192.9	192.275	192.8	191.125	194.175	191.6	191.675	194.9
W3(C10)	195.375	192.05	194.1	194.675	191.9	191.025	191.925	192.975	193.65	192.025	193.825	194.45
W3(C11)	195.525	191.475	192.6	191.85	192.325	193.525	193.275	192.575	194.95	191.725	191.05	195.125
W3(C12)	195.275	192	192.65	193.7	194.025	191.95	192.825	191.1	193.85	194.575	192.875	192.525
W4(C1)	194.25	194	194.675	192.325	192.275	192.825	193.425	194.125	194.425	195.975	194.925	193.9
W4(C2)	191.8	194.35	193.55	192.9	193.95	193.275	192.225	193.85	193.1	193.825	195.05	194.65
W4(C3)	193.5	192.6	194.075	191.875	192.55	191.925	191.125	192.85	194.575	191.3	194.225	194.15
W4(C4)	193.25	191.575	192.125	193.8	191.025	192.8	191.1	194.95	192.2	191.225	193.15	195.675
W4(C5)	192.05	194.375	191.85	192.725	195.225	191.75	193.05	195.025	194.55	192.875	194.9	195.325
W4(C6)	192	195.3	192.175	192.45	193.975	194.05	193.775	193.65	191.725	192.075	195.45	193.375
W4(C7)	193.925	191.975	192.3	194.025	193.525	191.5	193.575	194.6	192.425	191.675	194.45	195.725
W4(C8)	192.5	192.65	194.625	191.9	192.1	193.175	192.575	194.175	192.95	192.35	195.075	194.8
W4(C9)	191.775	191	193.7	191.425	191.375	193.725	195.2	192.775	192.025	193.3	195.125	195.55
W4(C10)	192.15	194.275	193.325	193.875	191.95	191.625	192.475	193.35	191.325	191.05	193	195.7
W4(C11)	192.925	194.1	192.675	191.4	192.625	191.825	193.45	192.75	191.275	192.25	192.525	194.525
W4(C12)	191.475	191.075	193.025	193.075	194.325	191.65	192.975	193.475	191.6	191.45	191.175	193.675
W5(C1)	194.35	194.625	193.875	192.625	193.725	192.975	192.85	191.725	191.225	194.9	195.725	193.225
W5(C2)	191.575	194.075	194.025	191.375	191.75	193.45	193.65	191.6	192.35	193	193.9	195.6
W5(C3)	195.3	192.675	193.8	193.525	192.825	192.475	192.775	194.55	191.45	195.05	194.8	194.825
W5(C4)	192.65	192.175	192.325	195.225	191.625	195.2	193.475	191.275	191.3	194.45	194.65	195.475
W5(C5)	194.275	194.675	191.4	192.55	194.05	192.575	193.85	192.2	191.675	191.175	195.55	195.5
W5(C6)	191.075	193.7	191.9	192.275	193.275	193.575	195.025	191.325	192.25	193.15	194.15	194.875
W5(C7)	194	192.125	192.725	194.325	191.825	193.775	194.175	194.575	193.825	195.125	195.7	195.575
W5(C8)	192.6	193.025	192.9	191.95	191.5	193.05	192.75	192.025	192.075	194.925	195.675	194.75

Mapping	Hop1	Hop2	Hop3	Hop4	Hop5	Hop6	Hop7	Hop8	Hop9	Hop10	Hop11	Hop12
W5(C9)	194.375	192.3	193.075	192.1	191.925	191.1	194.125	193.1	191.05	195.45	194.525	195.65
W5(C10)	191.975	193.55	191.425	193.975	191.65	191.125	194.95	192.95	195.975	192.525	195.325	194.85
W5(C11)	191	193.325	192.45	191.025	193.175	192.225	194.6	194.425	192.875	194.225	193.675	192.7
W5(C12)	194.1	191.85	191.875	193.95	192.8	193.425	193.35	192.425	193.3	195.075	193.375	194.775
W6(C1)	194.075	192.9	193.975	193.175	191.1	193.35	194.55	192.25	194.45	195.55	195.575	191.35
W6(C2)	192.175	193.8	194.325	191.925	192.575	194.6	191.325	193.3	194.925	195.325	193.225	195.425
W6(C3)	193.7	192.45	195.225	191.825	192.975	194.95	193.1	191.675	195.075	193.9	194.75	195
W6(C4)	193.025	191.9	192.625	194.05	191.125	194.125	192.425	192.875	195.05	195.7	195.6	194.2
W6(C5)	193.55	193.875	191.025	192.825	193.575	192.75	191.6	191.3	195.125	193.375	195.65	193.2
W6(C6)	191.85	193.075	191.95	193.725	193.45	194.175	192.2	195.975	194.225	194.65	194.825	195.625
W6(C7)	194.625	192.325	192.55	192.8	192.225	195.025	192.025	191.45	193	194.525	194.85	193.625
W6(C8)	192.675	191.875	191.375	191.65	193.775	193.85	194.425	191.05	193.15	195.725	195.475	194.7
W6(C9)	194.675	192.725	193.95	191.5	192.475	193.475	191.725	192.35	192.525	194.15	192.7	191.15
W6(C10)	192.125	194.025	192.1	193.275	193.425	192.775	191.275	192.075	194.9	193.675	195.5	194.725
W6(C11)	192.3	191.425	192.275	191.625	193.05	193.65	194.575	191.225	191.175	194.8	194.775	194.3
W6(C12)	193.325	191.4	193.525	191.75	195.2	192.85	192.95	193.825	195.45	195.675	194.875	193.125
W7(C1)	193.8	191.375	193.275	193.05	193.475	192.95	191.675	194.225	195.7	195.65	193.625	194.4
W7(C2)	191.9	195.225	192.8	192.475	192.75	194.575	195.975	195.45	195.725	195.5	191.35	193.6
W7(C3)	193.075	192.275	194.05	192.225	193.35	191.275	192.35	195.125	195.675	193.225	194.7	191.525
W7(C4)	191.875	191.95	193.175	193.575	192.775	191.725	193.825	191.175	193.9	194.85	195.425	195.175
W7(C5)	194.025	193.975	191.625	192.975	194.175	194.425	193.3	195.05	194.525	194.875	191.15	194.475
W7(C6)	191.4	193.95	191.65	191.1	194.6	192.025	191.3	194.9	194.8	195.6	195	193.4
W7(C7)	192.9	192.625	192.825	195.2	193.65	192.2	191.05	195.075	195.325	192.7	194.725	191.25
W7(C8)	192.45	193.525	191.925	193.425	195.025	191.6	191.225	192.525	194.65	195.575	194.2	193.75
W7(C9)	193.875	192.55	191.75	193.775	194.95	192.425	192.25	194.925	193.675	194.825	194.3	191.2
W7(C10)	192.325	194.325	191.5	193.45	192.85	193.1	192.875	193.15	195.55	194.775	193.2	192.375
W7(C11)	192.725	192.1	193.725	191.125	193.85	191.325	191.45	194.45	193.375	194.75	193.125	191.7
W7(C12)	191.425	191.025	191.825	192.575	194.125	194.55	192.075	193	194.15	195.475	195.625	191.55

Mapping	Hop1	**Hop2**	**Hop3**	**Hop4**	**Hop5**	**Hop6**	**Hop7**	**Hop8**	**Hop9**	**Hop10**	**Hop11**	**Hop12**
W8(C1)	195.225	191.925	193.45	193.85	192.425	192.075	195.125	194.8	194.85	191.15	191.25	195.275
W8(C2)	191.95	194.05	195.2	194.95	194.425	191.45	194.9	194.15	195.575	193.2	194.4	195.525
W8(C3)	193.95	193.725	193.575	193.65	192.95	192.875	194.925	194.525	195.475	191.35	193.75	195.375
W8(C4)	193.525	191.65	193.05	194.175	193.1	192.25	193	193.375	193.225	194.725	193.6	195.4
W8(C5)	194.325	193.275	191.125	193.35	192.025	191.225	195.45	193.9	192.7	195.625	191.2	195.15
W8(C6)	191.025	191.75	193.425	193.475	194.575	191.05	195.05	195.55	194.75	195.425	191.525	195.775
W8(C7)	191.375	193.175	192.975	194.125	191.325	191.3	192.525	195.675	195.5	194.3	192.375	194.5
W8(C8)	192.275	191.825	192.475	192.85	192.2	193.3	194.45	193.675	195.6	193.625	195.175	194.975
W8(C9)	193.975	192.825	192.575	195.025	191.275	193.825	194.225	195.725	194.775	195	191.7	195.25
W8(C10)	192.625	192.8	193.775	194.6	194.55	192.35	191.175	194.65	195.65	193.125	194.475	195.1
W8(C11)	192.55	191.5	191.1	192.775	191.6	195.975	195.075	195.7	194.875	194.7	191.55	195.35
W8(C12)	192.1	191.625	192.225	192.75	191.725	191.675	193.15	195.325	194.825	194.2	193.4	192.4
W9(C1)	194.05	192.475	194.6	191.6	193.825	193.15	194.525	194.75	194.725	191.2	194.5	191.475
W9(C2)	191.65	193.575	194.125	191.275	191.225	195.075	195.55	194.825	193.625	194.475	195.275	192.925
W9(C3)	191.75	191.1	194.175	191.325	192.075	191.175	195.725	192.7	194.2	194.4	194.975	192.15
W9(C4)	191.825	193.425	193.85	192.025	192.35	194.225	195.325	194.875	191.35	192.375	195.525	191.775
W9(C5)	192.8	193.45	192.775	192.95	191.05	194.45	194.15	193.225	194.3	193.4	195.25	192.5
W9(C6)	191.625	192.575	192.85	192.425	191.45	192.525	193.9	195.65	194.7	193.6	195.375	193.925
W9(C7)	191.925	193.05	193.35	191.725	195.975	195.05	193.675	195.475	193.2	191.7	195.1	192
W9(C8)	193.725	192.225	194.95	194.55	191.3	195.45	195.7	194.775	195.425	191.25	195.4	192.05
W9(C9)	193.275	192.975	192.75	192.2	192.875	193	194.8	195.575	193.125	191.525	195.35	193.25
W9(C10)	193.175	195.2	195.025	194.575	191.675	194.925	193.375	195.6	191.15	191.55	195.15	193.5
W9(C11)	192.825	193.775	193.475	193.1	193.3	194.9	195.675	194.85	195.625	193.75	192.4	191.8
W9(C12)	191.5	191.125	193.65	194.425	192.25	195.125	194.65	195.5	195	195.175	195.775	194.25
W10(C1)	193.575	194.95	194.575	193.3	193	194.65	192.7	194.7	192.375	195.25	192	194.1
W10(C2)	193.425	194.175	191.725	192.875	194.45	195.675	195.65	195	191.25	195.15	191.475	191
W10(C3)	192.575	193.475	192.025	195.975	193.15	193.375	195.575	194.3	195.175	195.275	192.05	191.975
W10(C4)	192.225	192.85	191.6	191.05	194.925	194.8	195.5	195.625	194.4	195.1	192.925	194.375

Mapping	Hop1	**Hop2**	**Hop3**	**Hop4**	**Hop5**	**Hop6**	**Hop7**	**Hop8**	**Hop9**	**Hop10**	**Hop11**	**Hop12**
W10(C5)	195.2	194.6	193.1	192.075	192.525	195.7	194.825	191.35	191.7	195.775	193.25	192.6
W10(C6)	191.125	192.75	194.55	193.825	195.075	193.675	193.225	191.15	193.75	195.525	192.15	194
W10(C7)	192.475	193.85	192.95	192.25	194.9	193.9	194.775	194.2	194.475	195.35	193.5	191.075
W10(C8)	191.1	193.65	191.275	191.675	195.05	194.15	194.85	193.125	193.6	194.5	191.775	194.275
W10(C9)	193.45	193.35	194.425	191.3	191.175	195.325	194.75	193.625	191.55	195.375	191.8	192.65
W10(C10)	193.05	194.125	192.2	191.45	195.125	195.725	194.875	195.425	191.2	192.4	192.5	195.3
W10(C11)	192.975	195.025	192.425	192.35	195.45	195.55	195.475	194.725	193.4	194.975	194.25	191.575
W10(C12)	193.775	192.775	191.325	191.225	194.225	194.525	195.6	193.2	191.525	195.4	193.925	194.35
W11(C1)	194.175	191.275	191.45	195.45	195.325	195.6	194.3	193.75	195.1	193.25	191.075	193.325
W11(C2)	192.85	192.025	192.25	191.175	195.7	195.475	191.15	191.525	194.5	192.5	194.1	192.3
W11(C3)	192.75	192.425	191.05	194.9	194.65	194.875	193.625	191.7	195.4	191.475	194.275	192.125
W11(C4)	193.65	194.55	193.3	192.525	195.725	194.75	193.2	193.4	195.275	193.5	191	194.675
W11(C5)	194.125	194.575	192.35	193.15	193.675	194.85	195	194.4	195.35	193.925	192.65	192.675
W11(C6)	192.775	194.425	191.675	193	195.675	194.775	191.35	191.2	194.975	192.925	191.975	194.625
W11(C7)	194.95	191.6	192.075	194.225	195.55	193.225	193.125	195.175	195.15	191.8	195.3	191.85
W11(C8)	193.475	191.325	192.875	195.125	193.9	194.825	194.725	191.55	195.525	192	194.375	193.55
W11(C9)	194.6	192.95	191.225	195.05	193.375	195.5	194.7	191.25	192.4	192.15	191.575	193.025
W11(C10)	193.85	191.725	191.3	195.075	194.525	195.575	195.625	193.6	195.25	194.25	192.6	193.7
W11(C11)	193.35	192.2	193.825	194.925	194.15	195.65	194.2	192.375	195.775	192.05	194.35	192.175
W11(C12)	195.025	193.1	195.975	194.45	194.8	192.7	195.425	194.475	195.375	191.775	194	194.075
W12(C1)	192.025	192.875	195.075	194.15	195.5	195.425	191.7	194.975	193.5	192.65	191.85	191.425
W12(C2)	194.55	191.05	194.225	193.375	194.85	194.2	191.2	195.375	192	192.6	193.325	192.725
W12(C3)	194.425	193.825	192.525	195.55	195.6	195.625	191.25	195.35	191.775	194.1	193.55	192.325
W12(C4)	191.325	191.675	195.45	193.675	195.575	194.7	194.475	195.775	191.475	195.3	192.3	193.875
W12(C5)	191.725	191.45	194.925	194.65	194.775	194.725	191.525	195.275	191.8	194	193.025	192.45
W12(C6)	193.1	191.225	195.125	195.325	195.475	193.125	194.4	195.25	192.05	191	192.125	192.9
W12(C7)	191.275	193.3	193.15	194.8	195.65	191.35	191.55	195.4	192.5	191.575	193.7	191.4
W12(C8)	192.425	195.975	191.175	194.525	193.225	195	192.375	192.4	192.925	191.075	194.675	194.025

Mapping	Hop1	**Hop2**	**Hop3**	**Hop4**	**Hop5**	**Hop6**	**Hop7**	**Hop8**	**Hop9**	**Hop10**	**Hop11**	**Hop12**
W12(C9)	194.575	192.075	194.45	193.9	194.875	193.2	193.75	194.5	194.25	191.975	192.175	191.875
W12(C10)	191.6	192.25	195.05	195.675	192.7	193.625	193.4	195.525	193.25	194.35	192.675	193.075
W12(C11)	192.95	191.3	193	195.725	194.825	191.15	195.175	195.1	193.925	194.275	194.075	191.9
W12(C12)	192.2	192.35	194.9	195.7	194.75	194.3	193.6	195.15	192.15	194.375	194.625	193.8
W13(C1)	191.05	191.175	195.675	194.825	193.2	193.6	195.35	192.05	195.3	193.025	191.4	192.1
W13(C2)	191.675	192.525	194.8	194.875	194.725	195.175	195.25	192.15	191.075	192.675	191.425	192.55
W13(C3)	191.225	193	193.675	195.65	195.425	193.4	194.5	191.8	194.375	193.325	194.025	192.625
W13(C4)	195.975	195.125	194.15	194.775	193.625	193.75	195.15	193.925	194.1	193.7	192.725	193.975
W13(C5)	192.25	195.075	195.725	195.6	193.125	192.375	195.375	191.475	191.575	194.625	191.875	192.275
W13(C6)	192.35	194.45	194.525	195.5	194.2	191.55	195.275	193.25	194.275	192.3	192.325	191.375
W13(C7)	192.875	195.45	194.65	194.75	191.15	194.4	192.4	191.775	192.6	192.175	193.075	191.025
W13(C8)	193.825	194.9	193.375	192.7	191.35	191.525	195.1	194.25	191	191.85	193.875	194.325
W13(C9)	191.45	193.15	195.7	193.225	195.625	194.475	194.975	192	194.35	192.125	191.9	193.525
W13(C10)	193.3	194.225	193.9	195.475	194.3	191.25	195.775	192.925	192.65	194.075	192.45	193.95
W13(C11)	192.075	195.05	195.325	195.575	195	191.2	195.4	193.5	194	193.55	193.8	191.95
W13(C12)	191.3	194.925	195.55	194.85	194.7	191.7	195.525	192.5	191.975	194.675	192.9	195.225
W14(C1)	192.525	193.375	195.475	195	194.475	195.525	191.8	194.275	193.7	191.875	191.025	191.5
W14(C2)	195.125	193.675	194.75	195.625	192.375	195.4	193.25	191.975	191.85	192.45	192.1	192.825
W14(C3)	194.45	195.325	194.775	191.15	193.6	195.775	192	191.575	194.675	191.425	194.325	193.175
W14(C4)	194.9	194.525	194.825	193.125	191.25	194.975	192.5	194	193.325	193.075	192.55	193.275
W14(C5)	194.225	195.675	195.575	195.425	191.55	195.1	192.15	194.1	192.175	192.9	193.525	193.725
W14(C6)	194.925	195.7	192.7	193.2	195.175	192.4	191.475	192.65	193.55	192.725	192.625	191.925
W14(C7)	191.175	194.15	195.6	194.7	191.2	195.275	194.25	194.375	192.675	191.9	193.95	191.625
W14(C8)	193	195.55	194.875	194.3	194.4	195.375	193.5	194.35	192.3	191.4	193.975	192.8
W14(C9)	195.075	194.65	194.85	191.35	193.4	195.15	192.05	191.075	194.075	192.325	191.95	191.825
W14(C10)	195.45	194.8	193.225	194.2	191.7	194.5	193.925	191	193.025	193.8	192.275	191.75
W14(C11)	193.15	193.9	195.5	193.625	191.525	195.25	191.775	195.3	194.625	194.025	195.225	191.65
W14(C12)	195.05	195.725	195.65	194.725	193.75	195.35	192.925	192.6	192.125	193.875	191.375	194.05

Mapping	Hop1	**Hop2**	**Hop3**	**Hop4**	**Hop5**	**Hop6**	**Hop7**	**Hop8**	**Hop9**	**Hop10**	**Hop11**	**Hop12**
W15(C1)	193.675	194.875	194.2	191.525	195.15	192.925	191.575	193.55	193.075	193.525	191.625	193.775
W15(C2)	194.525	194.775	194.7	193.4	195.1	191.775	192.65	192.125	191.4	192.275	191.5	192.975
W15(C3)	195.7	195.5	193.125	191.2	195.525	193.925	191.075	192.175	193.875	192.1	192.8	193.05
W15(C4)	195.55	192.7	195	191.55	194.5	192.05	192.6	194.625	191.425	193.95	192.825	193.45
W15(C5)	194.8	195.475	193.625	193.6	192.4	193.5	191.975	193.325	191.9	191.375	191.825	191.1
W15(C6)	195.725	194.85	194.3	194.475	195.4	194.25	194.1	193.025	194.025	192.55	193.175	192.475
W15(C7)	193.375	194.825	195.425	193.75	195.25	191.475	194.35	194.675	192.45	191.95	191.75	191.125
W15(C8)	195.325	195.65	195.625	191.7	195.275	192.15	195.3	194.075	192.725	191.025	193.275	195.2
W15(C9)	195.675	195.6	194.725	194.4	195.775	192.5	194.275	191.85	193.8	192.625	191.65	192.225
W15(C10)	194.15	194.75	191.35	195.175	195.35	192	194	192.3	191.875	195.225	193.725	192.575
W15(C11)	194.65	193.225	193.2	191.25	195.375	193.25	194.375	193.7	192.9	194.325	194.05	193.425
W15(C12)	193.9	195.575	191.15	192.375	194.975	191.8	191	192.675	192.325	193.975	191.925	193.575
W16(C1)	194.775	195.625	195.175	195.375	192.5	191	192.175	194.025	193.95	191.825	191.125	195.025
W16(C2)	192.7	193.125	193.75	195.775	193.5	194.375	193.025	192.325	191.025	193.725	193.775	193.35
W16(C3)	194.85	193.2	191.55	195.25	192.925	194	191.85	191.9	193.975	191.5	195.2	193.85
W16(C4)	195.65	194.3	191.525	192.4	192	194.275	192.675	192.9	192.1	191.75	192.975	194.6
W16(C5)	194.75	194.2	191.25	195.525	194.25	195.3	192.125	191.425	191.95	191.925	192.225	193.475
W16(C6)	195.575	194.725	191.7	195.15	191.775	194.35	193.325	191.875	194.325	192.825	193.05	194.95
W16(C7)	194.875	195	193.6	194.975	193.25	194.1	194.075	193.875	192.275	191.65	192.575	192.775
W16(C8)	195.5	191.15	193.4	195.35	191.475	191.975	193.7	193.8	192.55	191.625	193.45	194.125
W16(C9)	195.475	195.425	192.375	195.275	193.925	192.6	193.55	191.4	195.225	193.175	193.425	193.65
W16(C10)	194.825	194.7	194.4	195.4	191.8	191.075	194.625	192.725	193.525	194.05	191.1	192.75
W16(C11)	195.6	191.35	194.475	194.5	192.15	192.65	194.675	193.075	191.375	192.8	193.575	192.85
W16(C12)	193.225	193.625	191.2	195.1	192.05	191.575	192.3	192.45	192.625	193.275	192.475	194.175

APPENDIX E: SIMULATION RESULTS FOR FILES F3, F4, AND F5

The shaded channels in each file are those used to monitor performances (channels A, B, C, and D) of Figure 13.

HOP 1	HOP 2	HOP 3	HOP 4	HOP 5
File1 (THz)	File2 (THz)	File3 (THz)	File4 (THz)	File5 (THz)
193.325	192.45	191.025	193.175	192.225
191.75	193.425	193.475	194.575	191.05
191.175	195.675	194.825	193.2	193.6
193.7	191.9	192.275	193.275	193.575
193.65	191.275	191.675	195.05	194.15
192.75	194.55	193.825	195.075	193.675
191.7	195.375	194.25	191.075	193.55
194.15	195.6	194.7	191.2	195.275
195.35	192.15	194.35	191.85	194.025
193	193.675	195.65	195.425	193.4
195.1	191.8	192.6	194.675	193.8
193.3	193.15	194.8	195.65	191.35
194.925	195.55	194.85	194.7	191.7
191.675	195.45	193.675	195.575	194.7
191.25	195.25	193.5	194.275	192.175
193.175	192.975	194.125	191.325	191.3
193.95	191.65	191.1	194.6	192.025
191.025	191.825	192.575	194.125	194.55
193.15	195.7	193.225	195.625	194.475
191.075	193.025	193.075	194.325	191.65
191.125	193.65	194.425	192.25	195.125
194.975	191.475	194.375	192.175	191.4
195.775	191.775	191.975	192.675	192.725
194.075	194.025	191.375	191.75	193.45
192.25	195.05	195.675	192.7	193.625
192.575	192.85	192.425	191.45	192.525
193.575	194.125	191.275	191.225	195.075
192.525	194.8	194.875	194.725	195.175
192.4	192.05	194	193.7	193.875
191.45	194.925	194.65	194.775	194.725
191.1	194.175	191.325	192.075	191.175
191	193.7	191.425	191.375	193.725
194.35	193.55	192.9	193.95	193.275
193.425	193.85	192.025	192.35	194.225
193.075	191.95	193.725	193.45	194.175
191.95	193.175	193.575	192.775	191.725
195.225	192.8	192.475	192.75	194.575
193.05	193.35	191.725	195.975	195.05

194.05	195.2	194.95	194.425	191.45
193.55	191.425	193.975	191.65	191.125
195.3	192.175	192.45	193.975	194.05
192.875	195.075	194.15	195.5	195.425
194.375	191.85	192.725	195.225	191.75
195.05	195.325	195.575	195	191.2
191.625	192.225	192.75	191.725	191.675
194.025	192.1	193.275	193.425	192.775
194.275	193.325	193.875	191.95	191.625
193.8	194.325	191.925	192.575	194.6
192.35	194.9	195.7	194.75	194.3
192.85	191.6	191.05	194.925	194.8
195.075	195.725	195.6	193.125	192.375
191.825	192.475	192.85	192.2	193.3
191.425	192.275	191.625	193.05	193.65
194.325	191.5	193.45	192.85	193.1
194.45	194.525	195.5	194.2	191.55
195.15	194.25	192.65	192.3	192.9
193.925	194.375	192.125	192.45	192.55
195.975	191.175	194.525	193.225	195
193.525	191.925	193.425	195.025	191.6
193.85	192.95	192.25	194.9	193.9
192.65	194.625	191.9	192.1	193.175
193.375	195.475	195	194.475	195.525
191.5	191.1	192.775	191.6	195.975

APPENDIX F: SIMULATION RESULTS FOR HOPS IN FILES F3, F4, AND F5

Simulation results for hop number 3 (File F3)

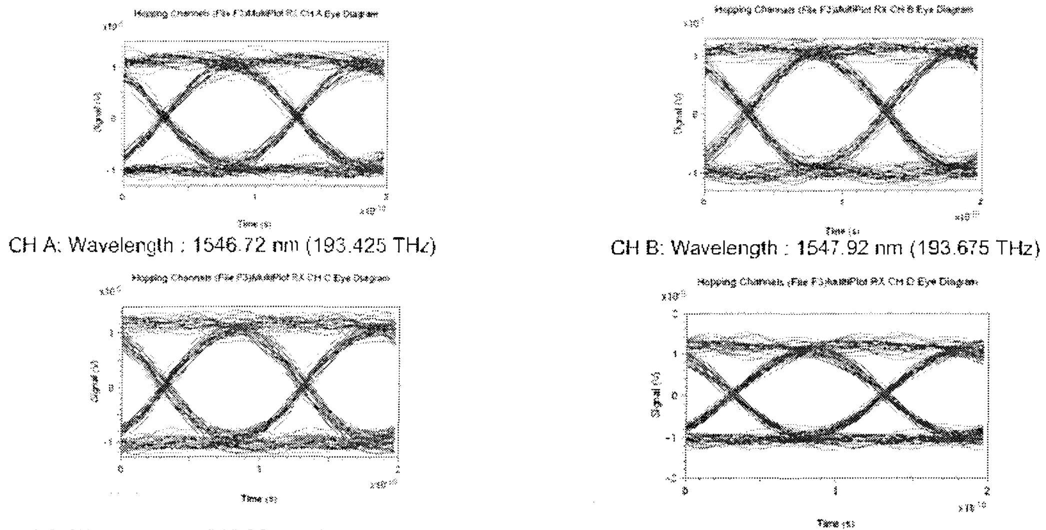

CH A: Wavelength : 1546.72 nm (193.425 THz)

CH B: Wavelength : 1547.92 nm (193.675 THz)

CH C: Wavelength : 1545.32 nm (194 THz)

CH D: Wavelength : 1562.23 nm (191.9 THz)

Figure 35: Eye pattern for 3rd hop

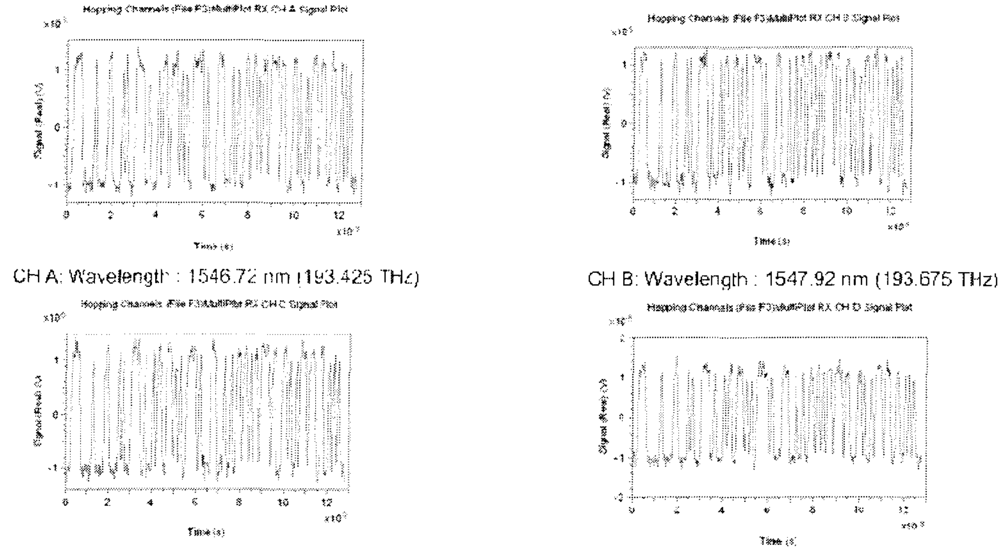

CH A: Wavelength : 1546.72 nm (193.425 THz)

CH B: Wavelength : 1547.92 nm (193.675 THz)

CH C: Wavelength : 1545.32 nm (194 THz)

CH D: Wavelength : 1562.23 nm (191.9 THz)

Figure 36: Signal output of 3rd hop

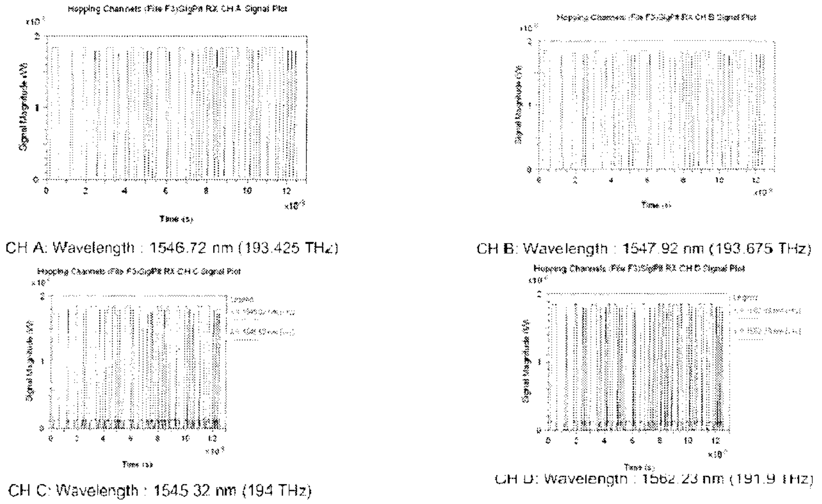

CH A: Wavelength : 1546.72 nm (193.425 THz)

CH B: Wavelength : 1547.92 nm (193.675 THz)

CH C: Wavelength : 1545.32 nm (194 THz)

CH D: Wavelength : 1562.23 nm (191.9 THz)

Figure 37: Cross channel interference in 3rd hp

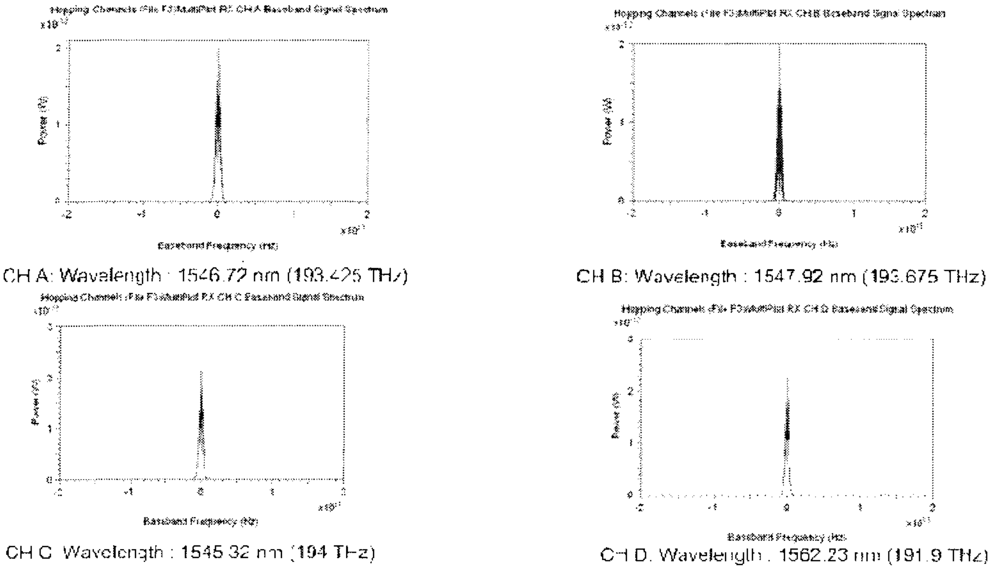

CH A: Wavelength : 1546.72 nm (193.425 THz)

CH B: Wavelength : 1547.92 nm (193.675 THz)

CH C Wavelength : 1545.32 nm (194 THz)

CH D. Wavelength . 1562.23 nm (191.9 THz)

Figure 38: Signal stability for 3rd hop

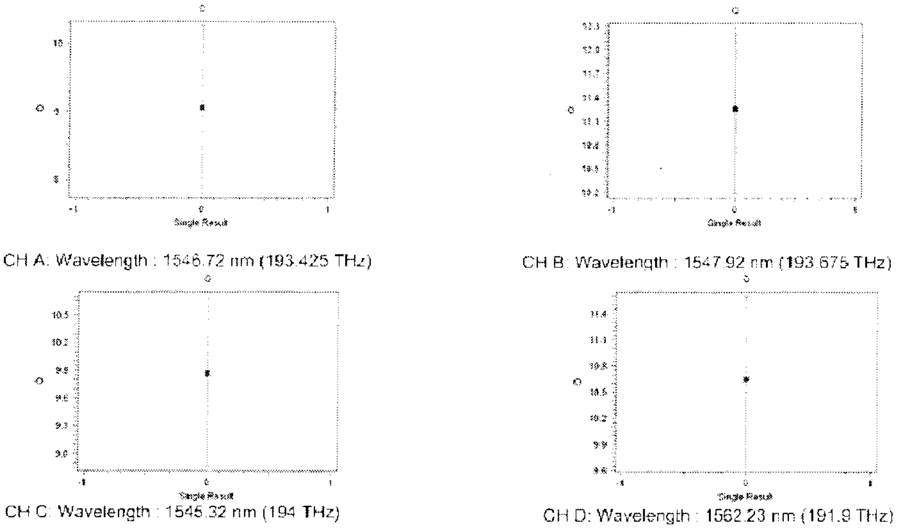

CH A: Wavelength : 1546.72 nm (193.425 THz)

CH B: Wavelength : 1547.92 nm (193.675 THz)

CH C: Wavelength : 1545.32 nm (194 THz)

CH D: Wavelength : 1562.23 nm (191.9 THz)

Figure 39: Q-Parameter for 3rd hop

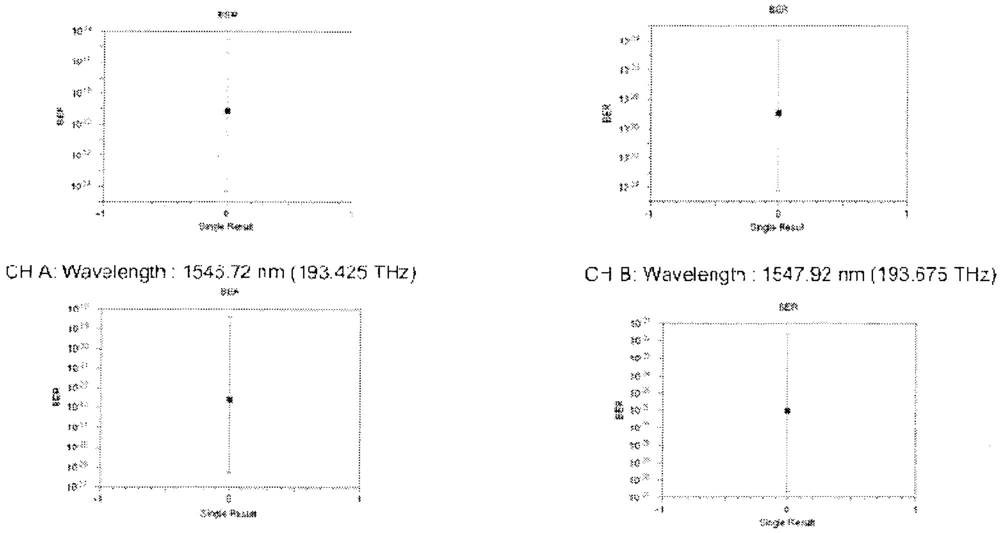

CH A: Wavelength : 1545.72 nm (193.425 THz)

CH B: Wavelength : 1547.92 nm (193.675 THz)

CH C: Wavelength : '545.32 nm (194 THz)

CH D: Wavelength : 1562.23 rm (191.9 THz)

File F4 wavelength hopping simulation results

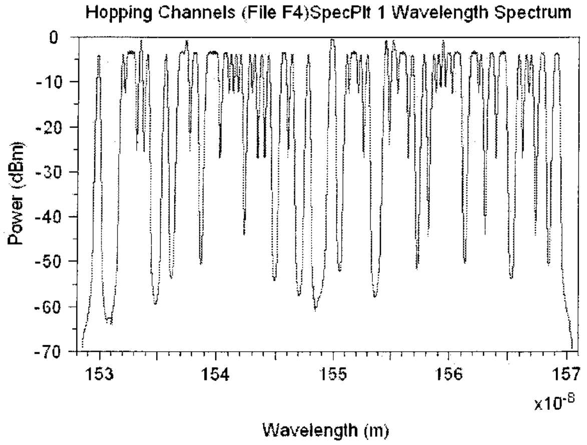

Figure 40: Spectrum of 4th hop

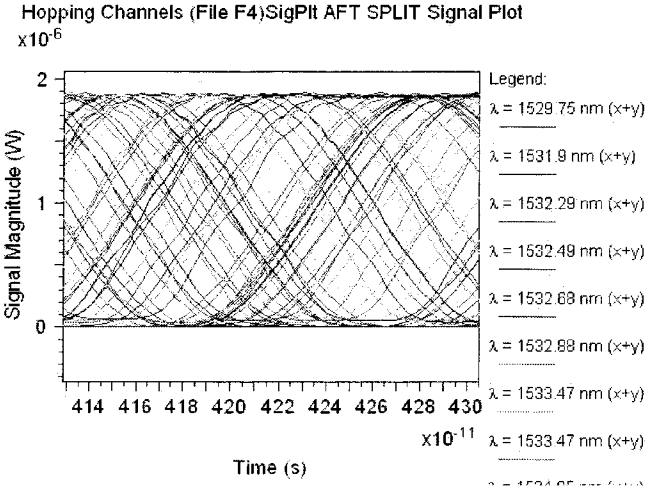

Figure 41: Signals on shared fiber link

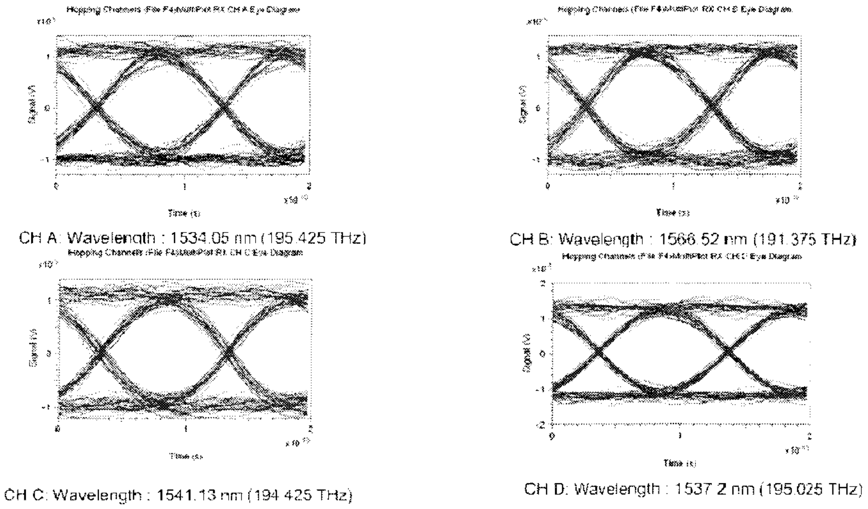

CH A: Wavelength : 1534.05 nm (195.425 THz)

CH B: Wavelength : 1566.52 nm (191.375 THz)

CH C: Wavelength : 1541.13 nm (194.425 THz)

CH D: Wavelength : 1537.2 nm (195.025 THz)

Figure 42: Eye patterns of 4th hop

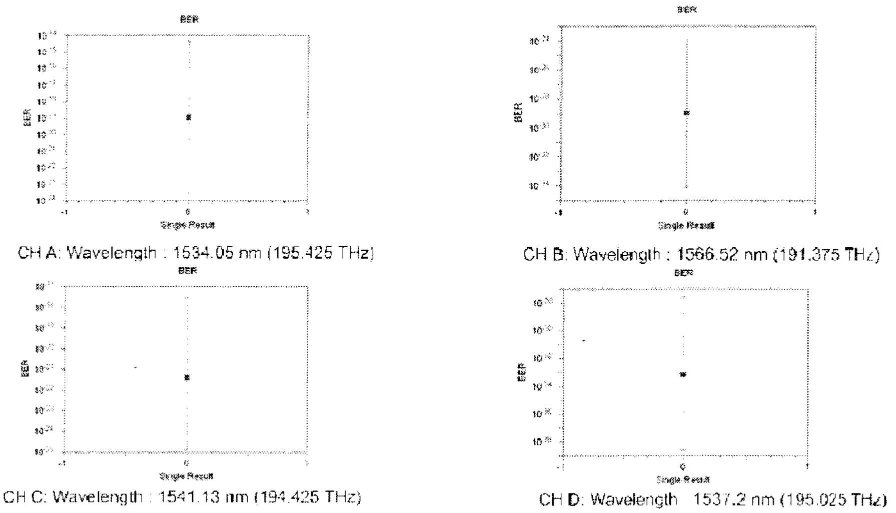

CH A: Wavelength : 1534.05 nm (195.425 THz)

CH B: Wavelength : 1566.52 nm (191.375 THz)

CH C: Wavelength : 1541.13 nm (194.425 THz)

CH D: Wavelength : 1537.2 nm (195.025 THz)

Figure 43: BER of 4th hop

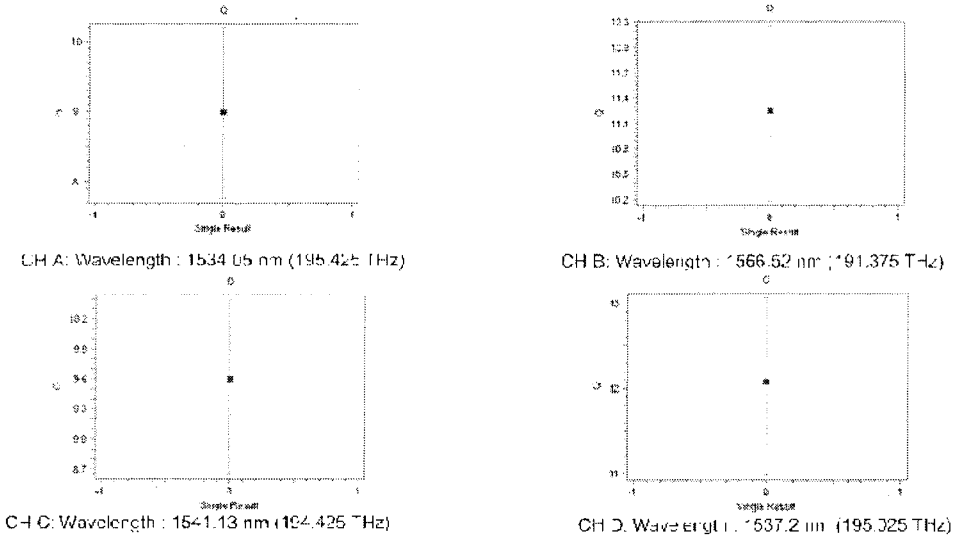

CH A: Wavelength : 1534.05 nm (195.425 THz)

CH B: Wavelength : 1566.52 nm (191.375 THz)

CH C: Wavelength : 1541.13 nm (194.425 THz)

CH D: Wavelength : 1537.2 nm (195.025 THz)

Figure 44: Q parameter of 4th hop

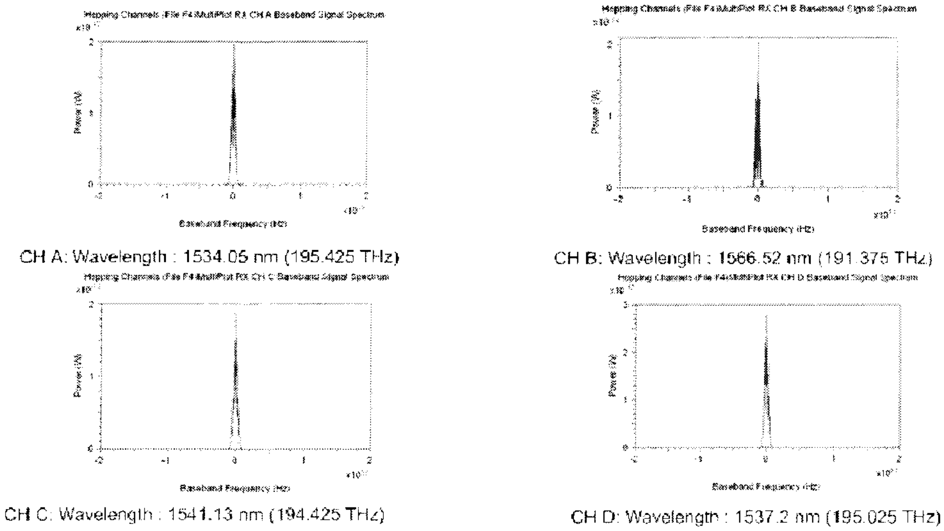

CH A: Wavelength : 1534.05 nm (195.425 THz)

CH B: Wavelength : 1566.52 nm (191.375 THz)

CH C: Wavelength : 1541.13 nm (194.425 THz)

CH D: Wavelength : 1537.2 nm (195.025 THz)

Figure 45: Signal stability of 4th hop

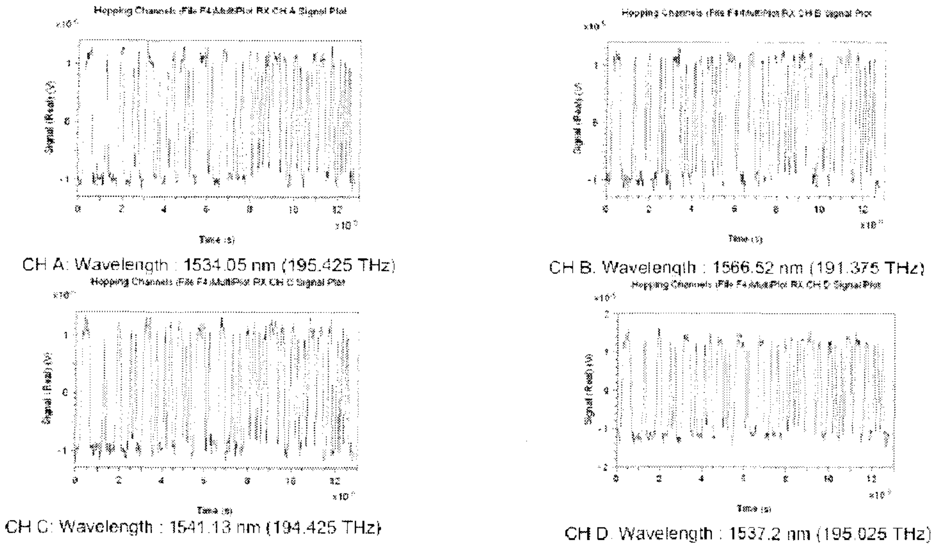

CH A: Wavelength : 1534.05 nm (195.425 THz)

CH B: Wavelength : 1566.52 nm (191.375 THz)

CH C: Wavelength : 1541.13 nm (194.425 THz)

CH D: Wavelength : 1537.2 nm (195.025 THz)

Figure 46: Signal output of 4th hop

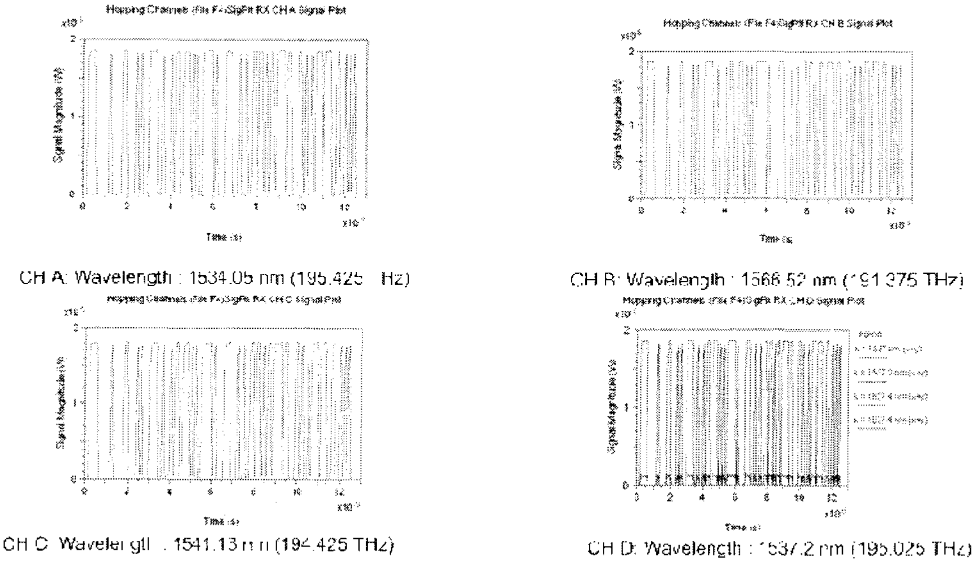

CH A: Wavelength : 1534.05 nm (195.425 THz)

CH B: Wavelength : 1566.52 nm (191.375 THz)

CH C: Wavelength : 1541.13 nm (194.425 THz)

CH D: Wavelength : 1537.2 nm (195.025 THz)

Figure 47: Cross channel interference of 4th hop

File F5 wavelength hopping simulation results

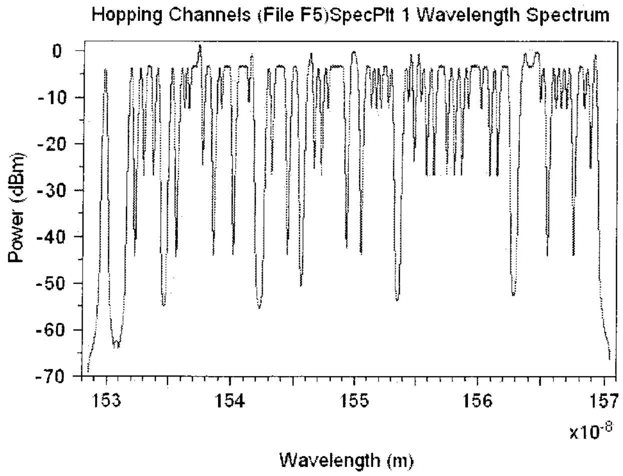

Figure 48: Spectrum of 4th hop

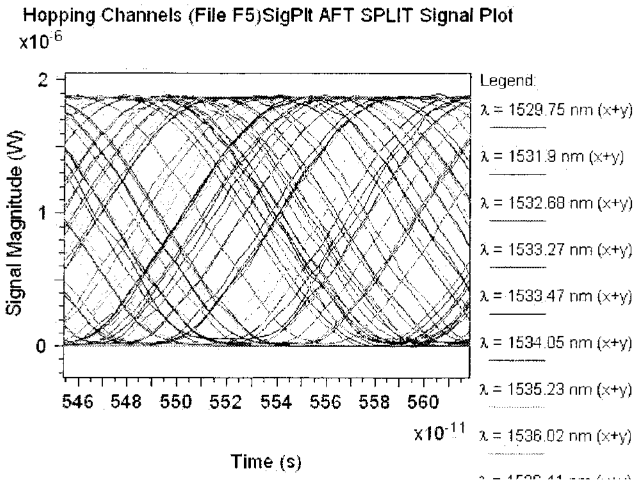

Figure 49: signal on shared link for 5th hop

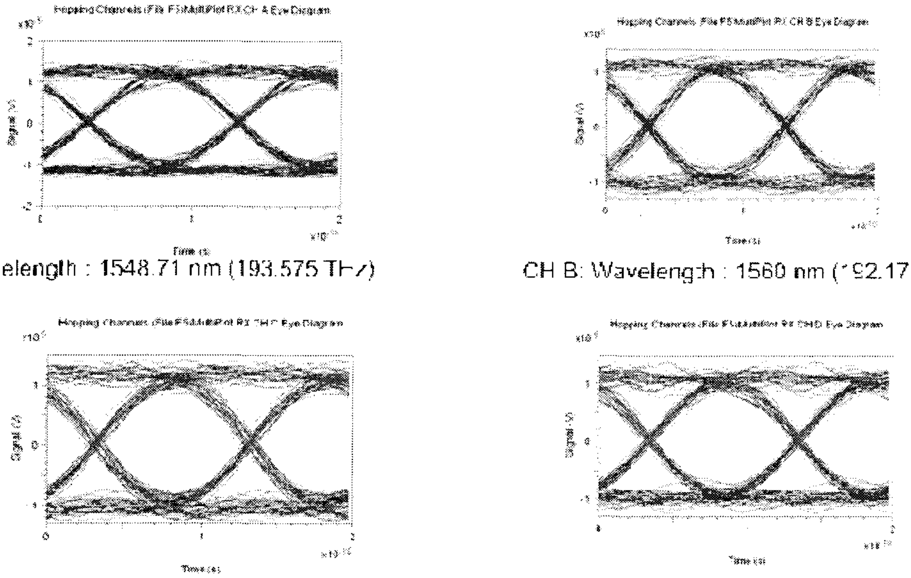

CH A: Wavelength : 1548.71 nm (193.575 THz)

CH B: Wavelength : 1560 nm (192.175 THz)

CH C: Wavelength : 1539.57 nm (194.725 THz)

CH D: Wavelength : 1537.40 nm (195 THz)

Figure 50: Eye pattern of 5th hop

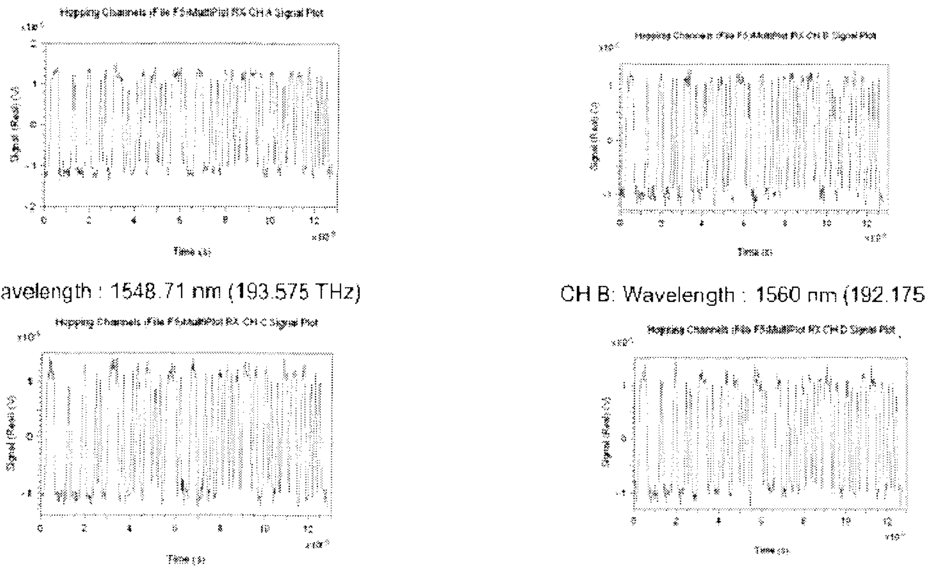

CH A: Wavelength : 1548.71 nm (193.575 THz)

CH B: Wavelength : 1560 nm (192.175 THz)

CH C: Wavelength : 1539.57 nm (194.725 THz)

CH D: Wavelength : 1537.40 nm (195 THz)

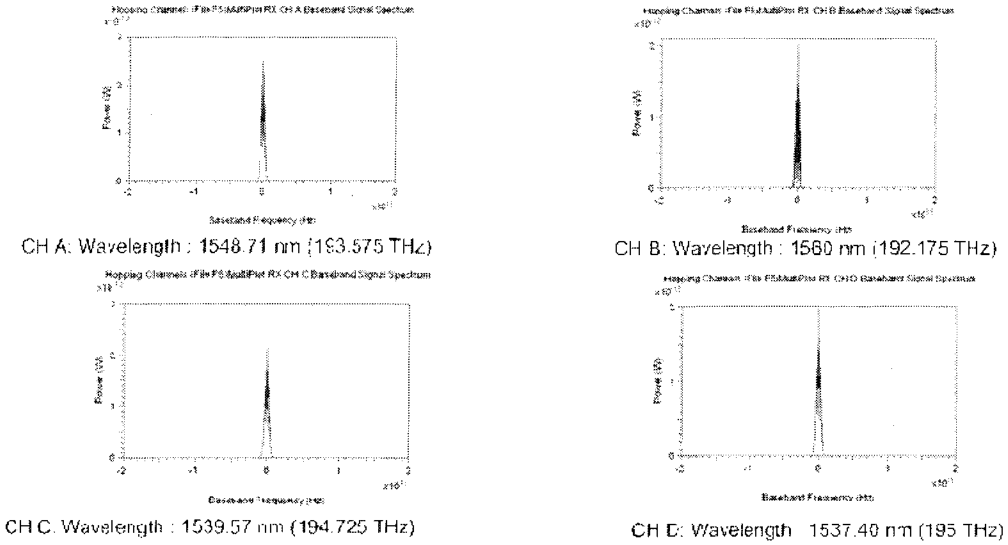

CH A: Wavelength : 1548.71 nm (193.575 THz)

CH B: Wavelength : 1560 nm (192.175 THz)

CH C: Wavelength : 1539.57 nm (194.725 THz)

CH D: Wavelength 1537.40 nm (195 THz)

Figure 51: Stability of 5th hop

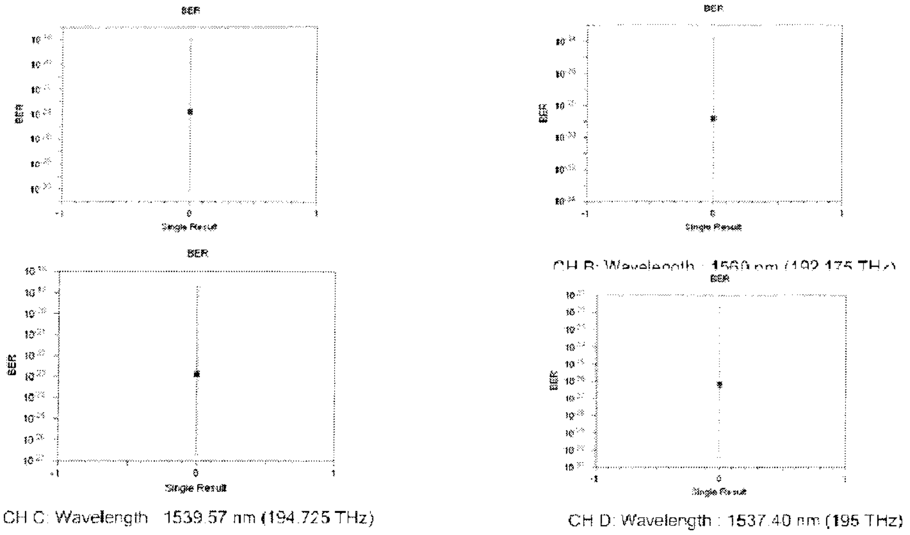

CH B: Wavelength : 1560 nm (192.175 THz)

CH C: Wavelength 1539.57 nm (194.725 THz)

CH D: Wavelength : 1537.40 nm (195 THz)

Figure 52: BER of 5th hop

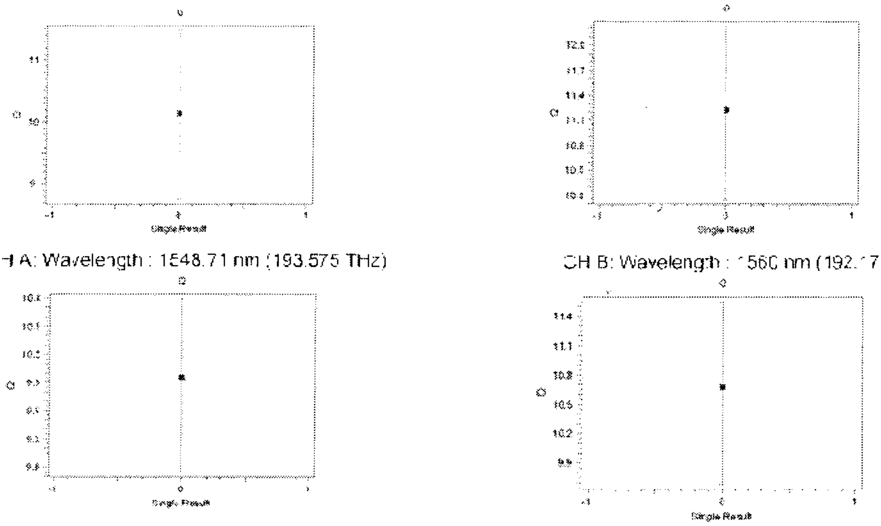

CH A: Wavelength : 1548.71 nm (193.575 THz)

CH B: Wavelength : 1560 nm (192.175 THz)

CH C Wavelength : 1539.57 nm (194.725 THz)

CH D. Wavelength . 1537.40 nm (195 THz)

Figure 53: Q pattern of 5th hop

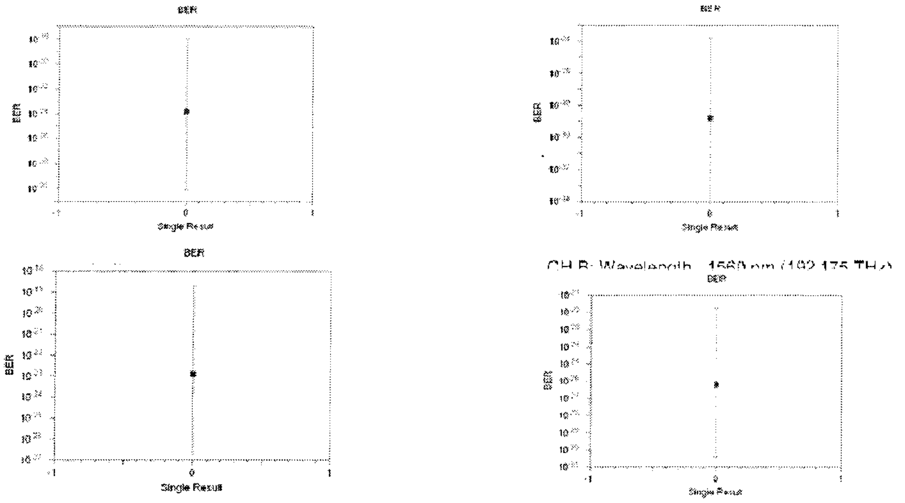

CH B: Wavelength 1560 nm (192.175 THz)

CH C Wavelength : 1539.57 nm (194.725 THz)

CH D Wavelength : 1537.40 nm (195 THz)

Figure 54: BER of 5th hop

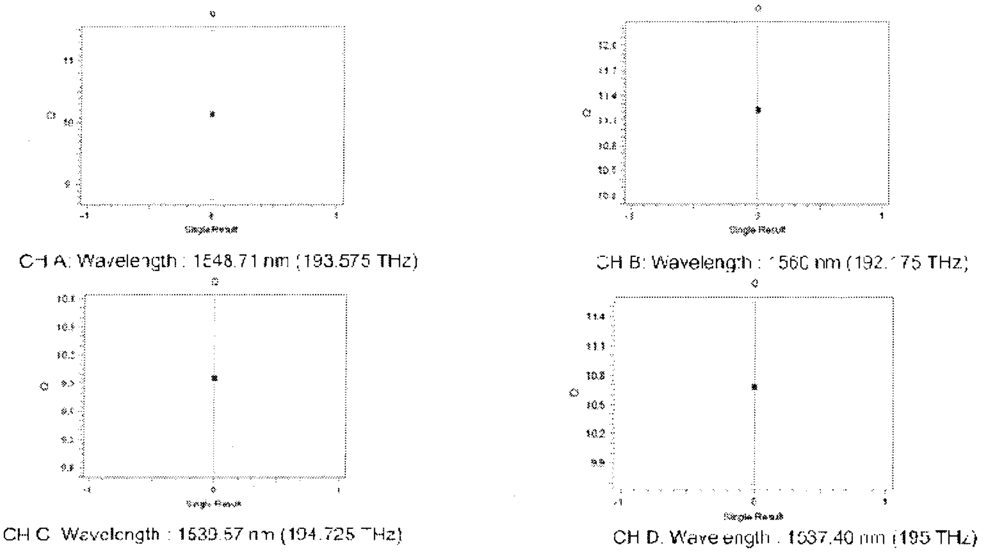

CH A: Wavelength : 1548.71 nm (193.575 THz)

CH B: Wavelength : 1560 nm (192.175 THz)

CH C Wavelength : 1539.57 nm (194.725 THz)

CH D. Wavelength . 1537.40 nm (195 THz)

Figure 55: Q pattern of 5th hop

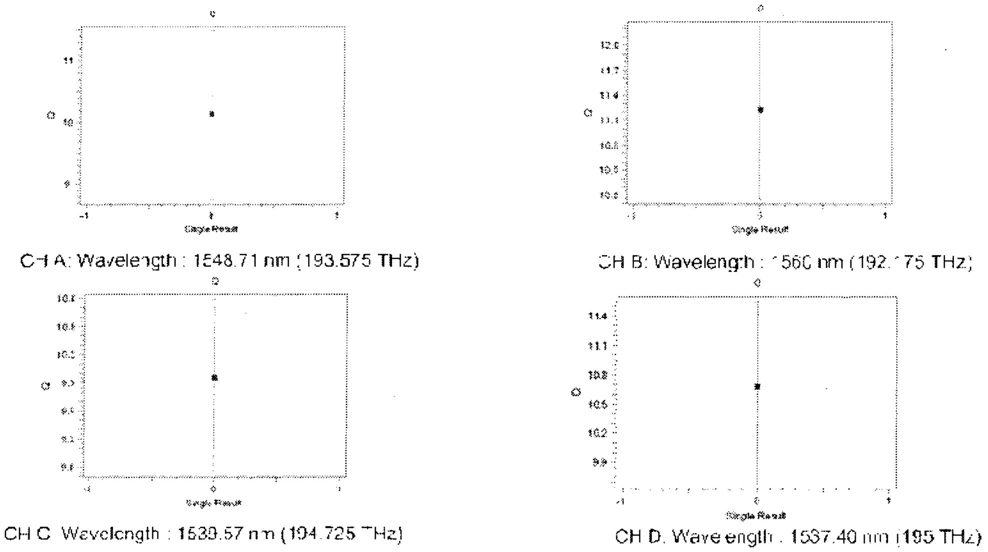

CH A: Wavelength : 1548.71 nm (193.575 THz)

CH B: Wavelength : 1560 nm (192.175 THz)

CH C Wavelength : 1539.57 nm (194.725 THz)

CH D. Wavelength . 1537.40 nm (195 THz)

Figure 56: Q pattern of 5th hopop

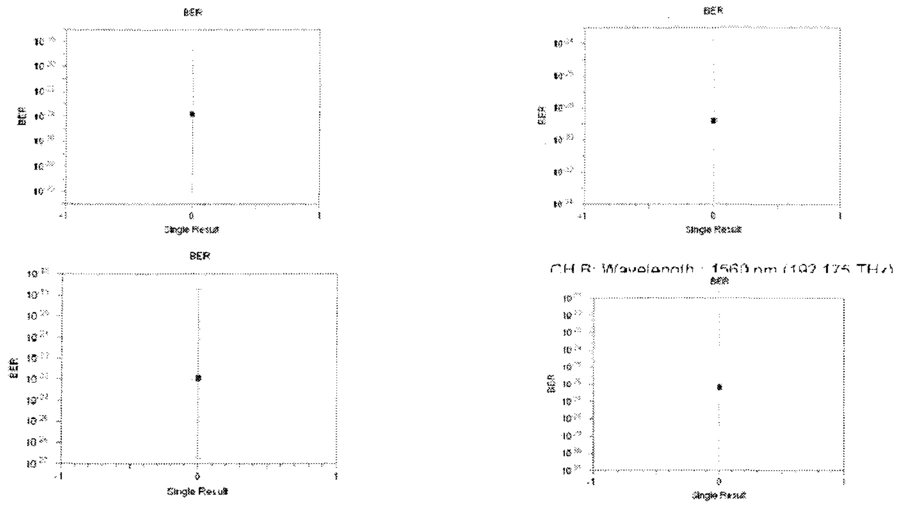

CH B: Wavelength : 1560 nm (192.175 THz)

CH C Wavelength : 1539.57 nm (194.725 THz)

CH D: Wavelength : 1537.40 nm (195 THz)

Figure 57: BER of 5th hop

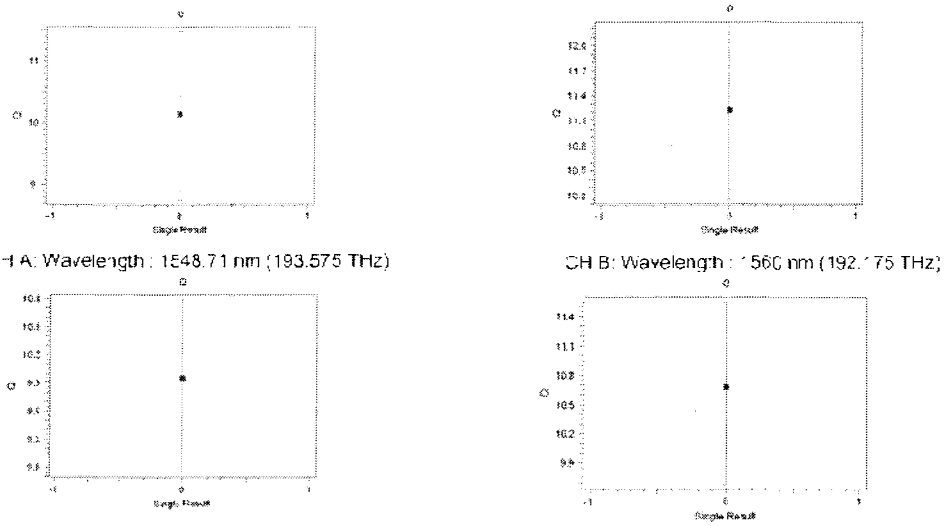

CH A: Wavelength : 1548.71 nm (193.575 THz)

CH B: Wavelength : 1560 nm (192.175 THz)

CH C Wavelength : 1539.57 nm (194.725 THz)

CH D. Wavelength : 1537.40 nm (195 THz)

Figure 58: Q pattern of 5th hop

BIBLIOGRAPHY

[1] Borella, M.S., Jue, J. P., Banerjee, D., Ramamurthy, B., and Mukherjee, B., "Optical components for WDM lightwave networks," *Proceedings of the IEEE*, Vol. 85, No. 8, pp. 1274-1307, Aug. 1997.

[2] Park, S.-J., Lee, C.-H., Jeong, K.-T., Park, H.-J., Ahn, J.-G., and Song, K.-H., "Fiber-to-the-home services based on wavelength-division-multiplexing passive optical network," *Journal of Lightwave Technology*, Vol. 22, No. 11, pp. 2582-2591, Nov. 2004.

[3] Stok A., and Sargent, E.H., "The role of optical CDMA in access networks," IEEE Communications Magazine, pp. 83-87, Sept. 2002..

[4] Harstead, E., "System requirements for optical components in the loop," *Lucent Technologies Inc. Lasers and Electro-Optics Society Annual Meeting*, p. 7, Nov. 1996.

[5] Medard, M., Marquis, D., Barry, R.A., and Finn, S.G., "Security issues in all-optical networks," *Network IEEE*, Vol. 11, No. 3, pp. 42-48, May-June 1997.

[6] Hamad, A.M., and Kamal, A.E. "A survey of multicasting protocols for broadcast-and-select single-hop networks," *IEEE Network*, pp. 36-48, July/Aug. 2002.

[7] Ramaswami, R., and Sivarajan, K.N., *Optical Networks, Practical Perspective*, 2d ed., San Francisco: Morgan Kaufmann Publishers, 2002, p.2.

[8] Gumaste, A., and Antony, T. *DWDM Network Designs and Engineering Solutions*, Indianapolis, IN: Cisco Press, pp. 147-148.

[9] Sherif, S.R., Hadjiantonis, A., Ellinas, G., Assi, C., and Ali, M.A, "A novel decentralized ethernet-based PON access architecture for provisioning differentiated QoS," *Journal of Lightwave Technology*, Vol. 22, No. 11, pp. 2483–2497, Nov. 2004.

[10] Paré, L.-R., "Cost effective broadband architecture for metro networks," *Lasers and Electro-Optics Society (LEOS), 16th Annual Meeting of the IEEE*, Vol. 2, pp. 612-613, 2003.

[11] *Heavy Reading, Real World Research,* http://www.heavyreading.com/document.asp?site=heavyreading&doc_id=9324page_number=3 (retrieved 14 Jan. 2006).

[12] G.983.1, Telecommunication Standardization Sector of ITU (10/98)—Series G: Transmission Systems and Media, Digital Systems and Networks—Broadband Optical Access Systems Based on Passive Optical Networks (PON).

[13] IEEE Std 802.3ah™-2004, (Amendment to IEEE Std 802.3™-2002 as amended by IEEE Stds 802.3ae™-2002, 802.3af™-2002, 802.3aj™-2003, and 802.3ak™-2004).

[14] Asatani, K., and Maeda, Y., "Access network architectural issues for future telecommunication networks," *IEEE Communications Magazine*, pp. 110-114, Aug. 1998.

[15] Kramer, G., and Pesavento, G., "Ethernet passive optical network (EPON): Building a next-generation optical access network," *IEEE Communications Magazine*, Feb. 2002.

[16] Zheng, J., and Mouftah, H.T., "Media access control for Ethernet passive optical networks: An overview." *IEEE Communications Magazine*, Feb. 2005.

[17] Harris, J.S., Jr., "Tunable long-wavelength vertical-cavity lasers: The engine of next generation optical networks?" *IEEE Journal of Selected Topics in Quantum Electronics*, Vol. 6, No. 6, pp. 1145–1160, Nov.-Dec. 2000.

[18] Shrikhande, K.V., Lentine, A.L., Nuss, M.C., Kogelnik, H., Krishnamoorthy, A.V., Avenarius, M, and Kazovsky, L.G., "Fiber-to-the-home/desktop using Ethernet," *IEEE Journal on Selected Areas in Communications*, Vol. 18, No. 10, pp.2004-2016, Oct. 2000.

[19] Chan, C.-K., Sherman, K.L., and Zirngibl, M., "A fast 100-channel wavelength-tunable transmitter for optical packet switching," *IEEE PhotonicsTechnology Letters*, Vol. 13, No. 7, July 2001.

[20] Mynbaev, D.K., and Scheiner, L.L., *Fiber-Optic Communications Technology*, Upper Saddle River, NJ: Prentice Hall, 2001.

[21] Yasaka, H., Okuno, M., and Sugahara, H., "Device technologies for photonic networks" *NTT Photonics Laboratories*, Vol. 1, No. 8, Nov. 2003.

[22] Bengi, K., *Optical Packet Access Protocols for WDM Networks*, Norwell, MA: Kluwer Academic Publishers, 2002.

[23] Kimura, H.A., Tohmon, G., Nishikawa, T., Uno, T., and Morikura, S., "High performance optical receiver using hybrid integration in line photodiode module and preamplifiers fir passive optical network."

[24] Parker, M.C., and Mears, R.J., "Digitally tunable wavelength filter and laser," *IEEE Photonics Technology Letters*, Vol. 8, No. 8, pp. 1007-1008, Aug. 1996.

[25] Tachikawa, Y., and Okamoto, K., "Arrayed wave guide granting laser and their applications to tuning-free wavelength routing," *IEE Proc. Optoelectronics,* Vol. 143, No. 5, Oct. 1996.

[26] International Telecommunication Union, (ITU-T) G.694.1, Telecommunication Standardization Sector of ITU, "Spectral grids for WDM applications: DWDM frequency grid," SERIES G: Transmission systems and media, digital systems and networks transmission media characteristics—Characteristics of optical components and subsystems: ITU-T Study Group 15 (2001-2004) and approved under the WTSA Resolution 1 procedure on 13 June 2002.

[27] Sarlet, G., Morthier, G., and Baets, R., "Wavelength and mode stabilization of widely tunable SG-DBR and SSG-DBR lasers," *IEEE Photonics Technology Letters*, Vol. 11, No. 11, Nov. 1999.

[28] Sugihwo, F., Lin, C.-C., Eyres, L.A., Fejer, M.M., and Harris, J.S., Jr., "Broadly-tunable narrow-linewidth micromachined laser/photodetector and phototransistor," Electron Devices Meeting, 1998. *IEDM '98 Technical Digest International*, pp. 665-668, 6-9 Dec. 1998.

[29] Misono, M., Henmi, N.; Hosoi, T., and Fujiwara, M., "High-speed wavelength switching and stabilization of an acoustooptic tunable filter for WDM network in broadcasting stations," *IEEE Photonics Technology Letters*, Vol. 8, No. 4, pp. 572-574, April 1996.

[30] Sadot, D., and Boimovich, E., "Tunable optical filters for dense WDM networks" *IEEE Communications Magazine*, Vol. 36, No. 12, pp. 50-55, Dec. 1998.

[31] Westphal, F.-J., Hermes, T., Hilbk, U., Meissner, P., and Schmidt, F., "Transmissive star coupler based experimental dense WDM-LANs interconnected via a central node," Flat Panel Display Technology/Technologies for a Global Information Infrastructure/ICs for New Age Lightwave Communications/RF Optoelectronics, *1995 Digest of the LEOS Summer Topical Meetings*, pp. 20-21, 7-11 Aug. 1995.

[32] Kauer, M., Girault, M., Leuthold, J., Honthaas, J. Pellegri, O., Goullancourt, C., and Zirngib, M., "16-channel digitally tunable external-cavity laser with nanosecond switching time," *IEEE Photonics Technology Letters*, Vol. 15, No. 3, March 2003.

[33] Krainer, L. Spiiliier, G.J., Kilburn, I.J., Golding, P.S., Crosby, S.A., Brownell, M., and Weingarten, K.J., "C-band tunable 25-GHz passively mode-locked Er:Yb:glass laser," GigaTera, Inc. and Ultrafmt Laser Physics, Zurich, Swrtzerland.

[34] Yoshikuni, Y. "Semiconductor optical Devices for WDM networks," NTT Opto-Electronics Laboratories, Kanagawa, Japan.

[35] Hammond, B., Su, B. Mathews, J., Chen, J., and Schwarts, E., "Integrated wavelength locker for tuneable laser applications," Digital Optics Corporation, Charlotte, NC.

[36] Huang, Y., Heritage, J.P., and Mukherjee, B. "Connection provisioning with transmission impairment consideration in optical WDM networks with high-speed channels," *Journal of Lightwave Technology*, Vol. 23, No. 3, March 2005.

[37] Strand, J., Chiu, A.L., and Tkach, R., "Issues for routing in the optical layer," *IEEE Communications Magazine*, February 2001.

[38] Ueda, H., Okada, K., Ford, B., Mahony, G., Hornung, S., Faulkner, D., Abiven, J., Durel, S., Ballart, R., and Erickson, J., "Deployment status and common technical specifications for a B-PON system," *IEEE Communications Magazine*, Vol. 39, No. 12, pp. 134-141, Dec. 2001.

[39] Davey, R.P., Healey, P., Hope, I., Watkinson, P., Payne, D.B., Marmur, O., Ruhmann, J., and Zuiderveld, Y., "DWDM reach extension of a GPON to 135 km," *Optical Fiber Communication Conference 2005 Technical Digest*, Vol. 6, p. 3, 6-11 March 2005.

[40] Strand, J., and Chiu, A., Eds., "RFC 4054—impairments and other constraints on optical layer routing," Network Working Group, AT&T, May 2005

[41] Newhouse, M., and Liu, Y., "System needs for dispersion compensation," Symposium on Requirements and Techniques of Dispersion Compensation Lucent Technologies, *OFC '97 Technical Digest*, 1997.

[42] Downie, J.D., Annunziata, F., Filios, A., Kennedy, T., Kim, D., and Oh, S., "Large effective area non-zero dispersion shifted fiber in metro/provincial network environments," *Proceedings of SPIE*, Vol. 5279, 2004.

[43] Belahlou, A., Bickham, S., Chowdhury, D., Diep, P., Evans, A., Grochocinski, J.M., Han, P., Kobyakov, A., Kumar, S., Luther, G., Mauro, J.C., Yihong Mauro, Mlejnek, M., Muktoyuk, M.S.K., Murtagh, M.T., Raghavan, S., Ricci, V., Sevian, A., Taylor, N., Tsuda, S., Vasilyev, M., and Wang, L., "Fiber design considerations for 40 Gb/s systems," *Journal of Lightwave Technology*, Vol. 20, No. 12, pp. 2290-2305, Dec. 2002.

[44] Judy, A. F., "Optimizing fiber dispersion for DWDM systems" *OFC 97 Technical Digest*, 1997.

[45] Agrawal, G.P., "Light wave technology telecommunication system," Hoboken, NJ: John Wiley and Sons, 2005.

[46] Yang, G.-C., and Kwong, W.C., "Performance comparison of multiwavelength CDMA and WDMA CDMA for fiber-optic network," *IEEE Transactions on Communications*, Vol. 45, No. 11, Nov. 1999.

[47] Xu, B., and Brandt-Pearce, M., "Comparison of FWM- and XPM-induced crosstalk using the volterra series transfer function method," *Journal of Lightwave Technology*, Vol. 21, No. 1, Jan. 2003,

[48] Thing, V.L.L., P. Shum, P., and Rao, M.K., "Channel allocation algorithm for WDM systems," *OSA 2003, Optics Express*, Vol. 11, No. 11, pp. 1322-1327, June 2003.

[49] Chan, S.C., Lu, M., Udpa, S.S., Udpa, L., and Jacobson, D.W., "All-optical dense WDM wide-area communication network," *IEEE 39th Midwest Symposium on Circuits and Systems*, Vol. 3, pp. 1157-1160, 18-21 Aug. 1996.

[50] Minn, S., and Won, Y.-H., "Upper-bounds on bit error rate of OCDMA systems using the time spreading/wavelength-hopping codes", School of Engineering, Information and Communication University, IEEE Publication document number 0-9803-5947-X00, 2000.

[51] Federal Information Processing Standards Publication 191, "Specifications for Guidelines for The Analysis Local Area Network Security," FIPS PUB 191, 9 Nov. 1994.

[52] Mědard, M., Marquis, D., and. Chinn, S.R., "Attack detection methods for all-optical networks," *IEEE Network*, pp. 42-48, May/June 1997.

[53] Canetti, Garay, J., Itkis, G., Micciancio, D., Naor, M., and Pinkas, B., "Multicast security: A taxonomy and some efficient constructions," *INFOCOMM'99*, pp. 708-716, March 1999.

[54] Islam, M.N., "Information assurance and system survivability in all-optical networks." Xtera Communications, Allen, TX.

[55] Liu, Z., Campbell, R.,H., and M Mickuna, M.D., "Active security support for active networks," *IEEE Transactions on Systems, Man and Cypernetics—Part C: Applications and Reviews,* Vol. 33, No. 4, Nov. 2003.

[56] Thomas, S., and Wagner, D., "Insecurity in ATM-based passive optical networks," Wave7 Optics, University of California, Berkeley.

[57] Bhatia, S., and Barto, R., "Performance of the IEEE 802.3 EPON registration scheme under high load," Society of Photo-Optical Instrumentation Engineers, 2004.

[58] ITU-T Recommendation G.984.1—Gigabit-capable Passive Optical Networks (GPON): General Characteristics," March 2003.

[59] Rho, S.-S., and Kim, S.-H., "Security model and authentication protocol in EPON-based optical access network," Gwangiu University, Korea, 2003.

[60] Chan, H., Hodjat, A., Shi, J., Wesel, R., and Verbauwhede, I., "Streaming encryption for a secure wavelength and time domain hopped optical network," *Proceedings of the International Conference on Information Technology: Coding and Computing* (ITCC'04), 2004.

[61] Keshavarzian, A., and Salehi, J.A., "Optical orthogonal code acquisition in fiber-optic CDMA systems via the simple serial-search method," *IEEE Transactions on Communications*, Vol. 50, No. 3, March 2002.

[62] Qiao, Y., Qi, J, Pu, H., Chen, S., and Guan, K., "A new scheme for WDM-based passive optical access network," *Communication Technology Proceedings*, International Conference WCC – ICCT, IEEE 0-7803-6394-9/00, 2000.

[63] Bengi K., *Optical Packet Access Protocols for WDM Networks*, Norwell, MA: Kluwer Academic Publishers, 2002.

[64] Simov, B. H., Jue, J.P., and Tridandapani, S., *Integrating Security in the MAC Layer of WDM Networks*, Norwell, MA: Kluwer Academic Publishers, 2001.

[65] Chung, F.R.K., and Salehi, J.A., "Optical orthogonal codes: Design, analysis, and application," *IEEE Transactions on Information Theory*, Vol. 35, No. 3, May 1989.

[66] Salehi, J.A., "Code division multiple access techniques in optical fiber networks, Part I: Fundamental principles," *IEEE Transactions on Communications*, Vol. 37, No. 8, pp. 824-8333, 1989.

[67] Fathallah, H., Rusch, L.A., and LaRochelle, S., "Passive optical fast frequency-hop CDMA communications system," *Journal of Lightwave Technology*, Vol. 17, No. 3, pp. 397-405, March 1999.

[68] Shake, T.H., "Security performance of optical CDMA against eavesdropping," *Journal of Lightwave Technology*, Vol. 23, No. 2, Feb. 2005.

[69] Stinson, D.R., *Cryptography: Theory and Practice*, 2d ed., Boca Raton, FL: CRC Press, 2002.

[70] Profet, K.J., Lavine, C.H., and Meyer, K.R., "The risk of trust vs the cost of assurance—Trades in the implementation of a secure LAN," *IEEE Proceedings on Aerospace Applications Conference*, 1994

[71] You, Y., and Chandra, K., "Time series models for Internet data traffic," *Proceedings of the 24th Conference on Local Computer Networks, LCN-99,* Oct. 1999.

[72] Yang, G.-Y., and Kwong, W.C., *Prime Codes with Applications to CDMA Optical and Wireless Network*, pp. 44, 247, Artech House Mobile Communication Series, 2002.

[73] Stok A., and Sargent, E.H., "Lighting the local area: Optical code-division multiple access and quality of service provisioning," *IEEE Network,* Nov./Dec. 2000.

[74] Touch, P., Bannister, J.D., and Kamath, J.A., "The need for media access control in optical CDMA networks," *INFOCOM 2004, 23rd Annual Joint Conference of the IEEE Computer and Communications Societies,* Vol. 4, pp. 2208-2219, 7-11 March 2004.

[75] Kwong, W.C., Yang; G.C., Baby, V., Bres, C.-S., and Prucnal, P.R., "Multiple-wavelength optical orthogonal codes under prime-sequence permutations for optical CDMA," *IEEE Transactions on Communications*, Vol. 53, No. 1, pp. 117-123, Jan. 2005.

[76] Andonovic, I., and Tancevski, L., "Incohernet optical code division multiple access systems," IEEE Paper 07-7803-3567-8/-8/96.

[77] Mendez, A.J., Gagliardi, R.M., Hernandez, V.J., Bennett, C.V., and Lennon W.J., "High-performance optical CDMA system based on 2-D optical orthogonal codes," *Journal of Lightwave Technology*, Vol. 22, No. 11, Nov. 2004.

[78] Kramer, G., Mukherjee, B., and Pesavento, G., "Ethernet PON (ePON): Design and analysis of an optical access network," *IEEE Journal*, Aug. 2000.

[79] Djordjevic, I.B., and Vasic, B., "Novel combinatorial constructions of optical orthogonal codes for incoherent optical CDMA systems," *Journal of Lightwave Technology*, Vol. 21, No. 9, Sept. 2003.

[80] Chan, H.H., Elmirghani, J.M.H., and Cryan, R. A., "Performance evaluation of PPM under different orthogonal coding schemes," IEEE Paper 0-7803-4788-9/98.

[81] Kim, S., Yu, K., and Park, N., "A new family of space/wavelength/time spread three-dimensional optical code for OCDMA networks," *Journal of Lightwave Technology*, Vol. 18, No. 4, April 2000.

[82] Tancevski, L., and Andonvic, I., "Hybrid wavelength hopping/time spreading schemes for use in massive optical network with increase security," *Journal of Lightwave Technology*, Vol. 14, No. 12, Dec. 1996.

[83] Tancevski, L., Andonvic, I., and Budin, J., "Secure optical network architecture utilizing wavelength hopping/time spreading code," *IEEE Photonics Technology*, Vol. 7, No. 5, May 1995.

[84] Park, S., Kim, B.K., and Kim, B.W., "An OCDMA scheme to reduce multiple access interference and enhance performance for optical subscriber access networks," *ETRI Journal*, Vol. 26, No. 1, pp. 13-20, Feb. 2004.

[85] Kwong, W.C., Yang, G.-Y., Baby, V., Bres, C.-S., and Prucnal, P.R., "Multiple-wavelength optical orthogonal codes under prime-sequence permutations for optical CDMA," *IEEE Transactions on Communications* Vol. 53, No. 1, pp. 117-123, Jan. 2005.

[86] Maric, S.V., Kostic, Z.I., and Titlebaum, E.L., "A new family of optical code sequences for use in spread-spectrum fiber-optic local area networks," *IEEE Transactions on Communications*, Vol. 41, No. 8, pp. 1217-1221, Aug. 1993.

[87] Tancevski, L., Andonovic, I., Tur, M., and Budin, J., "Massive optical LANs using wavelength hopping/time spreading with increased security," *Photonics Technology Letters*, Vol. 8, No. 7, pp. 935-937, July 1996.

[88] Tancevski, L., and Andonovic, I., "Wavelength hopping/time spreading code division multiple access systems," *Electronics Letters*, Vol. 30 No. 17, pp. 1388-1390, Aug. 1994.

[89] Guruprasad, A., Pandey, P., and Prashant, B., "Security features in Ethernet switches for access networks," *TENCON 2003, Conference on Convergent Technologies for Asia-Pacific Region*, Vol. 3, pp. 1211-1214, 15-17 Oct. 2003.

[90] Tatsuta, T. Yoshida, Y., and Maeda, Y., "Standardization of G-PON (gigabit passive optical network) in ITU-T," *NTT Technical Review*, Vol. 1, No. 7, pp. 89-93, Oct. 2003.

[91] Andonovic, I., and Tancevski, L., "Incohernet optical code division multiple access systems," *IEEE 4th International Symposium on Spread Spectrum Techniques and Applications Proceedings*, Vol. 1, pp. 424-430, 22-25 Sept. 1996.

[92] Tancevski, L., Andonovic, I., Tur, M., and Budin, J., "Hybrid wavelength hopping/ time spreading code division multiple access system," *IEE Proceedings—Optoelectronics*, Vol. 143, No. 3, June 1996.

[93] Kwong, W.C., and Yang, G.-C., "Multiple-length multiple-wavelength optical orthogonal codes for optical CDMA systems supporting multirate multimedia services," *IEEE Journal on Selected Areas in Communications*, Vol. 22, No. 9, Nov. 2004.

[94] Lee, S.-S., and Seo, S.W., "New construction of multiwavelength optical orthogonal codes," *IEEE Transactions on Communications*, Vol. 50, No. 12, pp. 2003-2008, Dec. 2002.

[95] Stok, A., and Sargent, E.H., "Comparison of diverse optical CDMA codes using a normalized throughput metric," *IEEE Communications Letters*, Vol. 7, No. 5, pp. 242-244, May 2003.

[96] Yang, G.C., "Variable-weight optical orthogonal codes for CDMA networks with multiple performance requirements," *IEEE Transactions on Communications*, Vol. 44, No. 1, Jan. 1996.

[97] Kwong, W.C., and Yang, G.-C., "Design of multilength optical orthogonal codes for optical CDMA multimedia networks," *IEEE Transactions on Communications*, Vol. 50, No. 8, Aug. 2002.

[98] Winzer, P.J., Pfennigbauer, M., and Essiambre, R.-J., "Coherent crosstalk in ultra dense WDM systems," *Journal of Lightwave Technology*, Vol. 23, No. 4, pp. 1734-1744, April 2005.

[99] Jepsen, T.C., "The basics of reliable distributed storage networks," *IT Pro*, May-June 2004.

[100] Shi, C., and Bhargava, B., "An efficient MPEG video encryption algorithm," *Reliable Distributed Systems, Proceedings of the 17th IEEE Symposium*, pp. 381-386, 20-23 Oct. 1998.

[101] BBC News website. "Supercomputer doubles own record," http://news.bbc.co.uk/1/hi/technology/4386404.stm (retrieved 13 Jan. 2006).

[102] TOP500 Supercomputer Sites. "26th TOP500 list," SC|05 Conference, 15 Nov. 2005," http://www.top500.org/lists/2005/11/TOP10_Nov2005.pdf, (retrieved 13 Jan. 2006).